Engineered plasma cells: a novel platform for long-term delivery of biologics to treat leukemia and other diseases

Tyler F. Hill

A dissertation

submitted in partial fulfillment of the

requirements for the degree of

Doctor of Philosophy

University of Washington

2023

Reading Committee:

Richard G. James, Chair

David J. Rawlings

Andrew A. Oberst

Program Authorized to Offer Degree:

Molecular & Cellular Biology

University of Washington

Abstract

Engineered plasma cells: a novel platform for long-term delivery of biologics to treat leukemia and other diseases

Tyler F. Hill

Advances in genome-engineering have enabled the generation of human plasma cells that secrete therapeutic proteins and are capable of long-term *in vivo* engraftment in humanized mouse models. To assist the clinical translation of engineered plasma cells (ePCs), we present three key studies evaluating: a) engineering approaches for optimized expression and secretion of non-immunoglobulin G (IgG)-like bispecific antibodies by human plasma cells to treat leukemias *in vivo*; b) a humanized mouse model to assess engraftment function and pharmacokinetics of adoptively transferred autologous ePC; and c) a novel B cell signaling BCR/Ab-screening method to evaluate highly expressed monoclonal antibodies for secretion by ePCs. We show that human ePCs expressing either anti-CD19 x anti-CD3 (blinatumomab) or anti-CD33 x anti-CD3 bispecific antibodies mediate T cell activation and direct T cell killing of specific primary human cell subsets and leukemia cell lines *in vitro* and *in vivo*. We demonstrate that the presence of autologous human hematopoietic cells in immunodeficient mice permits the establishment of a robust model for studying the *in vivo* biology and potential therapeutic benefit of long-lived human ePCs. Finally, we developed a B cell signaling-based method for the screening of BCRs for use as recombinant monoclonal antibody therapy and in engineered B cells and ePCs. Collectively, these findings support further development of ePCs for use as a durable system for the treatment of acute leukemias, and potentially other diseases.

TABLE OF CONTENTS

ACKNOWLEDGEMENTS

First, I would like to thank my boss, Dr. Richard James. It is hard to find a mentor who is both passionate about B cell therapies/genome-engineered cell therapies and also equally passionate about mentoring students. I have never had a mentor more willing to make time for me than Rich. Even when he is neck deep in grant and paper writing, he has made time for me. Anybody who talks to Rich long enough will know that Rich loves to talk about science. I remember a great many long evening conversations where we talked about what is known or not known, exciting or boring about a wide range of scientific topics. He thinks big and deeply. His willingness to talk and think deeply about a given scientific project were invaluable to my training and definitely have made me a better scientist. I am also incredibly grateful for the other support Rich has provided (scientific writing, experimental design, sending me to conferences etc.) throughout my training. Without Rich, none of this would have been possible. Many many many thanks.

I would also like to thank Dr. David Rawlings. Dr. Rawlings has provided me with incredible scientific guidance throughout my training as a co-mentor and committee member. Dr. Rawlings regularly provided key feedback on experimental designs, interpretation of findings and most importantly helped me contextualize my projects within the greater scientific field. I am grateful for all his thorough and useful feedback on my F30 grant application, manuscripts and this dissertation. Additionally, Dr. Rawlings also provided key reagent support such as providing human $CD34^+$ cells. His calm demeanor and ability to coach me to think more deeply about the strange findings (like when my humanized mice had GvHD early on in my training) has made me a far better, more relaxed and productive scientist.

I would like to thank my collaborator Dr. Andrew McGuire. His insights were invaluable in progressing my research on AMMO-1 secreting ePCs. He not only provided key guidance and

reagents but also performed pseudo-neutralization and binding affinity assays. I learned a lot from him, and my projects definitely benefited from his keen troubleshooting.

I would like to thank my collaborator Dr. Sarah Tasian. Her perspective as a pediatric oncologist was key to the success of the study presented in Chapter 2. Dr. Tasian provided many of the leukemia cell lines. Dr. Tasian also provided incredibly useful feedback on study design and implications. Her rapid and often humorous feedback was greatly appreciated.

I would also like to thank my thesis advisory committee members, Andrew Oberst and Julie Overbaugh. Andrew Oberst from early on was able to pick out interesting findings and ask great questions that helped shape my research. Julie Overbaugh was key to keeping me focused and on track to complete my research. She also offered assistance and reagents related to lentiviral transduction of T cells (and potentially B cells). I consider myself blessed that they would take time from their busy schedules to support my training in ways that go way beyond the average committee member.

I would be terribly remiss if I failed to acknowledge the many many research scientists that have assisted me in ways both big and small along the way. I want to specifically thank the amazing SCRI research scientists that I have been lucky to work with including Nathan Camp, Nikita Trivedi, Tingting Zhang, Emma Suchland, Iana Meitlis, Andee Ott, Parnal Narvekar, Gregory Asher, Anna Helmers, and Claire Stoffers. I could not have done this without you.

More thanks to my fellow SCRI graduate students; Rene Cheng, Malika Hale, Cade Ito, Ragan Pitner and Warren Anderson. I could not have asked for a better group of peers to share the north carrels with. I benefited immensely from being able to casually ask you all scientific questions, questions about training and to just to socialize with all of you. I will miss you all dearly and hope to get to work with you all again in the future.

I'd like to thank my family and friends. I'm sure that my training up here in Seattle has made it harder for us to stay close. I hope that you know that your phone calls and visits meant

the world to me. I also appreciate your flexibility and good grace with me and my unpredictable experimental schedule. Thanks for all your support and love over these past years. Mom and Dad you are super parents and I couldn’t be luckier to have you.

Lastly, thanks for my loving partner, Anna. She was integral to keeping my keel even as I navigated through the rough and stressful waters of graduate school. Her constant encouragement, understanding, and belief in my abilities kept me motivated when nothing else could. She helped take care of me when I was too focused on science to take care of myself by swimming and cooking great meals with me. I especially want to thank her for being an amazing dog mom to our dog, Zala. I couldn't have asked for a better companion to share this incredible chapter of my life with.

Chapter 1.

INTRODUCTION AND BACKGROUND ON THE MOLECULAR ENGINEERING OF B CELLS AND PLASMA CELLS

1.1. FEATURES OF B CELLS AND PLASMA CELLS RELATED TO THEIR USE AS CELL THERAPIES

Cells of the B cell lineage are adaptive immune cells best known for their production of antibodies (Abs). During their life cycle, B cells undergo various stages of differentiation, leading to the adoption of diverse phenotypes and functions. The development of B cells initiates in the bone marrow, where genetic recombination events lead to the expression of a unique B cell receptor (BCR) conferring antigen specificity. Following this, mature naive B cells egress into the systemic circulation, distributing in both blood and lymphoid organs, seeking an encounter with their respective cognate antigens. When exposed to cognate antigens, appropriately stimulated naive B cells can undergo clonal expansion and differentiation, giving rise to diverse subsets. Among those differentiated subsets are long-lived plasma cells (PCs). For a more comprehensive and in-depth exploration of the intricate mechanisms governing the various B cell differentiation fates, we recommend referring to the following reviews by Jason Cyster and Stephen Nutt[1–3].

We consider long-lived PCs to be the optimal B cell subset for long term delivery of biologics, however, it is worth mentioning some of the functionalities of other B cell subsets and their potential applications. For instance, antigen-specific B cells of can undergo differentiation towards an IL-10 secretory regulatory B cell phenotype or alternatively be modified to function as tolerogenic antigen-presenting cells by expressing an antigen fused to the heavy chain (HC) of IgG, and thus facilitate immunological tolerance for autoimmune diseases or monogenic disorders[4–8]. Alternatively, B cells under the right activation conditions can present antigen such as tumor associated antigens and induce antigen-specific T cell responses as a potential cancer vaccine[9–11]. Another function of many antigen-specific B cells subsets is their ability to clonally expand when stimulated with cognate antigen which can allow for the priming/boosting of adoptively transferred cells[12–14] To date, adoptively transferred B cells have been used in

clinical trials as a cancer vaccine[15] and as a way to prevent infectious complications during stem cell transplantation[16]. These trials indicate that adoptive B cell immunotherapy is generally safe and associated with little toxicity. However, the cell product transferred in these trials contained a variety of B cell subsets with various functionalities and abilities which may not necessarily be beneficial in the context of a biologic secreting cell-based platform. For example, B cells that encounter cognate antigen can secrete inflammatory cytokines (IL-6 and IFNγ) that may enhance immunogenicity of biologic being secreted or lead to volatile levels of biologic through antigen-driven expansion of biologic-secreting cells.

To avoid these undesirable B cell functionalities and enhance desired PC functionality, one can *ex vivo* differentiate and select a B cell product that consists primarily of long-lived PCs during *in vitro* manufacturing [17–19]. BCR surface expression and antigen presentation machinery is downregulated as B cells approach terminally differentiated IgG class-switched long-lived PCs and thus reduces the antigen-dependent B cell functions we just mentioned[20–22]. Using long-lived PCs has several additional benefits as a platform for the delivery of therapeutic biologics. Firstly, B cells are easily accessible from peripheral blood and readily expand and differentiate into plasma cells. Secondly, differentiated PCs can survive for decades in the absence of further antigen stimulation or proliferation[23] which may allow for a continuous long-term secretion of biologics. Thirdly, PCs have a high secretory capacity (up to 10,000 Immunoglobulin (Ig) G molecules per second[24–26], which may allow for the use of a smaller cell dose to achieve therapeutic levels. Additionally, PCs have a propensity to migrate and persist in hard to access tissue sites such as the bone marrow and mucosal tissues allowing for more localized delivery of biologics[27–29]. Lastly, there is a wide range of tools available for the molecular engineering of B cells and PCs to express exogenous therapeutic proteins and peptides (see section 1.2).

1.2. SHORT HISTORY OF THE MOLECULAR ENGINEERING OF HUMAN B CELLS

The past decade has seen a major shift in technology allowing for the stable integration of transgenes into the genome of B cells and subsequent PCs. While we will focus on technologies that stably integrate transgenes, it is worth mentioning there are many methods that use of mRNA[30,31], naked/plasmid DNA[32,33], viral vectored episomal DNA[34–37] for the transient expression of exogenous transgenes in human B cells. Progress in the early days of engineering stable gene integration into B cells was challenging because traditional VSV-g integrative lentiviral vectors do not readily transduce human B cells[38]. However, the introduction of lentiviral vectors pseudotyped with RD114 cat endogenous virus, baboon endogenous virus, or measles virus glycoproteins have significantly augmented transduction efficiency[39–41]. Integrative lentiviral vectors have been used in proof of concept studies to engineer B cells to treat cancer[42] and infectious disease[43,44]. Additionally, the Sleeping Beauty (SB) transposon system has also been used to generate IUDA-secreting plasma cells[45]. However, the non-site-specific integration of lentiviral vectors and SB along with their tendency to integrate into transcriptionally active regions, poses an inherent risk of introducing harmful mutations[46]. Furthermore, both systems lack control over the viral copy number[47] (gene integration events for SB) or lentiviral promoter silencing[48].

In part to improve control over where transgenes insert in the genome, the B cell engineering field has moved towards the use of clustered regularly interspaced short palindromic repeats(CRISPR)/CRISPR associated protein (Cas9) technology coupled with homology directed repair to allow for the targeted integration of transgenes at specific loci in B cells. Cheong et al. were the first to show locus-specific editing using CRISPR/Cas9 in human B cells. Interestingly, they also showed the ability to induce class switch recombination in murine B cells[49]. Then in 2018, Hung et al. were able to use homology directed repair to generate the first CRISPR/Cas9 genome-engineered B cell to secrete a clinically-relevant biologic drug[50]. In

their seminal study, they used CRISPR/Cas9 ribonucleoprotein to cause a double stranded break at the safe harbor locus, CCR5. They then used AAV6 vectored homologous repair templates to deliver a gene cassette containing Factor IX, which is inserted into the CCR5 locus via the homology directed repair pathway. This has led to proof-of-concept studies using homology directed repair to engineer B cells that deliver biologic drugs to treat protein deficiency diseases[51,52] and viral infections[12,14,53–55]. For a more comprehensive and in-depth discussion of B cell engineering methods, we recommend referring to the following reviews by James Voss, Paula Cannon and François-Loïc Cosset[38,44,56,57]. While editing efficiency with CRISPR/Cas9 and AAV6 vectored repair templates remains challenging when trying to deliver large transgene payloads (>4.7kB)[58], it is now possible to engineer B cells and subsequent PCs to secrete a variety of biologics against a wide range of targets.

1.3. POTENTIAL APPLICATIONS OF ENGINEERED PLASMA CELLS FOR THE DELIVERY OF CHRONICALLY ADMINISTERED BIOLOGICS

In Section 1.1, we summarized data that indicate that PCs have several features that make them an excellent candidate for a long-term biotherapeutic delivery platform. In section 1.2, we established that it was possible to engineer PCs to secrete a wide variety of biologics. Combined, we can generate a biologic drug delivery platform with the potential of providing continuous stable levels of therapeutic biologics (Figure 1). The initial success in B cell engineering raises a range of key questions including: what are the potential clinical applications where ePC therapy would prove beneficial? How can we model the *in vivo* functionality of ePC therapies in a manner that is most biologically relevant to humans? How can we screen future potential biologics for technical feasibility and high secretion in an ePC therapy?

Diseases treated chronically through repeat infusions or injections such as monogenic protein deficiency disorders may benefit from a continuous *in vivo* source of exogenous replacement protein. Maintaining sustained and effective serum concentrations of the desired

exogenous protein is a significant hurdle in protein replacement therapy. This is further complicated by the propensity of recombinant drug therapy to elicit anti-drug immune responses that diminish or neutralize the therapeutic efficacy[59]. Exogenous protein secreting ePCs, due to their potential for long-term persistence, could offer a lifelong cure with just one injection. Moreover, these ePCs may present the exogenous protein peptides as a self-antigen, potentially reducing the immunogenicity associated with exogenous replacement protein therapies[60,61]. Both Hung et al. and Levy at al. have provided proof of concept that human engineered B cells and ePCs can produce human factor IX, the missing clotting factor in patients with hemophilia B[50,52]. In the future, we hope that researchers will use immunocompetent models to investigate whether delivering exogenous replacement protein via ePC results in lower immunogenicity compared to injected protein or gene therapies that cause the secretion of exogenous proteins from other tissues, such as the liver[62] or muscle[63]. Additionally, deficiencies of sphingomyelin phosphodiesterase 1 (*SMDP1*)[64], alkaline phosphatase (*ALPL*)[65] alpha-galactosidase A (*GLA*)[66] alpha-L- iduronidase (IDUA)[67] and many other monogenic protein and enzyme deficiency diseases that require repeated injection of recombinant proteins with short half-lives may also benefit from ePC-based therapies.

In addition to monogenic diseases, there is considerable interest in using ePCs to deliver biologics to provide protection against pathogens that are hard to vaccinate against such as HIV, EBV, dengue and RSV. Several groups have published data on genome-engineering strategies that insert anti-pathogen Ab transgenes into the immunoglobulin heavy chain locus, where they can be expressed using B cell-endogenous H chain constant gene exons, which allows them to function as both BCRs and subsequently as secreted therapeutic Abs[12,14,53,55]. Anti-pathogen Ab engineered B cells showed evidence of antigen-specific immune responses (HIV[12,14,55]) and *in vivo* protection (RSF[53]). These studies used murine B cells and, to date, no one has demonstrated *in vivo* functional protection using human anti-pathogen Ab secreting B

cells. Modeling anti-pathogen Ab secreting ePCs in a humanized small animal model susceptible to human tropic disease would allow for the functional testing of disease protection and is further explored in Chapter 3. Alternatively to anti-pathogen Abs, Vamva et al. were able to show antiviral activity *in vitro* when plasma cells engineered to produce an anti-HIV-1 immunoadhesin, eCD4-Ig, were cultured with NL4-3 HIV-1-infected SupT1 CD4+ T cells[40]. An additional strategy yet to be explored is the use of ePCs to deliver antiviral peptides such as enfuvirtide[68].

Hematological and non-hematological malignancies may be another indication where engineered B cells and ePCs may provide benefit. For example, Luo et al. show that ePCs that produce the checkpoint inhibitor, pembrolizumab, could suppress human melanoma growth in xenograft-tumor mice[42]. Page et al. provide a very comprehensive review of past and current strategies for exploiting adoptive transfer of modified and unmodified B cells to treat malignancies[38]. A strategy that has yet to be explored in proof of concept studies is the engineering of B cells to express BCRs/Abs against tumor-associated antigens. For example, expression of anti-EGFR, cetuximab, from ePCs may provide long lasting inhibition of EGFR growth pathways in a variety of tumors. Alternatively, one potential use in cancer discussed in Chapter 2 is the use of ePCs to deliver anti-cancer biologics such as blinatumomab, a bispecific t cell engager targeting CD19. In Chapter 2 we will further explore the use of ePCs as a delivery platform for the delivery of anti-cancer therapeutics.

Additional potential of biologics or therapeutic peptides that may benefit by being delivered by ePC are summarized in Figure 2. In the following chapters, we will present studies that show that ePCs cells secreting anti-cancer biologics suppress patient-derived leukemia in immunodeficient mice. We will establish an autologous adoptive ePC transfer humanized mouse model for a more biologically-relevant evaluation of ePC functionality against human

pathogens. Furthermore, we developed a novel human B cell-based BCR screening system to develop highly expressed mAbs for ePC therapies.

1.4. FIGURES

1.4.1. *Generalized workflow for the generation of autologous engineered plasma cell therapeutics*

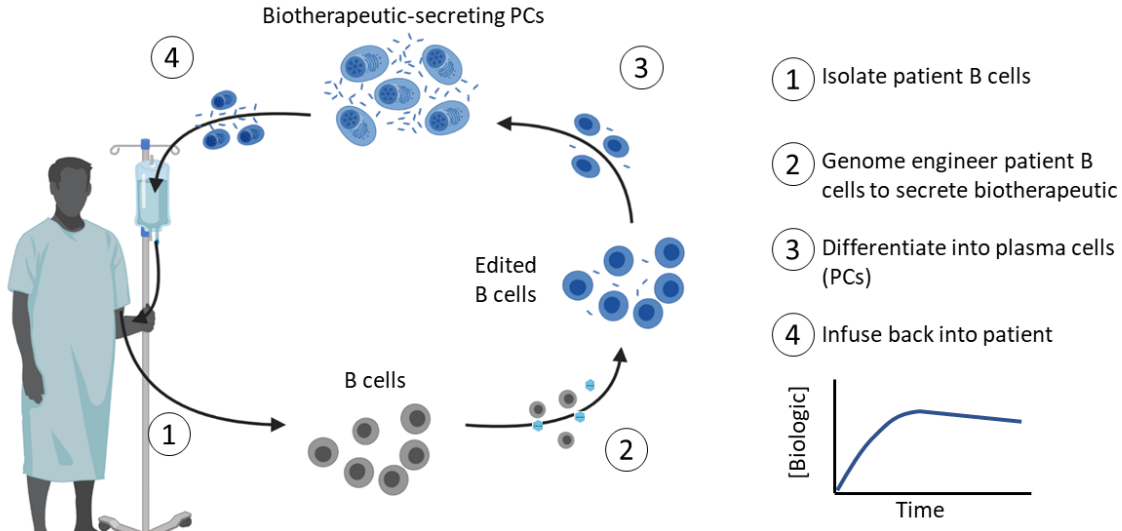

1.4.2. *Potential applications of ePC therapeutics*

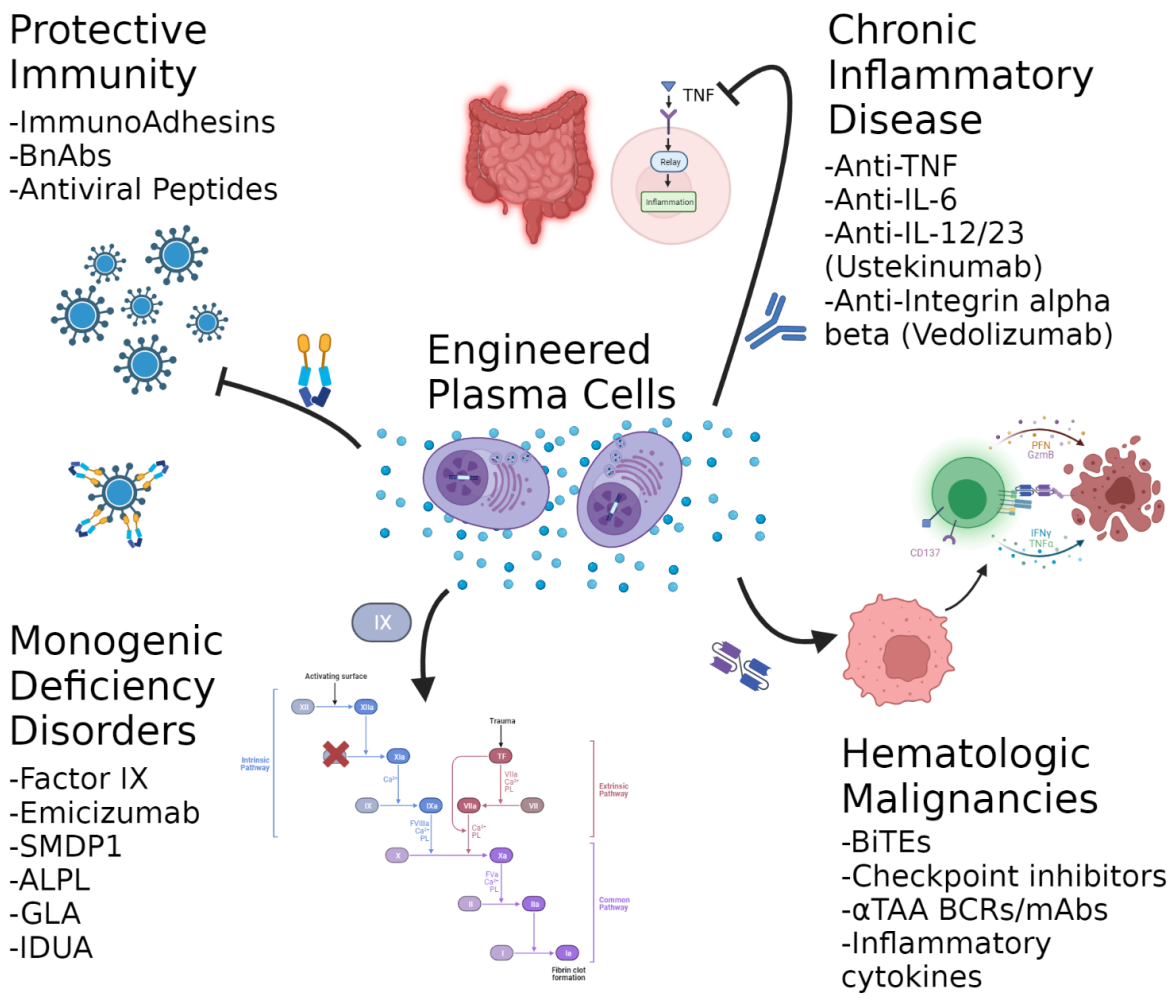

Engineered plasma cells can be engineered to produce a variety of therapeutic proteins to treat a variety of different diseases. Broadly neutralizing antibodies (BnAbs), Bispecific T cell engager (BiTE), Tumor associated antigen(TAA), Interleukin (IL).

1.5. BIBLIOGRAPHY

1. Laidlaw BJ, Cyster JG. Transcriptional regulation of memory B cell differentiation. *Nat Rev Immunol*. 2021;21(4):209-220.

2. Cyster JG, Allen CDC. B Cell Responses: Cell Interaction Dynamics and Decisions. *Cell*. 2019;177(3):524-540.

3. Nutt SL, Hodgkin PD, Tarlinton DM, Corcoran LM. The generation of antibody-secreting plasma cells. *Nat Rev Immunol*. 2015;15(3):160-171.

4. Matsumura Y, Watanabe R, Fujimoto M. Suppressive mechanisms of regulatory B cells in mice and humans. *Int Immunol*. 2023;35(2):55-65.

5. Wang X, Herzog RW, Byrne BJ, et al. Immune Modulatory Cell Therapy for Hemophilia B Based on CD20-Targeted Lentiviral Gene Transfer to Primary B Cells. *Mol Ther Methods Clin Dev*. 2017;5:76-82.

6. Wang X, Moghimi B, Zolotukhin I, Morel LM, Cao O, Herzog RW. Immune tolerance induction to factor IX through B cell gene transfer: TLR9 signaling delineates between tolerogenic and immunogenic B cells. *Mol Ther*. 2014;22(6):1139-1150.

7. Eynon EE, Parker DC. Small B cells as antigen-presenting cells in the induction of tolerance to soluble protein antigens. *J Exp Med*. 1992;175(1):131-138.

8. Gilbert KM, Weigle WO. Tolerogenicity of resting and activated B cells. *J Exp Med*. 1994;179(1):249-258.

9. Wennhold K, Weber TM, Klein-Gonzalez N, et al. CD40-activated B cells induce anti-tumor immunity in vivo. *Oncotarget*. 2017;8(17):27740-27753.

10. Ren H, Zhao S, Li W, et al. Therapeutic antitumor efficacy of B cells loaded with tumor-derived autophagasomes vaccine (DRibbles). *J Immunother*. 2014;37(8):383-393.

11. Wennhold K, Thelen M, Schlößer HA, et al. Using Antigen-Specific B Cells to Combine Antibody and T Cell-Based Cancer Immunotherapy. *Cancer Immunol Res*. 2017;5(9):730-743.

12. Nahmad AD, Raviv Y, Horovitz-Fried M, et al. Engineered B cells expressing an anti-HIV antibody enable memory retention, isotype switching and clonal expansion. *Nat Commun*. 2020;11(1):5851.

13. Nahmad AD, Lazzarotto CR, Zelikson N, et al. In vivo engineered B cells secrete high titers of broadly neutralizing anti-HIV antibodies in mice. *Nat Biotechnol*. 2022;40(8):1241-1249.

14. Huang D, Tran JT, Olson A, et al. Vaccine Elicitation of HIV Broadly Neutralizing Antibodies from Engineered B cells.

15. Biagi E, Rousseau R, Yvon E, et al. Responses to human CD40 ligand/human interleukin-2 autologous cell vaccine in patients with B-cell chronic lymphocytic leukemia.

Clin Cancer Res. 2005;11(19 Pt 1):6916-6923.

16. Winkler J, Tittlbach H, Roesler W, et al. Adoptive Transfer of Purified Donor-B-Lymphocytes after Allogeneic Stem Cell Transplantation: Results from a Phase I/IIa Clinical Trial. *Blood*. 2016;128(22):502-502.

17. Jourdan M, Caraux A, De Vos J, et al. An in vitro model of differentiation of memory B cells into plasmablasts and plasma cells including detailed phenotypic and molecular characterization. *Blood*. 2009;114(25):5173-5181.

18. Jourdan M, Cren M, Robert N, et al. IL-6 supports the generation of human long-lived plasma cells in combination with either APRIL or stromal cell-soluble factors. *Leukemia*. 2014;28(8):1647-1656.

19. Cheng RYH, Hung KL, Zhang T, et al. Ex vivo engineered human plasma cells exhibit robust protein secretion and long-term engraftment in vivo. *Nat Commun*. 2022;13(1):6110.

20. Delaloy C, Schuh W, Jäck HM, Bonaud A, Espéli M. Single-cell resolution of plasma cell fate programming in health and disease. *Eur J Immunol*. 2022;52(1):10-23.

21. Blanc P, Moro-Sibilot L, Barthly L, et al. Mature IgM-expressing plasma cells sense antigen and develop competence for cytokine production upon antigenic challenge. *Nat Commun*. 2016;7:13600.

22. Pinto D, Montani E, Bolli M, et al. A functional BCR in human IgA and IgM plasma cells. *Blood*. 2013;121(20):4110-4114.

23. Hammarlund E, Thomas A, Amanna IJ, et al. Plasma cell survival in the absence of B cell memory. *Nat Commun*. 2017;8(1):1781.

24. Eyer K, Doineau RCL, Castrillon CE, et al. Single-cell deep phenotyping of IgG-secreting cells for high-resolution immune monitoring. *Nat Biotechnol*. 2017;35(10):977-982.

25. Radbruch A, Muehlinghaus G, Luger EO, et al. Competence and competition: the challenge of becoming a long-lived plasma cell. *Nat Rev Immunol*. 2006;6(10):741-750.

26. Hibi T, Dosch HM. Limiting dilution analysis of the B cell compartment in human bone marrow. *Eur J Immunol*. 1986;16(2):139-145.

27. Roth K, Oehme L, Zehentmeier S, Zhang Y, Niesner R, Hauser AE. Tracking plasma cell differentiation and survival. *Cytometry A*. 2014;85(1):15-24.

28. Benet Z, Jing Z, Fooksman DR. Plasma cell dynamics in the bone marrow niche. *Cell Rep*. 2021;34(6):108733.

29. Wellford SA, Moseman AP, Dao K, et al. Mucosal plasma cells are required to protect the upper airway and brain from infection. *Immunity*. 2022;55(11):2118-2134.e6.

30. Coughlin CM, Vonderheide RH. Targeting adult and pediatric cancers via cell-based vaccines and the prospect of activated B lymphocytes as a novel modality. *Cancer*

Biol Ther. 2003;2(5):466-470.

31. Park MY, Kim HS, Woo SJ, et al. Efficient antitumor immunity in a murine colorectal cancer model induced by CEA RNA-electroporated B cells. *Eur J Immunol*. 2008;38(8):2106-2117.

32. Gerloni M, Rizzi M, Castiglioni P, Zanetti M. T cell immunity using transgenic B lymphocytes. *Proc Natl Acad Sci U S A*. 2004;101(11):3892-3897.

33. Colluru VT, McNeel DG. B lymphocytes as direct antigen-presenting cells for anti-tumor DNA vaccines. *Oncotarget*. 2016;7(42):67901-67918.

34. Jeon I, Lee JM, Shin KS, et al. Enhanced Immunogenicity of Engineered HER2 Antigens Potentiates Antitumor Immune Responses. *Vaccines (Basel)*. 2020;8(3). doi:10.3390/vaccines8030403

35. Kim YS, Kim YJ, Lee JM, et al. CD40-targeted recombinant adenovirus significantly enhances the efficacy of antitumor vaccines based on dendritic cells and B cells. *Hum Gene Ther*. 2010;21(12):1697-1706.

36. Kim EK, Seo HS, Chae MJ, et al. Enhanced antitumor immunotherapeutic effect of B-cell-based vaccine transduced with modified adenoviral vector containing type 35 fiber structures. *Gene Ther*. 2014;21(1):106-114.

37. White RE, Wade-Martins R, James MR. Infectious delivery of 120-kilobase genomic DNA by an epstein-barr virus amplicon vector. *Mol Ther*. 2002;5(4):427-435.

38. Page A, Hubert J, Fusil F, Cosset FL. Exploiting B Cell Transfer for Cancer Therapy: Engineered B Cells to Eradicate Tumors. *Int J Mol Sci*. 2021;22(18). doi:10.3390/ijms22189991

39. Sandrin V, Boson B, Salmon P, et al. Lentiviral vectors pseudotyped with a modified RD114 envelope glycoprotein show increased stability in sera and augmented transduction of primary lymphocytes and CD34+ cells derived from human and nonhuman primates. *Blood*. 2002;100(3):823-832.

40. Vamva E, Ozog S, Verhoeyen E, James RG, Rawlings DJ, Torbett BE. An optimized measles virus glycoprotein-pseudotyped lentiviral vector production system to promote efficient transduction of human primary B cells. *STAR Protoc*. 2022;3(1):101228.

41. Girard-Gagnepain A, Amirache F, Costa C, et al. Baboon envelope pseudotyped LVs outperform VSV-G-LVs for gene transfer into early-cytokine-stimulated and resting HSCs. *Blood*. 2014;124(8):1221-1231.

42. Luo B, Zhan Y, Luo M, et al. Engineering of α-PD-1 antibody-expressing long-lived plasma cells by CRISPR/Cas9-mediated targeted gene integration. *Cell Death Dis*. 2020;11(11):973.

43. Fusil F, Calattini S, Amirache F, et al. A Lentiviral Vector Allowing Physiologically Regulated Membrane-anchored and Secreted Antibody Expression Depending on B-cell Maturation Status. *Mol Ther*. 2015;23(11):1734-1747.

44. Page A, Fusil F, Cosset FL. Towards Physiologically and Tightly Regulated Vectored Antibody Therapies. *Cancers* . 2020;12(4).

45. Herbig EJ, Hyland K, Xu M, et al. 373. Expression of Human Iduronidase from Sleeping Beauty Engineered Human B Lymphocytes as a Cellular Therapy for Mucopolysaccharidosis Type I. *Mol Ther*. 2015;23:S148.

46. Jones RJ, DeBaun MR. Leukemia after gene therapy for sickle cell disease: insertional mutagenesis, busulfan, both, or neither. *Blood*. 2021;138(11):942-947.

47. Santeramo I, Bagnati M, Harvey EJ, et al. Vector Copy Distribution at a Single-Cell Level Enhances Analytical Characterization of Gene-Modified Cell Therapies. *Mol Ther Methods Clin Dev*. 2020;17:944-956.

48. Rintz E, Higuchi T, Kobayashi H, Galileo DS, Wegrzyn G, Tomatsu S. Promoter considerations in the design of lentiviral vectors for use in treating lysosomal storage diseases. *Mol Ther Methods Clin Dev*. 2022;24:71-87.

49. Cheong TC, Compagno M, Chiarle R. Editing of mouse and human immunoglobulin genes by CRISPR-Cas9 system. *Nat Commun*. 2016;7:10934.

50. Hung KL, Meitlis I, Hale M, et al. Engineering Protein-Secreting Plasma Cells by Homology-Directed Repair in Primary Human B Cells. *Mol Ther*. 2018;26(2):456-467.

52. Levy C, Fusil F, Amirache F, et al. Baboon envelope pseudotyped lentiviral vectors efficiently transduce human B cells and allow active factor IX B cell secretion in vivo in NOD/SCIDγc-/- mice. *J Thromb Haemost*. 2016;14(12):2478-2492.

53. Moffett HF, Harms CK, Fitzpatrick KS, Tooley MR, Boonyaratanakornkit J, Taylor JJ. B cells engineered to express pathogen-specific antibodies protect against infection. *Sci Immunol*. 2019;4(35). doi:10.1126/sciimmunol.aax0644

54. Voss JE, Gonzalez-Martin A, Andrabi R, et al. Reprogramming the antigen specificity of B cells using genome-editing technologies. *eLife*. 2019;8.

55. Hartweger H, McGuire AT, Horning M, et al. HIV-specific humoral immune responses by CRISPR/Cas9-edited B cells. *J Exp Med*. 2019;216(6):1301-1310.

56. Jeske AM, Boucher P, Curiel DT, Voss JE. Vector Strategies to Actualize B Cell-Based Gene Therapies. *J Immunol*. 2021;207(3):755-764.

57. Rogers GL, Cannon PM. Genome edited B cells: a new frontier in immune cell therapies. *Mol Ther*. 2021;29(11):3192-3204.

58. Allocca M, Doria M, Petrillo M, et al. Serotype-dependent packaging of large genes in adeno-associated viral vectors results in effective gene delivery in mice. *J Clin Invest*. 2008;118(5):1955-1964.

59. Pratt KP. Anti-Drug Antibodies: Emerging Approaches to Predict, Reduce or Reverse Biotherapeutic Immunogenicity. *Antibodies (Basel)*. 2018;7(2). doi:10.3390/antib7020019

60. Van Meerhaeghe T, Néel A, Brouard S, Degauque N. Regulation of CD8 T cell by B-cells: A narrative review. *Front Immunol*. 2023;14:1125605.

61. Bennett SR, Carbone FR, Toy T, Miller JF, Heath WR. B cells directly tolerize CD8(+) T cells. *J Exp Med*. 1998;188(11):1977-1983.

62. Rodríguez-Merchán EC, De Pablo-Moreno JA, Liras A. Gene Therapy in Hemophilia: Recent Advances. *Int J Mol Sci*. 2021;22(14). doi:10.3390/ijms22147647

63. Katneni UK, Alexaki A, Hunt RC, et al. Structural, functional, and immunogenicity implications of F9 gene recoding. *Blood Adv*. 2022;6(13):3932-3944.

64. Wasserstein MP, Schuchman EH. *Acid Sphingomyelinase Deficiency*. University of Washington, Seattle; 2023.

65. García-Fontana C, Villa-Suárez JM, Andújar-Vera F, et al. Epidemiological, Clinical and Genetic Study of Hypophosphatasia in A Spanish Population: Identification of Two Novel Mutations in The Alpl Gene. *Sci Rep*. 2019;9(1):9569.

66. Clarke JTR, West ML, Bultas J, Schiffmann R. The pharmacology of multiple regimens of agalsidase alfa enzyme replacement therapy for Fabry disease. *Genet Med*. 2007;9(8):504-509.

67. Jameson E, Jones S, Remmington T. Enzyme replacement therapy with laronidase (Aldurazyme®) for treating mucopolysaccharidosis type I. *Cochrane Database Syst Rev*. 2019;6(6):CD009354.

68. Matthews T, Salgo M, Greenberg M, Chung J, DeMasi R, Bolognesi D. Enfuvirtide: the first therapy to inhibit the entry of HIV-1 into host CD4 lymphocytes. *Nat Rev Drug Discov*. 2004;3(3):215-225.

Chapter 2.

HUMAN PLASMA CELLS ENGINEERED TO SECRETE BISPECIFICS DRIVE EFFECTIVE *IN VIVO* LEUKEMIA KILLING

A manuscript based on this chapter is under review at the journal Blood
Manuscript # BLD-2023-020747R1)

2.1. ABSTRACT

Bispecific antibodies are an important tool for the management and treatment of acute leukemias. Advances in genome-engineering have enabled the generation of human plasma cells that secrete therapeutic proteins and are capable of long-term *in vivo* engraftment in humanized mouse models. As a next step towards clinical translation of engineered plasma cells (ePCs) towards cancer therapy, here we describe approaches for the expression and secretion of bispecific antibodies by human plasma cells. We show that human ePCs expressing either fragment crystallizable domain deficient anti-CD19 x anti-CD3 (blinatumomab) or anti-CD33 x anti-CD3 bispecific antibodies mediate T cell activation and direct T cell killing of specific primary human cell subsets and B-acute lymphoblastic leukemia or acute myeloid leukemia cell lines *in vitro*. We demonstrate that knockout of the self-expressed antigen, CD19, boosts anti-CD19 bispecific secretion by ePCs and prevents self-targeting. Further, anti-CD19 bispecific-ePCs elicited tumor eradication *in vivo* following local delivery in flank-implanted Raji lymphoma cells. Finally, immunodeficient mice engrafted with anti-CD19 bispecific-ePCs and autologous T cells potently prevented *in vivo* growth of $CD19^+$ acute lymphoblastic leukemia in patient-derived xenografts. Collectively, these findings support further development of ePCs for use as a durable, local delivery system for the treatment of acute leukemias, and potentially other cancers.

2.2. INTRODUCTION

Immunotherapies that recruit cytotoxic T cells to kill cancer cells, such as bispecific antibodies, have played a significant role in the improved survival rates for patients with B-cell acute lymphoblastic leukemia (B-ALL)[1–4]. Blinatumomab is an anti-CD19 x anti-CD3 non-immunoglobulin G -like bispecific antibody (non-IgG-like bispecific; also called a bispecific T cell engager, BiTE™) that received FDA approval in 2014 for the treatment of patients with relapsed/refractory B-ALL [4,5]. Blinatumomab is now used in multiple B-ALL settings, including frontline therapy, as a bridge to transplantation, consolidation therapy, and as a low toxicity alternative to chemotherapy regimens[6]. A limitation of Blinotumamab[7] and other non-IgG-like bispecifics[8,9] is that these molecules lack fragment crystallizable domains and have short half-lives, which necessitate continuous high dose intravenous infusions. However, this intensive regimen can be challenging for patients, especially those with limited hospital access[10,11]. A range of methods have been utilized in an attempt to extend biologic half-life of non-IgG-like bispecifics[12], including conjugation with small molecules, fragment crystallizable domains, or albumin binding motifs. However, it remains unclear whether these fusion molecules will be effective, lack immunogenicity, and/or overcome the need for multiple continuous high-dose infusions.

We, and others, have explored using engineered plasma cells (ePCs) as a long-term biologic drug delivery platform[13–16]. Engineered B cell populations have been investigated in proof-of-concept studies to deliver biologic drugs to treat protein deficiency diseases[13,17], viral infections[18–22], and cancer[15,23]. Based on these observations, we predicted that adoptive transfer of bispecific expressing ePC might mitigate challenges related to both bispecific half-life and high dose systemic toxicity. Plasma cells are uniquely suited to deliver biologics over long periods due to their long lifespan[24] (half-life is estimated to be 11 to 200 years[25]), and high

secretory capacity (up to 10,000 IgG molecules per second[26–28]*),* Furthermore, *ex-vivo* generated ePCs resemble endogenous plasma cells, and can stably secrete therapeutically relevant levels of immunoglobulin for greater than one year in hIL6-humanized mice[14]. Because PCs[29,30] and ePCs[14] preferentially localize to bone marrow and other tissue microenvironments where progenitor B-ALL cells reside[31], we predicted that ePCs could harmonize with local bispecific delivery to induce potent anti-leukemia activity.

In this study, we describe a homology-directed repair strategy (HDR) based gene editing strategy for the generation of ePC that produce large quantities of anti-CD19 x anti-CD3 or anti-CD33 x anti-CD3 non-IgG-like bispecifics to target B-ALL or acute myeloid leukemia (AML), respectively. Our combined findings demonstrate that ePCs secreting bispecifics can promote T-cell driven killing of primary human cells, human leukemic cell lines *in vitro,* and patient-derived B-ALL xenografts *in vivo*. Based upon our preclinical results, we propose that ePC strategies could be translated to the clinic for evaluation of bispecific delivery to patients with acute leukemias, and other scenarios where half-life is limiting or local delivery could reduce on-target adverse effects.

2.3. MATERIALS AND METHODS

2.3.1. *B cell culturing and PC differentiation*

We isolated B cells from healthy human donors' PBMCs (Fred Hutchinson Cancer Research Center) using the EasySep Human B cell enrichment kit (Stem Cell Technologies). We obtained >95% purity for B cells defined by CD3 negativity and CD19 positivity. Isolated B cells were cultured in Iscove's modified Dulbecco's medium (Gibco), supplemented with 2-mercaptoethanol (55μM) and 10% FBS. For Figure 1, cells were cultured for seven days as described in Hung et al[13]. For experiments in Figure 2-6 cells were cultured as described in

Cheng et al[32]. Cell concentrations were kept between 5-15x10^5 live cells per ml. Cells for *in vivo* experiments were purified via CD3 bead depletion column (Miltenyi) prior to injection.

2.3.2. *AAV6 HDR CRISPR Cas9 Engineering of B cells*

Clustered regularly interspaced short palindromic repeats (CRISPR) RNAs (crRNAs) targeting the CCR5, JCHAIN, IgG1, Eμ[18], and CD19 (sequences in Table S1) were identified using the Broad Institute GPP sgRNA Designer (http://portals.broadinstitute.org/gpp/public/analysis-tools/sgrna-design) and synthesized (IDT) containing phosphorothioate linkages and 2′O-methyl modifications. crRNA and trans-activating crRNA (tracrRNA; IDT) single guide hybrids were mixed with 3uM Cas9 nuclease (Berkeley Labs) at a 1.2:1 ratio and delivered to cells by Lonza 3D (CA-137) or Maxcyte GTX (B cell 3) electroporation. After electroporation, cells were transferred into the activation medium (1.5x10^6cells/mL) in the presence of adeno-associated virus 6 (AAV6) vectors carrying homologous DNA repair templates (20% AAV by volume or viral copy of 1x10^4 per cell, Figure 1E schema). The medium was changed 24 hours following AAV6 administration. AAV6 vectors were produced as previously described[13] or manufactured by Sirion Biotech. Synthetic construct sequences can be found in GenBank (OQ743465-OQ743468).

2.3.3. *In vitro ePC-mediated killing assays (K562, PBMC, leukemia cell line, and self-killing assays)*

For the K562 killing assay, K562 cells were obtained from ATCC and lentivirally transduced to express either CD19 linked in cis to green fluorescent protein (GFP) (referred to as target cells) via self-cleaving P2A or BCMA linked in *cis* to BFP (referred to as control cells) and purified by flow cytometry assisted sorting. 5x10^3 target cells, 5x10^3 control cells and 5x10^4 $CD8^+$ T cells were incubated with either various dilutions of supernatants from genome-

engineered cells or media containing various concentrations of recombinant anti-CD19 x anti-CD3 bispecific (Invivogen, bimab-hcd19cd3) for 48 hours (Figure 1F-H& 3G-I). For the peripheral blood mononuclear cell (PBMC) killing assay, $2x10^5$ PBMCs and $4x10^4$ autologous $CD8^+$ T cells were incubated with either supernatants from engineered PCs or media containing recombinant anti-CD19 x anti-CD3 bispecific (Invivogen, bimab-hcd19cd3) or anti-CD33 x anti-CD3 bispecific (AMG 330) for 48 hours (Figure 2H-K). For leukemia cell line killing assay $5x10^3$ NALM-6 cells, 5e3 MOLM-14 cells and $5x10^4$ $CD8^+$ were incubated with either supernatants from engineered PCs or media containing recombinant bispecifics (Figure 2D-F). For the self-killing assay, $2x10^5$ genome-engineered B cells were incubated with autologous T cells at various effector to target ratios and cultured for 24 hours (Figure 3BE-F). Each assay was performed in 200uL in duplicate in 96 wells with RPMI-1640 supplemented with 10% FBS as the base media at 37°C and 5% CO_2. At the end of each assay, cells from duplicate wells were pooled, washed with PBS, stained according to Table S2, and analyzed by flow cytometry.

2.3.4. *In vivo assessment of ePCs against human B-cell malignancies*

All animal studies were performed according to AAALAC standards and were approved by the Seattle Children's Research Institute (SCRI) Institutional Animal Care and Use Committee. NOD.Cg-*Prkdc*^{scid} *Il2rg*^{tm1Wjl}/SzJ-c (NSG) mice were purchased from Jackson Laboratory and all mice were kept in a designated pathogen-free facility at SCRI. For the subcutaneous lymphoma flank model (Figure 4A-C), $2.5x10^5$ ePCs, $5x10^4$ autologous T cells, and $2.5x10^4$ luciferase transduced Raji cells (human Burkitt lymphoma cell line) were delivered subcutaneously to the right flank. For the disseminated leukemia experiments (Figure 5 and Figure 6), $2.5x10^6$-$15x10^6$ GFP or bispecific-ePCs were injected intravenously into NSG. The following day (Figure 5) or the two days prior (Figure 6) mice received $1x10^5$ luciferase expressing B-ALL cells intravenously (model NL482B [Children's Oncology Group unique specimen identifier PALJDL]). For Figure 5, the following day and three days later mice received

$1x10^5$ or $1x10^6$ T cells administered retro-orbitally. For Figure 6, $2.5x10^6$ T cells were injected retro-orbitally the day following ePC engraftment, Tumor burden was monitored by bioluminescence imaging using IVIS Lumina S5 (Perkin Elmer) following subcutaneous injection of luciferin (75-150 mg/kg). Peripheral blood was collected via submandibular bleed and processed to collect sera and quantify human T cell numbers. Mice were euthanized for harvesting of bone marrow and spleens that were processed via erythrocyte lysis (ACK lysis) and then immunophenotyped by flow cytometry to quantify human leukemia cell and plasma cell numbers (Table S2).

2.4. RESULTS

2.4.1. *Primary human B cells engineered by HDR-based gene editing secrete functional bispecifics*

To integrate a bispecific gene expression cassette into B cells, we adapted AAV-based HDR that we have used for delivery of transgenes in B cells at the safe harbor gene *CCR5*[13]. We designed *CCR5*-targeted HDR templates for delivery of Blue Fluorescent Protein (BFP) alone (as control) or an anti-CD19 x anti-CD3 bispecific cis-linked with GFP (heretofore referred to as a αCD19). We initiated gene editing by transfecting the activated human peripheral B cells with Cas9 ribonucleoprotein complexes (RNPs) containing guide RNAs targeting sequence within *CCR5*, and subsequently transduced with rAAV6 HDR donor vector (Figure 1A & S1A). We found that HDR integration rates were slightly lower with the vectors containing the αCD19 bispecifics when evaluated by digital droplet PCR (ddPCR; Figure S1B Figure 1B). However, despite similar integration rates the proportion of cells expressing the fluorescent reporter was substantially diminished in cells edited using the bispecific design, resulting in a significant drop in the ratio of fluorescent reporter marking to integration rate (Figure 1C-D).

We hypothesized that αCD19 bispecific expression could be increased by targeting transgene integration to loci that are natively expressed in B cells or plasma cells. Therefore, we built three additional AAV-based repair template designs for delivery of transgene cassettes to the highly expressed B cell loci *IGHG1*, *JCHAIN,* and a region proximal to an heavy chain enhancer, Eμ[18] (repair arms and sgRNA were previously described in [18]; overall schematic for all vectors, Figure 1E). Although the same ubiquitous viral-derived promoter (MND[33]) was used at all loci, we observed variable increases in GFP^+ percentage and GFP mean fluorescent intensity in B cells following delivery to the antibody-associated loci, relative to that at *CCR5* (Figure S1C-D). While integration was detected at all loci, we observed significant increases in the mean fluorescent intensity of the cis-linked GFP at the antibody loci relative to *CCR5* (Figure 1F-G).

To initially assess the functionality of the B cell-produced αCD19 bispecific, we developed a fluorescent reporter-based *in vitro* killing assay using a K562 cell line that stably expresses CD19, a reference K562 cell line, CD8+ T cells incubated with either recombinant αCD19 bispecific or with supernatants from engineered cells (Figure H). After 48 hours, flow cytometry was used to quantify T cell activation (percent $CD69^+CD137^+$) and specific lysis of $CD19^+$ target cells (Figure S2A). Recombinant αCD19 bispecific elicited dose and time-dependent increases in T cell activation and CD19-specific lysis (Figure S2B-C). Supernatants from B cells engineered to express the αCD19 bispecific induced T cell activation and specific lysis, whereas supernatants from GFP-engineered B cells did not (Figure 1I-J). We generated standard curves using recombinant bispecific T cell activation data to quantify the αCD19 bispecific concentrations in the supernatants derived from engineered B cells (Figure 1K). These findings indicate that primary human B cells can be engineered at various loci to express and secrete a functional αCD19 bispecific.

2.4.2. *Bispecific-ePCs exhibit in vitro activity against common leukemia target antigens*

We next asked whether *ex vivo*-differentiated human ePCs could produce bispecifics that specifically target primary human hematopoietic cells expressing physiological levels of candidate leukemia antigens (including CD19 or CD33) within a heterogeneous cell population. We built an Eμ locus-directed bispecific vector for delivery of an anti-CD33 x anti-CD3 bispecific (heretofore referred to as a αCD33 bispecific; Figure 2A)[8]. We introduced each Eμ locus-directed bispecific or GFP alone control into B cells using HDR-based editing and differentiated the edited population into ePCs as previously described (Figure S1A).[13,32] Following editing and differentiation, we observed detectable transgene expression with all vectors and donors (Figure 2B-C). Although we observed donor-dependent differences in relative expression of the plasma cell differentiation markers CD38 and CD138, introduction of the bispecifics did not impact differentiation into plasma cells (defined as $CD38^{++}$ $CD138^{+}$; Figure S3A-C), demonstrating that human plasma cells can be engineered to express bispecifics.

To investigate the functionality of bispecifics secreted by the ePCs to target physiological levels of antigen, we evaluated αCD19 and αCD33 ePC supernatants using two assays of heterologous cell populations. First, we applied recombinant bispecific to a PBMC killing assay wherein effector $CD8^{+}$ T cells were co-cultured with autologous PBMCs that contained B cell and myeloid cell subpopulations expressing endogenous levels of CD19 and CD33 respectively (Figure 2D). As expected, recombinant αCD19 bispecific elicited a dose-dependent decrease in IgM^{+} B cells (Figure S4B), whereas recombinant αCD33 bispecific elicited a dose-dependent decrease in $CD14^{+}$ $CD33^{+}$ monocytes (Figure S4B). Supernatants from both αCD19- and αCD33-ePCs elicited higher T cell activation relative to that from control GFP-ePCs (Figure 2E). Furthermore, supernatants from αCD19-ePCs specifically lysed IgM^{+} B cells (Figure 2F), while supernatants from αCD33-ePCs specifically lysed $CD33^{+}$ $CD14^{+}$ monocytes (Figure 2G). Secondly, we evaluated ePC supernatants in a leukemia cell line killing

assay wherein a $CD19^+$ precursor B-ALL cell line (NALM-6), a $CD33^+$ AML cell line (MOLM-14) and $CD8^+$ effector T cells were co-cultured for 48 hours (Figure 2D). Increasing concentrations of recombinant αCD19 bispecific led to increased lysis of NALM-6 cells whereas increasing concentrations of recombinant αCD33 bispecific led to increased lysis of MOLM-14 cells (Figure S5A-B). T cells showed upregulation of activation markers $CD69^+$ and $CD137^+$ when cultured with supernatants from ePCs producing either bispecific relative to supernatants from control GFP-ePCs (Figure 2H). Supernatants from αCD19- ePCs specifically lysed NALM-6 cells (Figure 2I), whereas supernatants from αCD33- ePCs cells specifically lysed MOLM-14 cells (Figure 2J). Together, these data show that ePCs secreting αCD19 or αCD33 bispecifics elicit specific T cell killing of PBMC subsets or leukemia cell lines expressing physiological levels of CD19 or CD33 respectively.

2.4.3. *CD19KO ePCs are protected from self-targeting and exhibit increased αCD19 bispecific secretion*

CAR T cells engineered to recognize T-cell antigens can kill other CAR T cells within the same cell product, resulting in diminished anticancer activity[34,35]. We hypothesized that upon T cell encounter, αCD19-ePCs could similarly elicit self-targeting (ie fratricide) due to their surface CD19 expression (Figure S6). To evaluate the degree of self-targeting, we incubated Eμ locus-directed GFP-ePCs or αCD19-ePCs with autologous T cells (Figure 3A). Addition of autologous T cells lead to a progressive decline in the proportion of αCD19-ePCs but not GFP-ePCs (Figure 3B; gating Figure S7), implying that CD19 self-targeting likely impacts αCD19-secreting ePCs. Based on these observations, we predicted that elimination of CD19 would prevent αCD19 bispecific-elicited self-targeting.

To knockout CD19, we co-delivered RNPs targeting CD19 with the Eμ locus-directed αCD19 bispecific editing reagents. The addition of the CD19-targeting RNPs resulted in >85% reduction in the proportion of CD19+ PCs (Figure 3C-D). CD19 knockout did not overtly impact

differentiation of edited B cells into plasmablasts or PCs in vitro (Figure S8C). Upon challenging these CD19 knockout αCD19-ePCs with T cells, we observed no differences in GFP percentage with increased starting T cell numbers (Figure 3E). When comparing CD19KO to CD19wt, only CD19wt αCD19-ePCs exhibited a significant decrease in edited cells at the highest T cell dose (Figure 3F). These data suggest that CD19 knockout protects αCD19-ePCs from self-targeted death.

An additional challenge with CD19 surface expression is that the αCD19 bispecific produced from ePCs may bind to surface CD19 and limit the quantity that is released by the cells. Therefore, we predicted that knocking out CD19 would increase the level of αCD19 bispecific in supernatants. To assess free bispecific in the context of knocking out CD19, supernatants from αCD19 ePCs (co-engineered with or without CD19 RNPs) were assessed using the K562 killing assay (Figure 1E). Supernatants from CD19KO αCD19-ePCs resulted in higher T cell activation, and higher αCD19 bispecific concentrations and a trend towards higher specific lysis when compared to CD19wt αCD19-ePCs (Figure 3G-I). Collectively these findings indicate that knocking out CD19 prevents self-targeting by T cells and boosts αCD19 bispecific levels.

Similar strategies could be employed for ePCs expressing biologics targeting additional B cell surface proteins. We individually knocked out the B cell surface markers CD19, MS4A1 (CD20), CD38 and TNFRSF17 (BCMA) to assess our ability to generate ePCs lacking these markers. Knock outs were confirmed by Inference of CRISPR Editing and by staining for surface expression (Supplemental 9A,C-D). None of the knockouts impacted cell expansion, viability, differentiation, or antibody secretion (Supplemental 9B-E). These data suggest that ePCs can be made that lack B cell associated antigens currently targeted in the clinic.

2.4.4. *αCD19 bispecific ePCs exhibit anti-tumor activity in vivo*

To begin to test whether bispecific-secreting ePCs maintained function *in vivo*, we used a subcutaneous flank model of B cell lymphoma wherein luciferase-expressing lymphoma target cells, autologous T cells and ePCs were co-delivered to the flanks of immune deficient mice (Figure 4A). The lymphoma cells engrafted similarly in all groups (day 1 time point, Figure 4C-D). However, at later time points, tumor burden decreased in mice that received αCD19-ePCs relative to mice that received control GFP-ePCs (Figure 4B-D). In the αCD19-ePCs group, reductions in tumor size were below background luminescence levels in >50% of the mice within 5 days (Figure 4B-D). These findings demonstrate that αCD19-ePCs can promote robust local anti-tumor responses *in vivo*.

In some clinical settings, non-IgG-like αCD19 bispecifics are used to treat high-risk B-ALL patients as a bridge to hematopoietic stem cell transplantation.[36–41] To potentially mimic this clinical scenario, we utilized a patient-derived, Philadelphia chromosome (PH)-like B-ALL xenograft model wherein $CD19^{KO}$ GFP or αCD19-ePCs were adoptively transferred into immunodeficient mice and subsequently followed 1 day later with intravenous transfer of luciferase expressing PH-like B-ALL cells (NL482B; *IL7R* gain–of-function, *SH2B3* deletion).[42,43] Effector T cells syngeneic with the ePCs were transferred retro-orbitally at 1 and 3 days after the B-ALL engraftment (Figure 5A). Control mice that received leukemia cells showed a steady increase in luciferase activity over time(Figure 5B-C). In contrast to control animals, mice that received αCD19-ePCs showed near complete leukemia control (Figure 5B-D). Consistent with these findings, the frequency of human T cells in the peripheral blood of the αCD19-ePC treated group trended higher, which is consistent with bispecific-driven T cell expansion *in vivo* (Figure 5E). Most importantly, the proportion of $CD19^{+}$ leukemia cells was markedly reduced in both the spleen and bone marrow in the αCD19-ePC treated cohort upon sacrifice at 34 days post-

leukemia cell transfer (Figure 5F). These findings demonstrate that bispecific-ePCs can limit in vivo growth and dissemination of a patient-derived leukemia in a B-ALL xenograft model.

Next, we tested the therapeutic potential of ePCs to treat established leukemia. Briefly, immunodeficient mice were intravenously engrafted with luciferase expressing PH-like B-ALL. After tumors were detectable by luciferase, $CD19^{KO}$ GFP or αCD19-ePCs, and syngeneic T cells were adoptively transferred (Figure 6A). In contrast to control animals which exhibited increases in luciferase, mice that received αCD19-ePCs exhibited leukemia control (Figure 6B-D), exemplified by a slight decrease in luminescence between day 3 and day 8 post tumor engraftment (Figure 6C). Almost no leukemic cells were detectable in the bone marrow of the αCD19-ePC treated mice (Figure 6H). Upon quantifying bispecific levels in sera, we found that mice that received αCD19-ePCs had detectable signals in the T cell activation assay (Figure 6E). Furthermore, the concentration of bispecific in the sera of αCD19-ePCs remained stable between days 12 and 20 (Figure 6F). Consistent with a stable source of bispecific, αCD19-ePCs plasma cells that expressed the cis-linked GFP reporter could be detected in the bone marrow of mice 18 days after receiving αCD19-ePCs, but not in control mice that did not receive ePCs (Figure 6H-I). Together these findings suggest that αCD19-ePCs stably engraft in the bone marrow where they secrete αCD19 bispecific at detectable levels that are sufficient to mediate and maintain leukemia clearance *in vivo.*

2.5. DISCUSSION

Engineered plasma cells comprise an emerging cell-based modality for high-level, sustained delivery of therapeutic proteins; herein, we report the novel use of ePCs to produce bispecific therapeutics. Using HDR-based editing, expression of two alternative clinical bispecifics, αCD19 and αCD33, was achieved across a range of candidate loci actively expressed in primary human B cells and PCs (Figure 1). B cells engineered to express

bispecifics could be differentiated into PCs that mediated specific killing of primary human cells and leukemia cell lines expressing CD19 or CD33, respectively (Figure 2). Further, knockout of the target antigen, CD19, led to a significant increase in functional αCD19 bispecific concentrations and prevented ePC self-targeting (Figure3). Finally, we show that αCD19 ePCs were capable of directing a T cell dependent anti-leukemia response against a locally engrafted cell line and, most notably, controlling the expansion of patient-derived leukemia xenograft, partially mimicking bispecific treatment in patients with high-risk B-ALL (Figure 4-6).

Persistent on-target off-tumor toxicity to normal bystander B cells is common in patients that respond to CD19-targeted chimeric antigen receptor (CAR) T cell therapy.[44–46] Similarly, ePC therapies targeting lymphoid malignancies have the potential to cause B cell aplasia, hypogammaglobulinemia and long-term dysfunction of the immune system. These treatment related sequelae may last beyond the desired treatment window given that the ePCs persisted for at leasts 18 days and that the phenotype of bispecific ePCs-engineered cells described in this study ($CD38^{++}$ $CD138^{+}$) resembles the phenotype of long-lived PCs isolated from human bone marrow[47]. ePCs engineered using similar methods can persist in humanized mice >1 year[14]. Antibiotics, intravenous immunoglobulin replacement therapy as well as vaccinations effectively manage hypogammaglobulinemia and recurrent infections seen in CD19-CAR treated patients[48,49], and may be effective for patients treated with αCD19 ePCs. To further mitigate on-target/off-tumor toxicity, ePCs could be engineered with a kill switch such as the clinically validated inducible caspase[50–52] suicide gene system.

A potential barrier for use of ePCs for treatment of leukemia, and possibly other lymphoid malignancies, is that ePCs[14,15,18] retain expression of surface markers targeted by many biologics (*eg.* CD19, CD20, CD38, and BCMA), which could result in self-targeting of the ePC. Consistent with this concept, we demonstrate that αCD19-ePCs express endogenous surface CD19 and are self-targeted in the presence of T cells. This phenomenon parallels

similar findings in chimeric antigen receptor T cells engineered to target T cell-associated antigens (ie fratricide)[53–55]. As CD19 is not critical for PC function[44,56], and is downregulated in long-lived PCs[47,56,57], our engineering strategy for dual CD19 knockout and expression of αCD19 at Eμ locus is unlikely to impact the ePC function or longevity. An alternative strategy to also achieve this goal would be to engineer only at the *CD19* locus. Our data suggest that ePCs could be engineered to utilize a range of candidate bispecifics or monoclonal antibody-based therapeutics targeting B cell expressed tumor targets. Like *CD19*, knockout or depletion of the lymphoma and myeloma targets *MS4A1* (also known as CD20)[58–61], and *CD38*[62,63] in plasma cells does not acutely impact durable antibody titers, a corollary of their longevity and secretory capacity. Knockouts of *MS4A1* and *CD38* did not impair our ability to generate ePCs. Thus, our findings imply that similar strategies could be used to generate ePCs expressing biologics in use for chronic lymphocytic lymphoma (CD20; glofitamab[64]), non-Hodgkin's lymphomas (CD20; rituximab[65], odronextamab[66], mosunetuzumab[67]) and multiple myeloma (CD38; daratumomab[68], Bi38[69]). In contrast, knockout of *TNFRSF17* (also known as BCMA) in mice decreases PC survival and eliminates the antibody response[70]; hence, knockout of *TNFRSF17* would likely hamper ePC longevity and/or function.

Our findings suggest that ePCs may provide benefits for delivery of protein therapeutics beyond delivery of bispecifics as studied here. Therapeutic protein biologics were the second most approved drugs from 2009 to 2017[71] and many suffer from suboptimal half-lives exemplified by blinatumomab[7]. Because of poor pharmacokinetics, many biologics used in chronic diseases require frequent (up to daily) and, in some cases, life-long dosing. Examples, include treatments for enzyme replacement (agalsidase beta; half-life of 56 to 76 minutes[72], factor IX; 18 to 40 hours[73], laronidase; 1.5 to 3.6 hours[74]), chronic autoimmune disorders (infliximab; 9.5 days[75] etanercept; 80 hours[76]), diabetes (liraglutide; 13 hours[77]) and human immunodeficiency virus (enfuvirtide 3.4 hours[78]). The potential for ePCs to persist long term[14]

and produce robust levels of exogenous protein could be a key to unlocking the therapeutic potential of biologics or therapeutic peptides that lack efficacy due to poor pharmacokinetics.

In summary, these findings demonstrate the potential for human ePCs to mediate anti-leukemia responses and marks a key step in the realization of ePC as therapies to treat cancer, auto-immune disorders and protein deficiency disorders. Further studies in humanized mice and non-human primates are warranted to fully understand the activity, longevity, and tissue localization of ePCs.

2.6. FIGURES

2.6.1. *Genome engineered primary human B cells secrete functional αCD19-bispecific in a locus dependent manner*

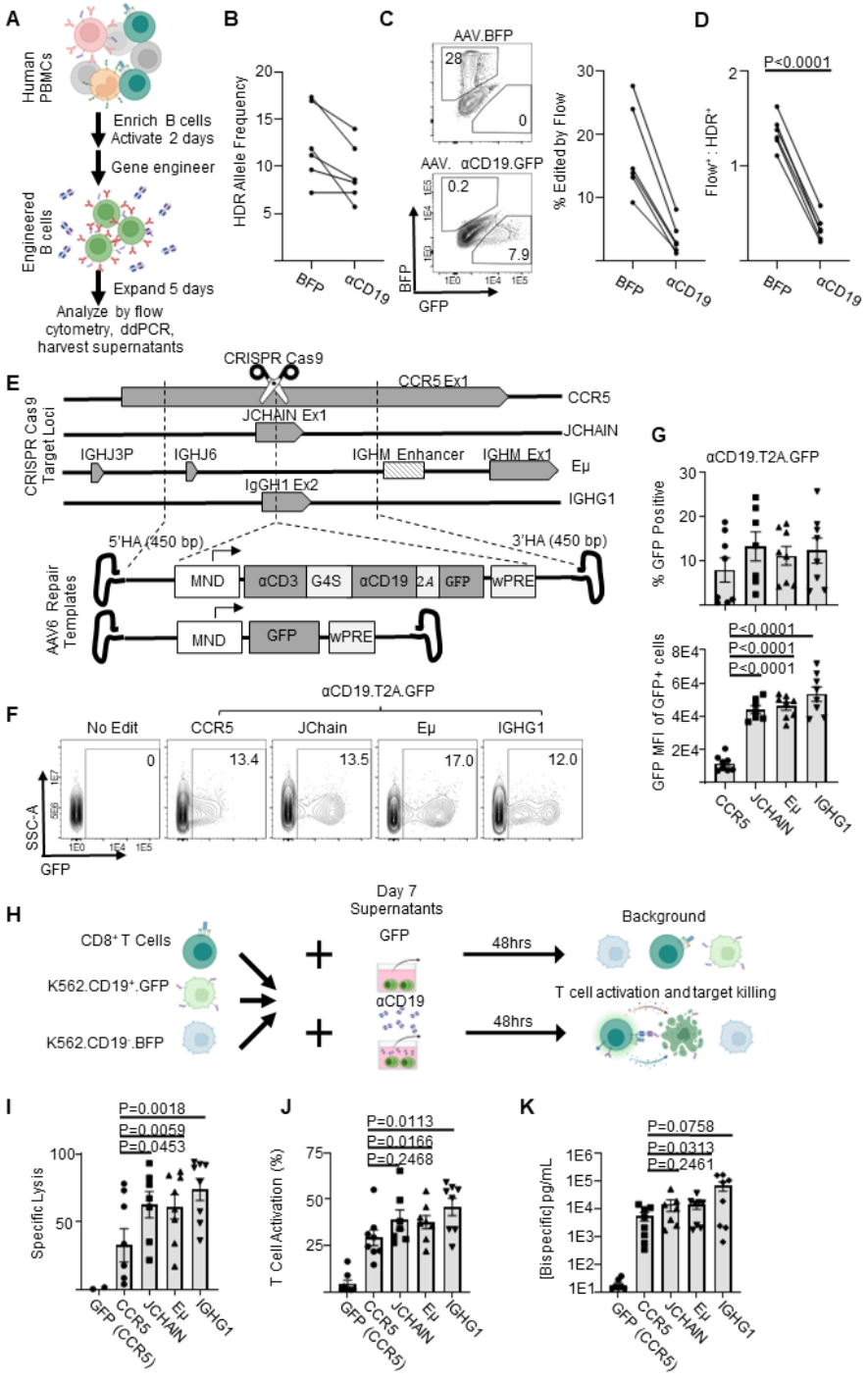

A) Schematic showing the experimental flow of a primary B cell experiment. Briefly, after isolation from PBMCs, B cells were edited to express either BFP or αCD19.T2A.GFP transgenes at CCR5 genetic loci via HDR-gene editing with AAV6 delivered DNA repair templates. Five days later genomic DNA, cells and supernatants were analyzed as indicated. **B)** Transgene integration at CCR5 locus shown here as HDR allele frequency was measured by ddPCR. **C)** Representative flow cytometry plots showing transgene expression of fluorescent proteins in engineered B cells shown and quantified as % edited of live cells. **D)** Ratio of engineering rate as determined by ddPCR vs flow cytometry. **E)** Schematic showing the editing strategies for delivery of GFP or αCD19.T2A.GFP to antibody-associated loci. **F)** Representative flow cytometry plots of αCD19.T2A.GFP edited B cells with **G)** the quantification of % edited and GFP mean fluorescent intensity of edited cells. **H)** K562 killing assay schema. Supernatants from edited B cells were incubated with target ($CD19^+$) and control ($CD19^-$) K562 cells with $CD8^+$ T cells for 48 hours. Cells were harvested for flow cytometry to obtain **I)** specific lysis of $CD19^+$ K562 and **J)** T cell activation (%$CD69^+CD137^+$ of $CD3^+$ cells). **K)** The concentration of bispecific in the supernatants as interpolated from %T cell activated data. Data are from five donors in five independent experiments. Error bars represent SEM. P values calculated using D) a paired student's t test and G,I-K) paired one-way ANOVAs with Dunnett’s posttest. Illustrations were created in part with biorender.com.

2.6.2. *Human plasma cells engineered to secrete anti-leukemia bispecifics specifically target cells expressing physiological levels of antigen*

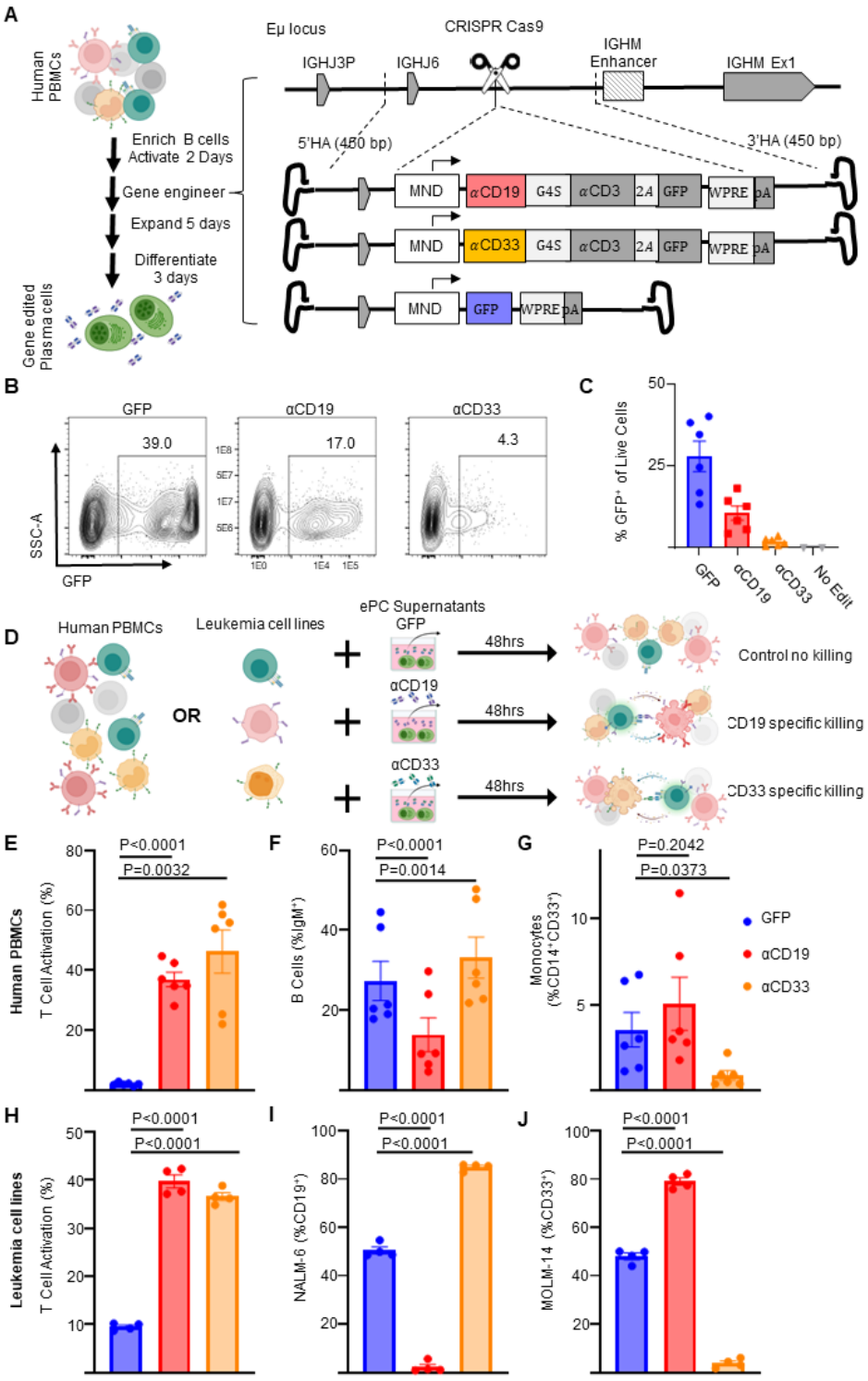

Primary human B cells were isolated and cultured for two days in activating media then edited.

A) Schematic showing how primary activated human B cells were edited to express GFP or αCD19.T2A.GFP or αCD33.T2A.GFP. After editing activated B cells, the engineered cells were then cultured in expansionary media for 5 days followed by differentiation into PCs over 3 days and cells and supernatants. **B)** Representative flow cytometry plots assessing editing via expression of GFP and **C)** quantification as % of live cells. **D)** Schematic illustrating *in vitro* PBMC or Leukemia cell line killing assays. Briefly, autologous $CD8^+$ T cells are co-cultured with PBMCs or mixed leukemia cell populations (NALM-6 and MOLM-14) in the presence of supernatants from ePCs for 48 hours. Flow cytometry was used to quantify **E)** T cell activation (%$CD69^+CD137^+$ of $CD3^+$ cells), **F)** the % B cells (IgM^+) of live cells, **G)** the % monocytes ($CD14^+CD33^+$) of live cells in PBMC cultures at the end of the 48-hour co-culture. Likewise flow cytometry was used to quantify **H)** T cell activation (%$CD69^+$,$CD137^+$ of $CD8^+$ cells), the frequency of **I)** NAML-6 ($CD19^+$) and **J)** MOLM-14 ($CD33^+$) in the leukemia cell line killing assay. In E-G, data were obtained from six donors in three independent experiments, and in H-J, data were obtained from four donors. Error bars represent SEM. P-values were calculated using paired one-way ANOVAs with Dunnett's posttest. Illustrations were created in part with biorender.com.

2.6.3. *CD19 knockout prevents self-targeting of αCD19- ePCs and increases αCD19-bispecific secretion*

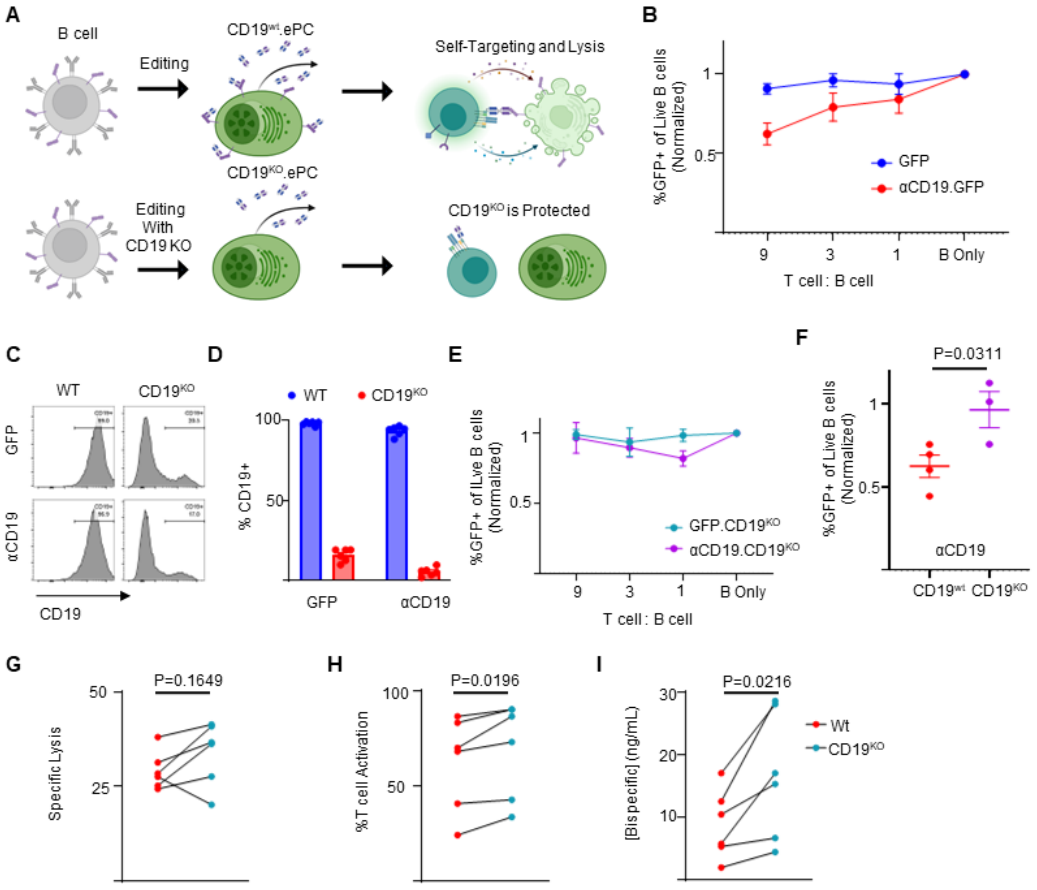

A) Schematic showing the self-targeting assay of ePCs with and without CD19 knockout. Primary human B cells were engineered to express either GFP or αCD19.T2A.GFP at the Eμ locus, and/or to eliminate CD19. These engineered cells were incubated with the indicated ratios of autologous T cells. **B)** After 24 hours, flow cytometry was used to calculate the percentage of GFP^+ of live $CD20^+$ B cells. The relative quantity of transgene-expressing cells was plotted. sgRNAs targeting CD19 were included to elicit knock out CD19 while engineering into the Eμ. Representative flow cytometry images **C)** and quantification **D)** of CD19 expression in engineered cells is shown. **E)** $CD19^{KO}$ cells were incubated with the indicated ratios of T cells for 24 hours. After incubation of edited cells with T cells, we used flow cytometry to quantify the % GFP^+ of $CD20^+$ cells. **F)** Combined data showing the GFP percentage following incubation of

edited cells with T cells at a nine:one ratio. **G-I)** Engineered B cells were further differentiated over 3 days into ePCs. Supernatants from $CD19^{KO}$ and WT αCD19 ePCs were incubated with T cells, K562 $CD19^{+}$ and K562 $CD19^{-}$ cells for 48 hours. **G)** Specific lysis of $CD19^{+}$ K562 and **H)** T cell activation (%$CD69^{+}CD137^{+}$ of $CD3^{+}$ cells) was quantified. **I)** αCD19 bispecific concentration was interpolated using recombinant αCD19 bispecific standards curves. These data are from four donors. Error bars represent SEM. P-values were calculated by paired one-way ANOVA with Dunnett's posttest (F) and paired student's T test (G-I). Illustrations created in part with biorender.com.

2.6.4. *CD19^{KO} PCs engineered to secrete αCD19 bispecific have anti-lymphoma efficacy in vivo*

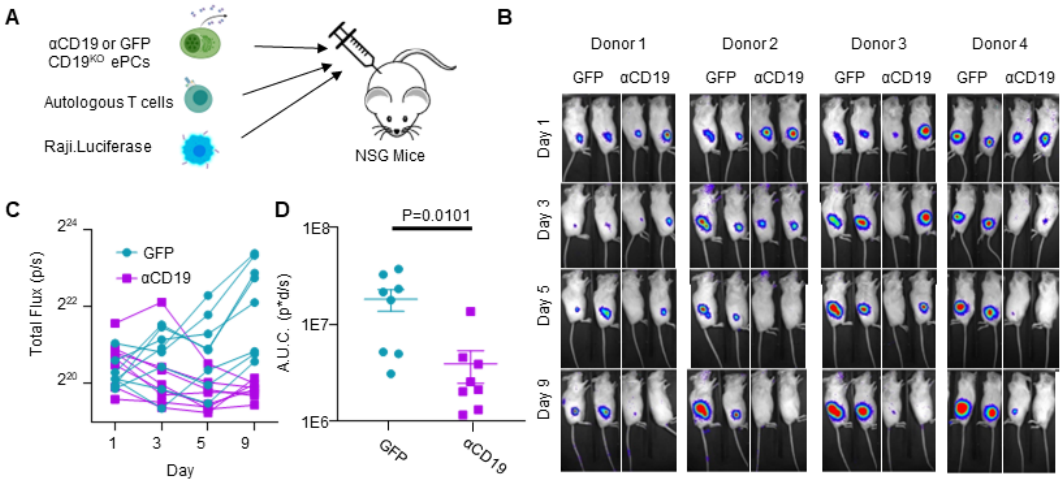

A) Schematic showing an *in vivo* model for lymphoma growth. Briefly, GFP.CD19^{KO} or αCD19.GFP.CD19^{KO} ePCs, autologous T cells, and luciferase expressing Raji cells were injected subcutaneously into the right flank of immunodeficient NSG mice. **B)** Representative bioluminescence images were obtained via *in vivo* imaging (color scale; min:8x10^3 max:1x10^5). **C)** Bioluminescence was quantified from each mouse as total flux and graphed over time. **D)** Area under the curve analysis was conducted with baseline correction of 6x10^5 flux. A-D) Data across 4 donors in two independent experiments with p-value calculated by unpaired student's t test. Illustrations created in part with biorender.com.

2.6.5. *CD19KO PCs engineered to secrete αCD19 bispecific can prevent leukemia engraftment*

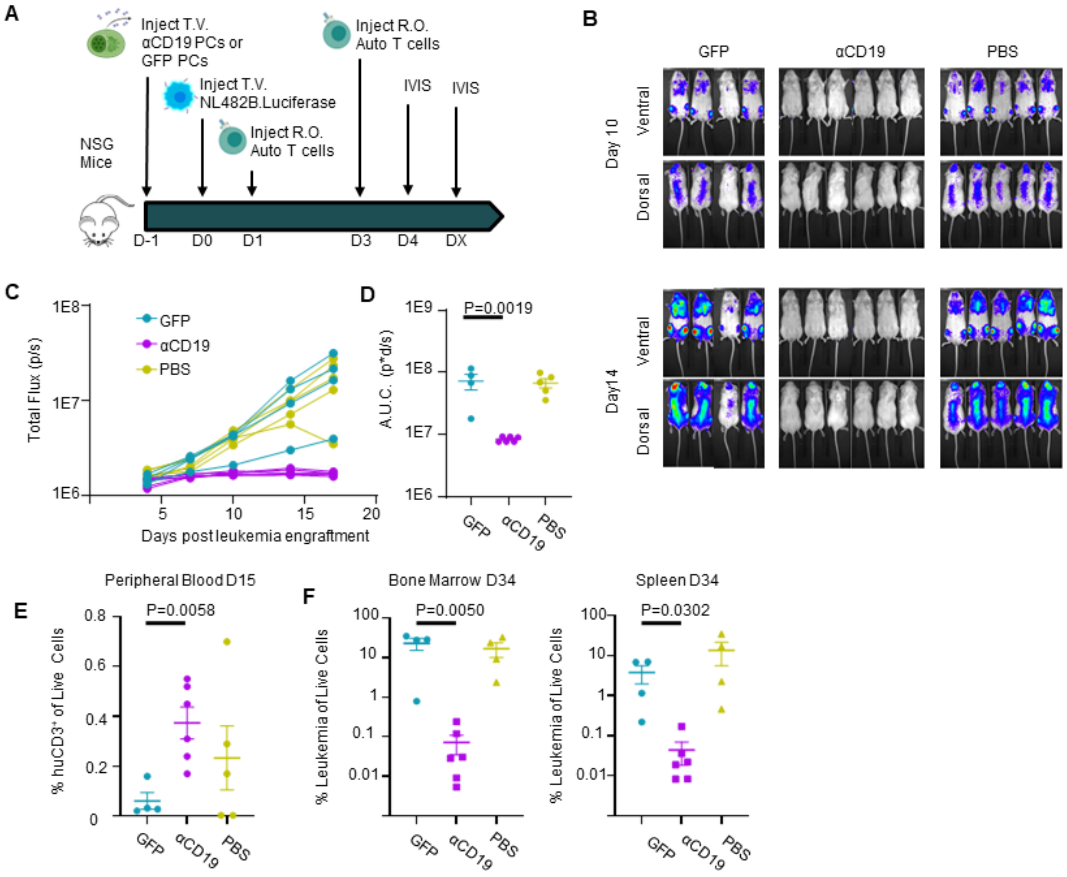

A) Schematic showing prophylactic treatment of a patient-derived xenograft model of high-risk ALL. Either GFP.CD19^{KO} or αCD19.GFP.CD19^{KO} ePCs were injected intravenously into immunodeficient NSG mice. 24 hours later, luciferase-labeled patient-derived NL482B [Children's Oncology Group unique specimen identifier PALJDL] cells were administered. Finally, we delivered T cells syngeneic to the ePCs in two doses by retro-orbital injection. **B)** Bioluminescent images showing dissemination of the luciferase-expressing leukemia cells (color scale; min:8x10^3 max:1x10^5). **C)** Leukemia growth was quantified via total bioluminescent flux at the indicated time points. **D)** Area under the curve analysis was conducted with baseline correction 1x10^6 flux. E**)** Peripheral blood flow analysis showing the percent of CD3+ cells of

singlet live cells is elevated in the αCD19 cohort. Mice were euthanized 34 days after leukemia engraftment and tissues were stained and analyzed by flow. **F)** The percent $CD19^+$ of live $CD45^+$ singlet cells shows suppression of leukemic cells in bone and spleens of the αCD19 ePC cohort. A-F) Data from one donor with p-values calculated by one-way unpaired ANOVA with Šídák's posttest (D) and unpaired student's T test between GFP and αCD19 cohorts (E-F). Illustrations created in part with biorender.com.

2.6.6. *αCD19 bispecific secreting ePCs can persist in bone marrow and treat established leukemia*

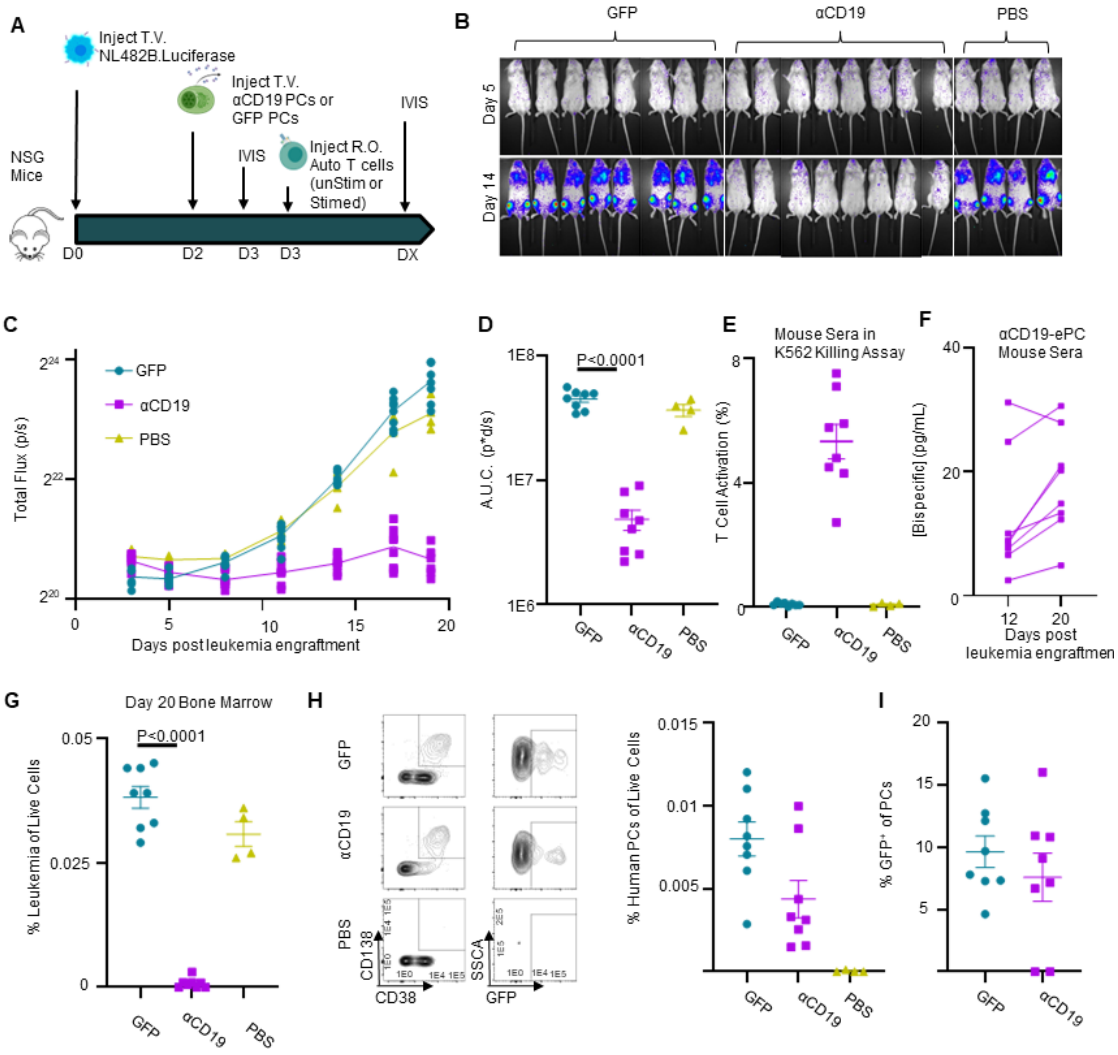

A) Schematic showing therapeutic treatment of a patient-derived xenograft model of high-risk ALL. Luciferase-labeled patient-derived NL482B [Children's Oncology Group unique specimen identifier PALJDL] cells were administered intravenously. After 48 hours, either GFP.CD19^{KO} or αCD19.GFP.CD19^{KO} ePCs were injected intravenously into immunodeficient NSG mice. 24 hours later, we delivered T cells syngeneic to the ePCs via retro-orbital injection. **B)** Bioluminescent images showing dissemination of the luciferase-expressing leukemia cells (color scale; min:5x10e^{3} max:5x10e^{4}). **C)** Leukemia growth was quantified via total bioluminescent flux at the indicated time points. **D)** Area under the curve analysis was conducted with baseline

correction $1.25x10^6$ flux. Peripheral blood sera from mice at day 12 and day 20 was collected and used in the previously described K562 Killing assay. **E)** Specific lysis of sera from mice twenty days post tumor engraftment is shown. **F)** Concentration of αCD19 bispecific in the mouse seras were interpolated from a standards curv*e.* Twenty days after tumor engraftment**,** bone marrow cells were harvested, stained, and analyzed by flow cytometry. **G)** The percent of tumor ($huCD19^+huCD45^+moCD45^-$) of live cells was quantified. H) Representative flow plots of human cells show plasma cells present in the bone marrow of mice that received ePCs. The percent of plasma cells ($huCD38^+huCD45^+moCD45$-$huCD138^+$) of live cells was calculated. **I)** The percentage of plasma cells that were GFP^+ was quantified and plotted. Data from one donor with p-values calculated by one-way unpaired ANOVA with Šídák's posttest. Illustrations created in part with biorender.com.

2.7. BIBLIOGRAPHY

1. Mullard A. FDA approves first CAR T therapy. *Nat Rev Drug Discov*. 2017;16(10):669.

2. Waldman AD, Fritz JM, Lenardo MJ. A guide to cancer immunotherapy: from T cell basic science to clinical practice. *Nat Rev Immunol*. 2020;20(11):651-668.

3. Siegel RL, Miller KD, Fuchs HE, Jemal A. Cancer Statistics, 2021. *CA Cancer J Clin*. 2021;71(1):7-33.

4. Kantarjian H, Stein A, Gökbuget N, et al. Blinatumomab versus Chemotherapy for Advanced Acute Lymphoblastic Leukemia. *N Engl J Med*. 2017;376(9):836-847.

5. Przepiorka D, Ko CW, Deisseroth A, et al. FDA Approval: Blinatumomab. *Clin Cancer Res*. 2015;21(18):4035-4039.

6. Halford Z, Coalter C, Gresham V, Brown T. A Systematic Review of Blinatumomab in the Treatment of Acute Lymphoblastic Leukemia: Engaging an Old Problem With New Solutions. *Ann Pharmacother*. 2021;55(10):1236-1253.

7. Zhu M, Wu B, Brandl C, et al. Blinatumomab, a Bispecific T-cell Engager (BiTE(®)) for CD-19 Targeted Cancer Immunotherapy: Clinical Pharmacology and Its Implications. *Clin Pharmacokinet*. 2016;55(10):1271-1288.

8. Ravandi F, Stein AS, Kantarjian HM, et al. A Phase 1 First-in-Human Study of AMG 330, an Anti-CD33 Bispecific T-Cell Engager (BiTE®) Antibody Construct, in Relapsed/Refractory Acute Myeloid Leukemia (R/R AML). *Blood*. 2018;132(Supplement 1):25-25.

9. Uy GL, Aldoss I, Foster MC, et al. Flotetuzumab as salvage immunotherapy for refractory acute myeloid leukemia. *Blood*. 2021;137(6):751-762.

10. Toksvang LN, Lee SHR, Yang JJ, Schmiegelow K. Maintenance therapy for acute lymphoblastic leukemia: basic science and clinical translations. *Leukemia*. 2022;36(7):1749-1758.

11. Apostolidou E, Lachowiez C, Juneja HS, et al. Clinical Outcomes of Patients With Newly Diagnosed Acute Lymphoblastic Leukemia in a County Hospital System. *Clin Lymphoma Myeloma Leuk*. 2021;21(11):e895-e902.

12. Strohl WR. Fusion Proteins for Half-Life Extension of Biologics as a Strategy to Make Biobetters. *BioDrugs*. 2015;29(4):215-239.

13. Hung KL, Meitlis I, Hale M, et al. Engineering Protein-Secreting Plasma Cells by Homology-Directed Repair in Primary Human B Cells. *Mol Ther*. 2018;26(2):456-467.

14. Cheng RYH, Hung KL, Zhang T, et al. Ex vivo engineered human plasma cells exhibit robust protein secretion and long-term engraftment in vivo. *Nat Commun*. 2022;13(1):6110.

15. Luo B, Zhan Y, Luo M, et al. Engineering of α-PD-1 antibody-expressing long-lived plasma cells by CRISPR/Cas9-mediated targeted gene integration. *Cell Death Dis*. 2020;11(11):973.

16. Page A, Laurent E, Nègre D, et al. Efficient adoptive transfer of autologous modified B cells: a new humanized platform mouse model for testing B cells reprogramming therapies. *Cancer Immunol Immunother*. 2022;71(7):1771-1775.

17. Levy C, Fusil F, Amirache F, et al. Baboon envelope pseudotyped lentiviral vectors efficiently transduce human B cells and allow active factor IX B cell secretion in vivo in NOD/SCIDγc-/- mice. *J Thromb Haemost*. 2016;14(12):2478-2492.

18. Moffett HF, Harms CK, Fitzpatrick KS, Tooley MR, Boonyaratanakornkit J, Taylor JJ. B cells engineered to express pathogen-specific antibodies protect against infection. *Sci Immunol*. 2019;4(35). doi:10.1126/sciimmunol.aax0644

19. Huang D, Tran JT, Olson A, et al. Vaccine Elicitation of HIV Broadly Neutralizing Antibodies from Engineered B cells.

20. Voss JE, Gonzalez-Martin A, Andrabi R, et al. Reprogramming the antigen specificity of B cells using genome-editing technologies. *eLife*. 2019;8.

21. Hartweger H, McGuire AT, Horning M, et al. HIV-specific humoral immune responses by CRISPR/Cas9-edited B cells. *J Exp Med*. 2019;216(6):1301-1310.

22. Nahmad AD, Raviv Y, Horovitz-Fried M, et al. Engineered B cells expressing an anti-HIV antibody enable memory retention, isotype switching and clonal expansion. *Nat Commun*. 2020;11(1):5851.

23. Page A, Hubert J, Fusil F, Cosset FL. Exploiting B Cell Transfer for Cancer Therapy: Engineered B Cells to Eradicate Tumors. *Int J Mol Sci*. 2021;22(18). doi:10.3390/ijms22189991

24. Manz RA, Thiel A, Radbruch A. Lifetime of plasma cells in the bone marrow. *Nature*. 1997;388(6638):133-134.

25. Amanna IJ, Carlson NE, Slifka MK. Duration of humoral immunity to common viral and vaccine antigens. *N Engl J Med*. 2007;357(19):1903-1915.

26. Eyer K, Doineau RCL, Castrillon CE, et al. Single-cell deep phenotyping of IgG-secreting cells for high-resolution immune monitoring. *Nat Biotechnol*. 2017;35(10):977-982.

27. Radbruch A, Muehlinghaus G, Luger EO, et al. Competence and competition: the challenge of becoming a long-lived plasma cell. *Nat Rev Immunol*. 2006;6(10):741-750.

28. Hibi T, Dosch HM. Limiting dilution analysis of the B cell compartment in human bone marrow. *Eur J Immunol*. 1986;16(2):139-145.

29. Marchand T, Pinho S. Leukemic Stem Cells: From Leukemic Niche Biology to Treatment Opportunities. *Front Immunol*. 2021;12:775128.

30. Benet Z, Jing Z, Fooksman DR. Plasma cell dynamics in the bone marrow niche. *Cell Rep*. 2021;34(6):108733.

31. Tasian SK, Bornhäuser M, Rutella S. Targeting Leukemia Stem Cells in the Bone Marrow Niche. *Biomedicines*. 2018;6(1). doi:10.3390/biomedicines6010022

32. Cheng RYH, de Rutte J, Ott AR, et al. SEC-seq: Association of molecular signatures with antibody secretion in thousands of single human plasma cells. *bioRxiv*. Published online August 26, 2022:2022.08.25.505190. doi:10.1101/2022.08.25.505190

33. Robbins PB, Yu XJ, Skelton DM, et al. Increased probability of expression from modified retroviral vectors in embryonal stem cells and embryonal carcinoma cells. *J Virol*. 1997;71(12):9466-9474.

34. Fleischer LC, Spencer HT, Raikar SS. Targeting T cell malignancies using CAR-based immunotherapy: challenges and potential solutions. *J Hematol Oncol*. 2019;12(1):141.

35. Gower M, Tikhonova AN. Avoiding fratricide: a T-ALL order. *Blood*. 2022;140(1):3-4.

36. Keating AK, Gossai N, Phillips CL, et al. Reducing minimal residual disease with blinatumomab prior to HCT for pediatric patients with acute lymphoblastic leukemia. *Blood Adv*. 2019;3(13):1926-1929.

37. Pawinska-Wasikowska K, Wieczorek A, Balwierz W, Bukowska-Strakova K, Surman M, Skoczen S. Blinatumomab as a Bridge Therapy for Hematopoietic Stem Cell Transplantation in Pediatric Refractory/Relapsed Acute Lymphoblastic Leukemia. *Cancers* . 2022;14(2). doi:10.3390/cancers14020458

38. Bargou R, Leo E, Zugmaier G, et al. Tumor regression in cancer patients by very low doses of a T cell-engaging antibody. *Science*. 2008;321(5891):974-977.

39. Mølhøj M, Crommer S, Brischwein K, et al. CD19-/CD3-bispecific antibody of the BiTE class is far superior to tandem diabody with respect to redirected tumor cell lysis. *Mol Immunol*. 2007;44(8):1935-1943.

40. Dreier T, Lorenczewski G, Brandl C, et al. Extremely potent, rapid and costimulation-independent cytotoxic T-cell response against lymphoma cells catalyzed by a single-chain bispecific antibody. *Int J Cancer*. 2002;100(6):690-697.

41. Dreier T, Baeuerle PA, Fichtner I, et al. T cell costimulus-independent and very efficacious inhibition of tumor growth in mice bearing subcutaneous or leukemic human B cell lymphoma xenografts by a CD19-/CD3- bispecific single-chain antibody construct. *J Immunol*. 2003;170(8):4397-4402.

42. Bride KL, Hu H, Tikhonova A, et al. Rational drug combinations with CDK4/6 inhibitors in acute lymphoblastic leukemia. *Haematologica*. 2022;107(8):1746-1757.

43. Maude SL, Tasian SK, Vincent T, et al. Targeting JAK1/2 and mTOR in murine xenograft models of Ph-like acute lymphoblastic leukemia. *Blood*. 2012;120(17):3510-3518.

44. Bhoj VG, Arhontoulis D, Wertheim G, et al. Persistence of long-lived plasma cells and humoral immunity in individuals responding to CD19-directed CAR T-cell therapy. *Blood*. 2016;128(3):360-370.

45. Maude SL, Frey N, Shaw PA, et al. Chimeric antigen receptor T cells for sustained remissions in leukemia. *N Engl J Med*. 2014;371(16):1507-1517.

46. Hill JA, Li D, Hay KA, et al. Infectious complications of CD19-targeted chimeric antigen receptor-modified T-cell immunotherapy. *Blood*. 2018;131(1):121-130.

47. Halliley JL, Tipton CM, Liesveld J, et al. Long-Lived Plasma Cells Are Contained within the CD19(-)CD38(hi)CD138(+) Subset in Human Bone Marrow. *Immunity*. 2015;43(1):132-145.

48. Topp M, Feuchtinger T. *Management of Hypogammaglobulinaemia and B-Cell Aplasia*. Springer; 2022.

49. Kampouri E, Walti CS, Gauthier J, Hill JA. Managing hypogammaglobulinemia in patients treated with CAR-T-cell therapy: key points for clinicians. *Expert Rev Hematol*. 2022;15(4):305-320.

50. Straathof KC, Pulè MA, Yotnda P, et al. An inducible caspase 9 safety switch for T-cell therapy. *Blood*. 2005;105(11):4247-4254.

51. Di Stasi A, Tey SK, Dotti G, et al. Inducible apoptosis as a safety switch for adoptive cell therapy. *N Engl J Med*. 2011;365(18):1673-1683.

52. Stavrou M, Philip B, Traynor-White C, et al. A Rapamycin-Activated Caspase 9-Based Suicide Gene. *Mol Ther*. 2018;26(5):1266-1276.

53. Cooper ML, Choi J, Staser K, et al. An “off-the-shelf” fratricide-resistant CAR-T for the treatment of T cell hematologic malignancies. *Leukemia*. 2018;32(9):1970-1983.

54. Mamonkin M, Rouce RH, Tashiro H, Brenner MK. A T-cell-directed chimeric antigen receptor for the selective treatment of T-cell malignancies. *Blood*. 2015;126(8):983-992.

55. Gomes-Silva D, Srinivasan M, Sharma S, et al. CD7-edited T cells expressing a CD7-specific CAR for the therapy of T-cell malignancies. *Blood*. 2017;130(3):285-296.

56. Mei HE, Wirries I, Frölich D, et al. A unique population of IgG-expressing plasma cells lacking CD19 is enriched in human bone marrow. *Blood*. 2015;125(11):1739-1748.

57. Arumugakani G, Stephenson SJ, Newton DJ, et al. Early Emergence of CD19-Negative Human Antibody-Secreting Cells at the Plasmablast to Plasma Cell Transition. *J Immunol*. 2017;198(12):4618-4628.

58. Hammarlund E, Thomas A, Amanna IJ, et al. Plasma cell survival in the absence of B cell memory. *Nat Commun*. 2017;8(1):1781.

59. Kuijpers TW, Bende RJ, Baars PA, et al. CD20 deficiency in humans results in impaired T cell-independent antibody responses. *J Clin Invest*. 2010;120(1):214-222.

60. Kozlova V, Ledererova A, Ladungova A, et al. CD20 is dispensable for B-cell receptor signaling but is required for proper actin polymerization, adhesion and migration of malignant B cells. *PLoS One*. 2020;15(3):e0229170.

61. Langley WA, Wieland A, Ahmed H, et al. Persistence of Virus-Specific Antibody after Depletion of Memory B Cells. *J Virol*. 2022;96(9):e0002622.

62. Hotchandani N, Fung H, Dulaimi E. CD38 Expression Loss in Multiple Myeloma Treated with Daratumumab. *Am J Clin Pathol*. 2016;146(suppl_1). doi:10.1093/ajcp/aqw151.007

63. Postigo J, Iglesias M, Cerezo-Wallis D, et al. Mice deficient in CD38 develop an attenuated form of collagen type II-induced arthritis. *PLoS One*. 2012;7(3):e33534.

64. Papazoglou D, Ysebaert L, Ioannou N, et al. S141: ELICITING ANTI-TUMOR T CELL ACTIVITY IN CHRONIC LYMPHOCYTIC LEUKEMIA WITH BISPECIFIC ANTIBODY-BASED COMBINATION THERAPY. *HemaSphere*. 2022;6:42.

65. Dotan E, Aggarwal C, Smith MR. Impact of Rituximab (Rituxan) on the Treatment of B-Cell Non-Hodgkin's Lymphoma. *P T*. 2010;35(3):148-157.

66. Bannerji R, Arnason JE, Advani RH, et al. Odronextamab, a human CD20×CD3 bispecific antibody in patients with CD20-positive B-cell malignancies (ELM-1): results from the relapsed or refractory non-Hodgkin lymphoma cohort in a single-arm, multicentre, phase 1 trial. *Lancet Haematol*. 2022;9(5):e327-e339.

67. Budde LE, Assouline S, Sehn LH, et al. Single-Agent Mosunetuzumab Shows Durable Complete Responses in Patients With Relapsed or Refractory B-Cell Lymphomas: Phase I Dose-Escalation Study. *J Clin Oncol*. 2022;40(5):481-491.

68. Abdallah N, Kumar SK. Daratumumab in untreated newly diagnosed multiple myeloma. *Ther Adv Hematol*. 2019;10:2040620719894871.

69. Fayon M, Martinez-Cingolani C, Abecassis A, et al. Bi38-3 is a novel CD38/CD3 bispecific T-cell engager with low toxicity for the treatment of multiple myeloma. *Haematologica*. 2021;106(4):1193-1197.

70. O'Connor BP, Raman VS, Erickson LD, et al. BCMA is essential for the survival of long-lived bone marrow plasma cells. *J Exp Med*. 2004;199(1):91-98.

71. Batta A, Kalra BS, Khirasaria R. Trends in FDA drug approvals over last 2 decades: An observational study. *J Family Med Prim Care*. 2020;9(1):105-114.

72. Clarke JTR, West ML, Bultas J, Schiffmann R. The pharmacology of multiple regimens of agalsidase alfa enzyme replacement therapy for Fabry disease. *Genet Med*. 2007;9(8):504-509.

73. Chhabra A, Spurden D, Fogarty PF, et al. Real-world outcomes associated with standard half-life and extended half-life factor replacement products for treatment of haemophilia A and B. *Blood Coagul Fibrinolysis*. 2020;31(3):186-192.

74. Jameson E, Jones S, Remmington T. Enzyme replacement therapy with

laronidase (Aldurazyme®) for treating mucopolysaccharidosis type I. *Cochrane Database Syst Rev*. 2019;6(6):CD009354.

75. Cornillie F, Shealy D, D'Haens G, et al. Infliximab induces potent anti-inflammatory and local immunomodulatory activity but no systemic immune suppression in patients with Crohn's disease. *Aliment Pharmacol Ther*. 2001;15(4):463-473.

76. Nestorov I, Zitnik R, DeVries T, Nakanishi AM, Wang A, Banfield C. Pharmacokinetics of subcutaneously administered etanercept in subjects with psoriasis. *Br J Clin Pharmacol*. 2006;62(4):435-445.

77. Sisson EM. Liraglutide: clinical pharmacology and considerations for therapy. *Pharmacotherapy*. 2011;31(9):896-911.

78. Cheng S, Wang Y, Zhang Z, et al. Enfuvirtide-PEG conjugate: A potent HIV fusion inhibitor with improved pharmacokinetic properties. *Eur J Med Chem*. 2016;121:232-237.

2.8. SUPPLEMENT

Supplemental Methods

Cell lines

K562 and Raji cell lines were obtained from the ATCC and cultured in RPMI 1640 supplemented with 10% fetal bovine serum. K562 were retroviral transduced with VSV-g pseudotyped virus containing CD19 in cis to GFP or BCMA (NP_001183) in cis to BFP and subsequently purified using fluorescence activated cell sorting (FACS) to generate target K562 $CD19^+$ GFP^+ and control reference K562 $BCMA^+$ BFP^+ cell lines. Raji were lentivirally transduced with firefly luciferase (AB261984.1) and enhanced green fluorescent protein (HM640279.1) and FACS-purified. NL428B cells expressing luciferase were provided by K. Thomas and S. Tasian. MOLM-14 cells lentiviral transduced to express GFP and luciferase were provided by S. Tasian.

Flow cytometry

Cells were stained according to staining panels in supplementary table 2. Flow cytometric analysis was performed on an LSR II flow cytometer (BD Biosciences) and events were analyzed using FlowJo software (Tree Star). Flow cytometry gating for fluorescent proteins, viability, and immunophenotyping can be found in supplementary figures.

Supplementary Figure Legends

Supplemental 1: High GFP editing efficiencies achieved at multiple loci

A) Schematic showing the protocols used for B cell expansion and differentiation. B cells were enriched from human PBMCs and cultured in activating media for two days. B cells were then engineered using homologous directed repair gene editing. Engineered cells were further expanded for 5 days. For figure 1 experiments only: engineered expanded B cells were

harvested on day 7 for ddPCR, flow cytometry, and supernatants for killing assays. In subsequent experiments, cells were then cultured at $1x10^6$/mL in cytokines driving differentiation towards PCs. B) Schematic showing the primer design for quantification of homology directed repair upon integration at the CCR5 locus. Integrated alleles and reference alleles were measured by ddPCR and used to calculate HDR allele frequency in Figure 1B. C) Gating strategy for determining the $\%GFP^+$ and GFP MFI of edited B cells at Day 7. Flow data was first gated on lymphocytes by SSC-A vs FSC-A. Lymphocytes were then gated on live cells ($AF350^-$). Live lymphocytes were then gated for single cells and analyzed for GFP expression. D) $\%GFP^+$ was calculated from singlet live cells and the mean fluorescent index was calculated from GFP^+ cells.

Supplemental 2: Recombinant bispecific results in dose and time dependent T cell activation and CD19-specific lysis in a K562 killing assay

Various concentrations of recombinant αCD19 bispecific were cultured with target (GFP^+:$CD19^+$) and control reference (BFP^+:$CD19^-$) K562 cells and $CD8^+$ T cells. Cells were harvested for analysis by flow cytometry after 48 hours. A) Gating strategy for flow cytometry of K562 killing assay. T cell activation is defined as the percent of live $CD8^+$ cells that are $CD69^+$ $CD137^+$. Specific lysis is calculated using the ratio of GFP^+:$CD19^+$ to BFP^+:$CD19^-$ cells normalized to the same ratio in the controls that received media only. B) Standard curves were interpolated for each experiment. Recombinant anti-CD19, anti-CD3 bispecific antibodies were added to the K562-CD8 T cell co-cultures. At the indicated concentration of bispecific, we quantified specific lysis and T cell activation as described in A). These standard curves were then used to back calculate the concentration of the supernatants from ePCs engineered to secrete the αCD19 bispecific in Figure 1J. C) T cell activation and specific lysis at various time

points with various concentrations of recombinant bispecific was determined. D) Time course showing optimal T cell activation and specific lysis at 48 hours using supernatants from ePCS.

Supplemental 3: Cells differentiated to day 10 maintain bispecific transgene expression and express phenotypic markers of plasma cells

B cells were enriched from human PBMCs and cultured in activating media for two days. B cells were then engineered to express GFP or αCD19.T2A.GFP or αCD33.T2A.GFP transgenes. Engineered cells were further expanded for 5 days and then cultured at $1x10^6$/mL in cytokines driving differentiation towards PCs for an additional 3 days. Engineered PCs were analyzed for PC phenotype by flow cytometry. A) Gating strategy for flow cytometry analysis of the PC phenotypes. B) Quantification of PC phenotype ($CD38^+$ $CD138^{+)}$ of singlet live lymphocytes in cells engineered to express the indicated bispecific antibodies. C) Representative flow plots and quantification of transgene positivity in bulk D10 cells or in the $CD38^+$ $CD138^+$ PC subsets.

Supplemental 4: PBMC killing assay shows specific lysis and specific T cell activation in a dose dependent manner

Human PBMCs and autologous $CD8^+$ T cells were co-cultured in the presence of either recombinant αCD19 bispecific or recombinant αCD33 bispecific for 48 hours. A) Cells were harvested and analyzed using the flow gating strategy shown. B) Cell frequencies were quantified and plotted by concentration of either αCD19 bispecific or αCD33 bispecific. Standards curves were interpolated by four parameter logistic based on T cell activation data.

Supplemental 5: Bispecifics drive T cell dependent specific lysis in a leukemia cell line killing assay

NALM-6 (B-ALL), MOLM-14 (AML) and autologous CD8+ T cells were co-cultured in the presence of either recombinant αCD19 bispecific or recombinant αCD33 bispecific for 48 hours. A) Cells were harvested and analyzed by flow cytometry using the gating strategy shown. B) NALM-6 (IgM^+) and MOLM-14 ($CD33^+$) cell frequencies were quantified and plotted as a function of the indicated bispecific concentrations. C) T cell activation ($CD69^+CD137^+$ of $CD8^+$) were quantified and plotted as a function of the indicated bispecific. Standard curves were interpolated by four parameter logistic based on T cell activation data.

Supplemental 6: CD19 surface staining on αCD19 engineered plasma cells

Primary human B cells were enriched from PBMCs and cultured in activating media for two days and then engineered to express GFP or αCD19.T2A.GFP at the Eμ locus. Engineered cells were then expanded and subsequently differentiated into plasma cells over an additional 8 days. A) Gating strategy to analyze CD19 expression on engineered cells (GFP^+). B) Quantification of CD19 mean fluorescent intensity on engineered cells (GFP^+) shown.

Supplemental 7: Flow cytometry gating Strategy for B cell self-targeting assay

Primary human B cells were enriched from PBMCs and cultured in activating media for two days and then engineered to express GFP or αCD19.T2A.GFP at the Eμ locus with or without CD19 knockout. Engineered cells were expanded for an additional 5 days. The expanded engineered cells were incubated with autologous T cells. After 24hrs the percentage of edited B cells was determined by flow cytometry according to the gating strategy shown.

Supplemental 8: CD19 knockout does not affect differentiation of bispecific engineered B cells into plasma cells

Primary human B cells were enriched from PBMCs and cultured in activating media for two days and then engineered to express GFP or αCD19.T2A.GFP at the Eμ locus with or without CD19 knockout. Edited cells were expanded for an additional 5 days. A) A slight trend towards lower viability was seen in cells that had CD19 knocked out. B) However, cell count remained high by day 7 of culturing. Engineered cells were further differentiated for 3 days into PCs. C) Cells were stained for surface markers and quantified as PCs ($CD38^{++}CD138^{+}$) and plasmablasts ($CD38^{++}CD138^{-}$). Data across 4 biologic donors.

Supplemental 9: Knockout of B cell tumor associated antigens does not affect the generation of engineered plasma cells

Primary human B cells were enriched from PBMCs and cultured in activating media for two days and then engineered to knock out various B cell tumor associated antigens. Edited cells were then expanded and differentiated into PCs A) gDNA from Day 10 cells were harvested and analyzed by Inference of CRISPR Editing (ICE). B) Cell counts and viability was quantified at various times during cell expansion and differentiation. Key B cell and plasma cell markers were stained and quantified at days 6 and day 10 by flow cytometry; C) representative flow plots shown (blue boxes highlight knockout relevant staining) and D) quantified as percent of live cells. E) IgM and IgG secretion was assessed by ELISA of supernatants of edited cells after differentiation. Data across two independent biologic donors.

Supplementary Figure 1

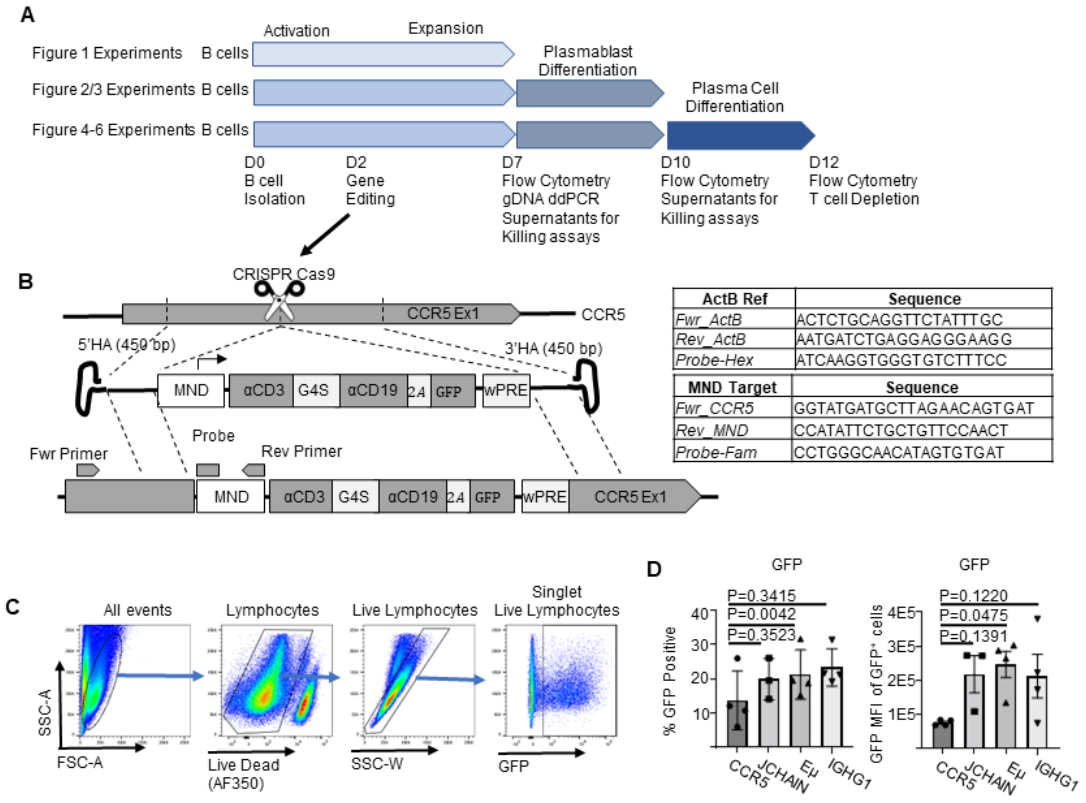

Supplementary Figure 2

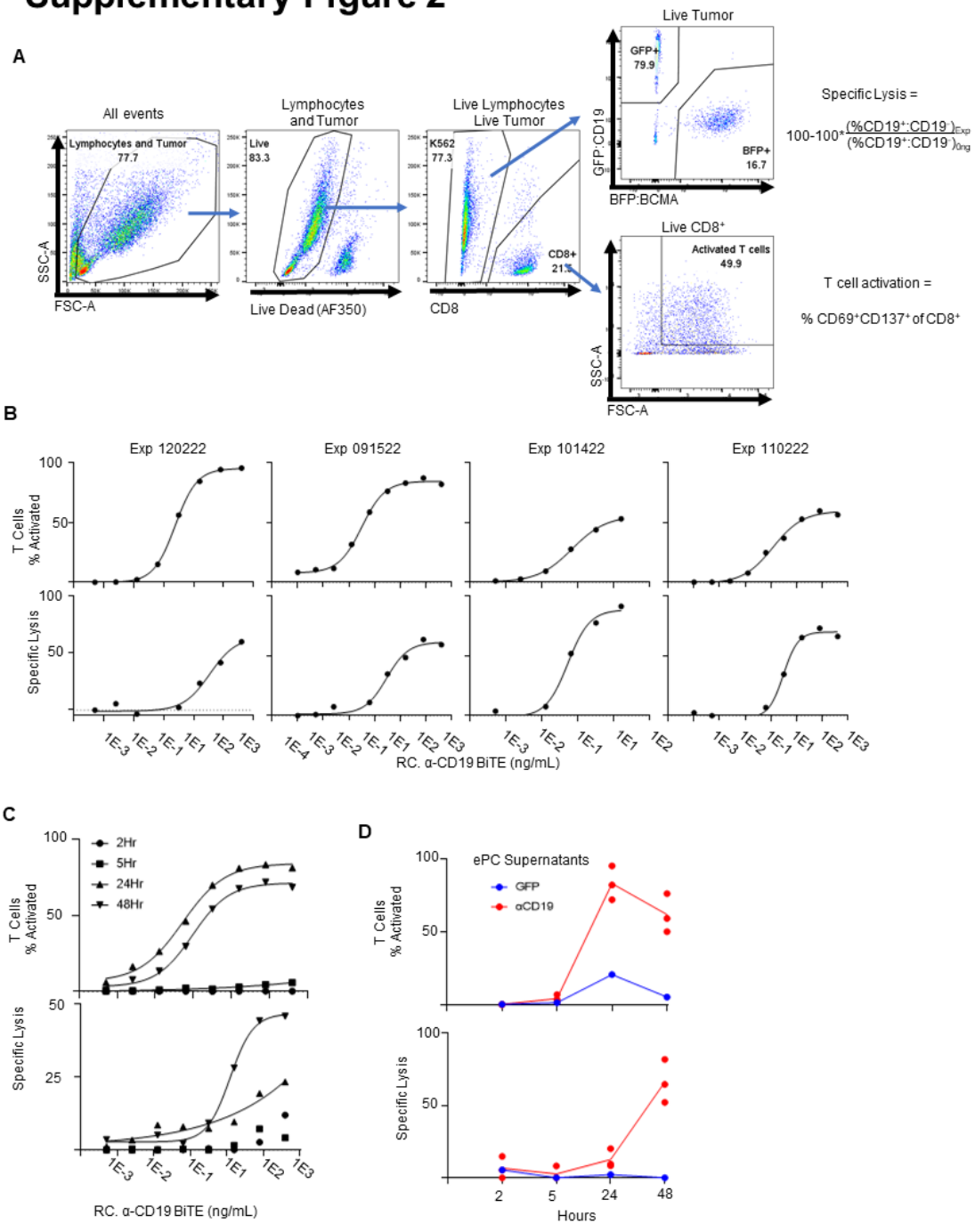

Supplementary Figure 3

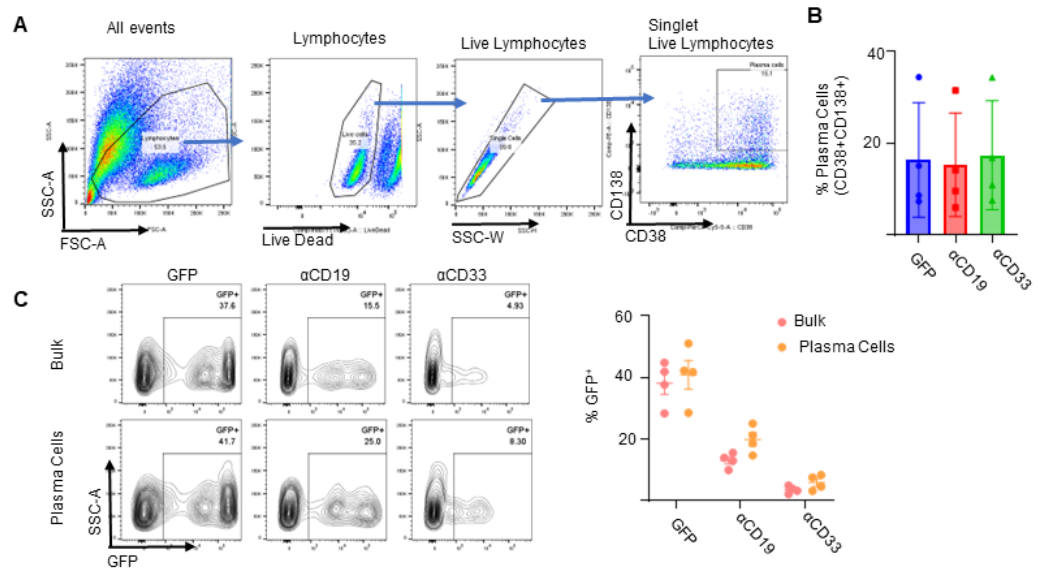

Supplementary Figure 4

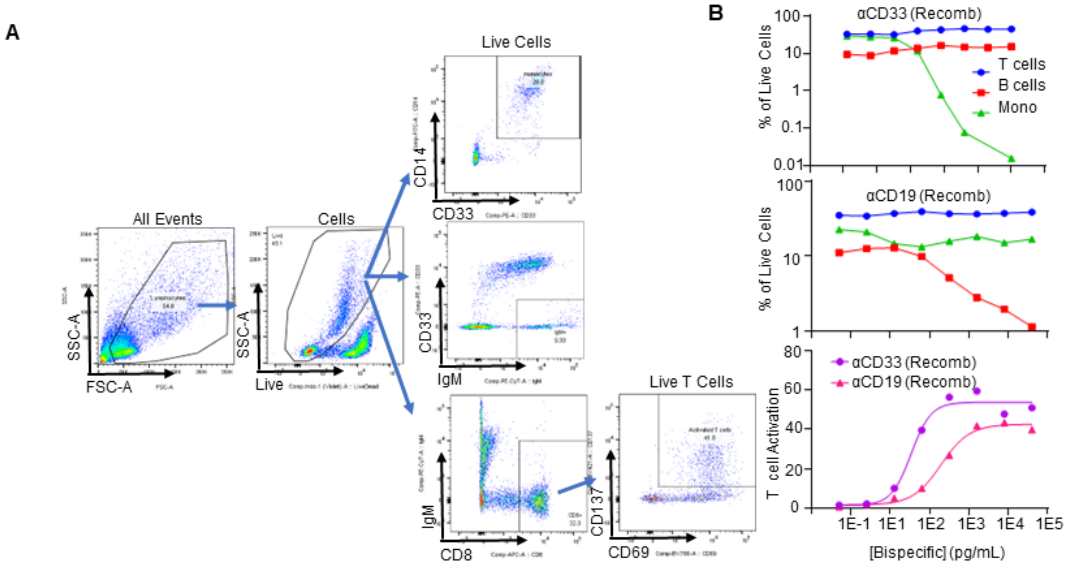

Supplementary Figure 6

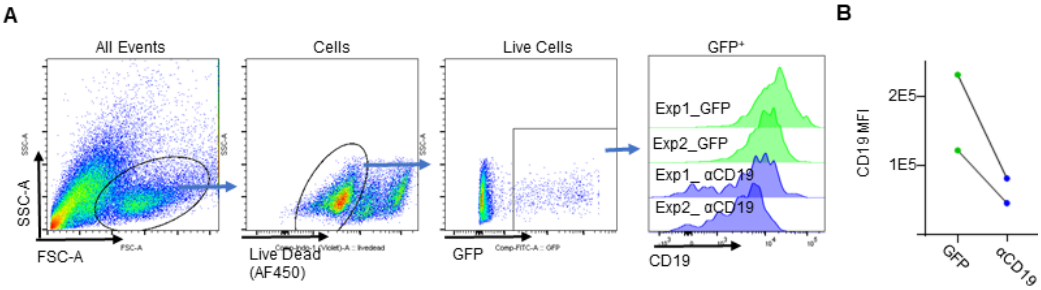

Supplementary Figure 7

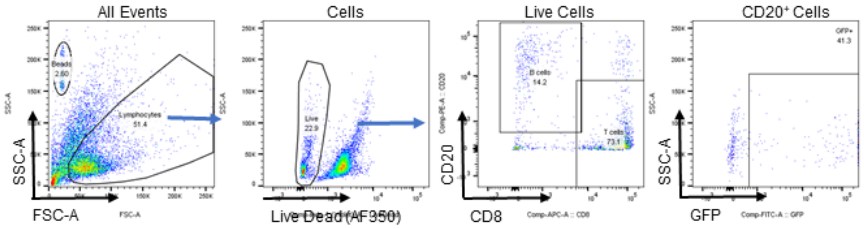

Supplementary Figure 8

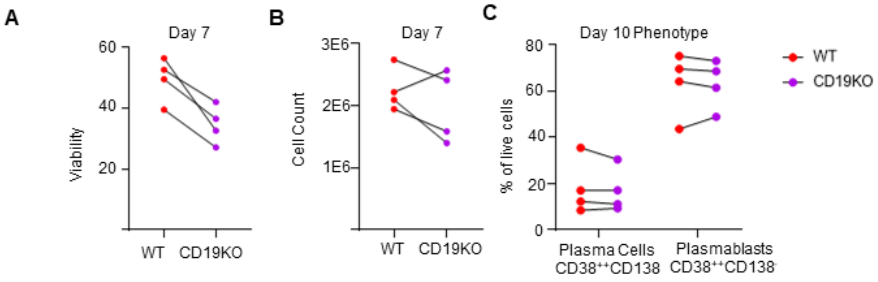

Supplementary Figure 9

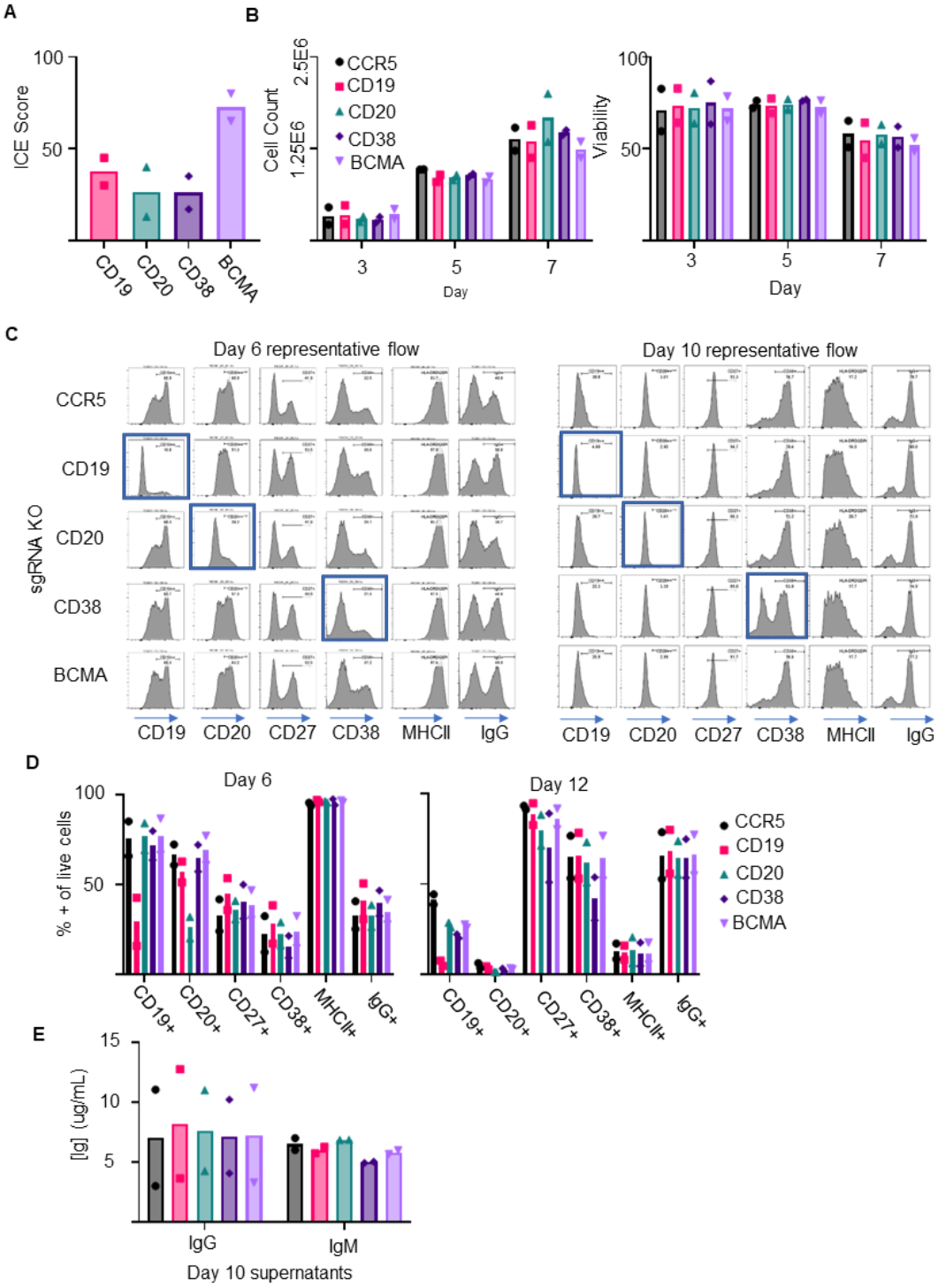

Supplementals Tables

Supplemental Table 1: CRISPR Guide Target Sequences

Guide Target	Sequence
CCR5	CAATGTGTCAACTCTTGACA
JCHAIN	AAGAACCATTTGCTTTTCTG
IgHG1	TGAGTTTTGTCACAAGATTT
Eμ	GTCTCAGGAGCGGTGTCTGT
CD19	CCTCGGGCCTGACTTCCATG

Supplemental Table 2: Flow Antibody Panels

B cell Phenotyping		
Item	**Vendor**	**Catalog**
PE-Cy7 anti-human CD19	Biolegend	302216
PerCP-Cy5.5 anti-human CD38	BD	BDB551400
PE anti-human CD138	Biolegend	356504
Brilliant Violet 605 anti-human CD3	Biolegend	317322
GFP	NA	NA
BFP	NA	NA
Alexa Fluor™ 350 NHS Ester (Succinimidyl Ester)	Fisher	A10168
K562 Killing Assay		
Item	**Vendor**	**Catalog**
BV786 anti-human CD69	Biolegend	310932
PE anti-human CD137	Biolegend	309804
APC anti-human CD8	Biolegend	344722
GFP	NA	NA
BFP	NA	NA
Alexa Fluor™ 350 NHS Ester (Succinimidyl Ester)	Fisher	A10168
PBMC Killing Assay		
Item	**Vendor**	**Catalog**
BV786 anti-human CD69	Biolegend	310932
PE anti-human CD137	Biolegend	309804
APC anti-human CD8	Biolegend	344722
FiTC anti-human CD14	Biolegend	325604
PE-Cy7 anti-human IgM	Biolegend	314531
PE anti-human CD33	Biolegend	303404
Alexa Fluor™ 350 NHS Ester (Succinimidyl Ester)	Fisher	A10168
Self-Killing Assay		
Item	**Vendor**	**Catalog**
BV786 anti-human CD69	Biolegend	310932
PE anti-human CD137	Biolegend	309804
APC anti-human CD8	Biolegend	344722
GFP	NA	NA
PE-Cy7 anti-human IgM	Biolegend	314531
PE anti-human CD20	BD	560961
Alexa Fluor™ 350 NHS Ester (Succinimidyl Ester)	Fisher	A10168
Mouse Tissue Staining		
Item	**Vendor**	**Catalog**
APC-Cy7 anti-human CD45	Biolegend	368516
Brilliant Violet 605 anti-mouse CD45	Biolegend	103155
Alexa Fluor™ 700 anti-human CD4	Biolegend	300526
PerCP-Cy5.5 anti-human CD38	BD	551400
PE anti-human CD138	Biolegend	352306
APC anti-human CD8	Biolegend	344722
BV786 anti-human CD3	Biolegend	317330
PE-Cy7 anti-human CD19	Invitrogen	25-0199-42

Chapter 3.

ENGRAFTMENT OF ENGINEERED PLASMA CELLS INTO HUMANIZED MICE SHOWS EARLY PROMISE FOR THE FEASIBILITY OF ENGINEERED PLASMA CELL THERAPIES

3.1. ABSTRACT

Advances in genome-engineering have enabled the generation of engineered plasma cells (ePCs) that secrete large quantities of therapeutic proteins. However, *in vivo* modeling of human ePCs has largely been limited to short-term studies following adoptive transfer of ePCs into immunodeficient mouse models including immuno-deficient NOD.Cg-*Prkdc*^{scid} *Il2rg*^{tm1Wjl}/SzJ (NSG) mice. Recent advances have shown improved ePC engraftment in immunodeficient mice that express human IL-6, but still have deficiencies (missing or lack of cross-species reactivity) in many key factors provided by human bone marrow stromal, myeloid and adaptive immune cells. In this study, we tested the hypothesis that immunodeficient mice humanized by engraftment of syngeneic human CD34+ hematopoietic peripheral stem cells would increase the engraftment potential of human ePCs. Further, we predicted that this approach might help to elucidate critical interactions between human PCs and human host BM-resident cells (myeloid cells and lymphocytes). Consistent with this concept, autologous ePCs engrafted more efficiently in NSG mice engrafted with syngeneic CD34 cells (NSG-huCD34) than in NSG control mice without. Further, ePCs in NSG-huCD34 mice secreted substantially higher levels of endogenous human antibodies (>100 IgG ug/mL for over 90 days) and engrafted in additional lymphoid compartments. ePCs migrated to and localized in the bone marrow and spleen and were retained in these locations based upon luciferase-based *in vivo and ex vivo* imaging, *ex vivo* flow analysis and histopathology. Plasma cells engineered to express an anti-EBV antibody produced robust levels for longer than 3 months. Anti-EBV levels remained stable relative to polyclonal-derived human IgG indicating that engineered plasma cells maintain similar fitness to non-engineered plasma cells. Taken together, these data demonstrate that the presence of autologous human hematopoietic cells in NSG-huCD34 mice permit the establishment of a robust model for studying the *in vivo* biology and potential therapeutic benefit of long-lived human ePCs.

3.2. INTRODUCTION

In the previous chapter, we established that human PCs can be engineered to secrete a therapeutic bispecific antibody that can effectively target leukemia cells in vivo. Importantly, we showed that the therapeutic bispecific was present in the sera and the ePCs were present in the bone marrow 20 days after engraftment (the timepoint where these animals were sacrificed). Taken together with our previous findings in hu-IL6 expressing NSG models[1], these observations suggest that human ePCs may be able to persist and secrete therapeutics for long periods of time. To begin to assess the longevity and function of ePCs in a physiological setting, we hypothesized that humanized mice could provide a more optimal platform to evaluate the functional capabilities of ePCs. Here, we describe development of an adoptive transfer humanized mouse model to better understand the biology, kinetics and localization of ePCs, as well as assess the functional potential of ePCs to deliver therapeutic monoclonal antibodies.

Numerous therapeutic monoclonal antibodies (mAbs) have been produced in the effort to better treat hematologic malignancies, solid tumors, immune disorders, hypercholesterolemia, asthma, osteoporosis, inflammatory bowel disease, and various infections.[2] In April 2021, the FDA approved the 100th mAb for clinical use in the USA[3]. However, many mAbs are prohibitively expensive and achieving therapeutic benefit requires repeated intravenous injections. For example, Eculizumab, a mAb that binds C5 and is used to treat paroxysmal nocturnal hemoglobinuria, costs $409,500 a year[6]. Furthermore, several antibody therapies require repeated injections or transfusions to provide long-term benefit. Repeated infusions can pose a logistical and quality of life challenge for patients that can lead to lower patient adherence[5,74,5] . Gene and cell therapies that aim to continuously produce mAbs *in vivo* are being investigated as a way to provide therapeutic levels of mAbs over long periods of time[8–10] with the goal of both improving patient adherence and decreasing costs[5].

Recent advances have made it feasible to genome engineer human B cells to continuously produce large quantities mAbs.[8,11–13] Engineered B cells that are differentiated into engineered plasma cells (ePCs) are uniquely suited to deliver mAbs over long periods due to their long lifespan[14] (half-life is estimated to be 11 to 200 years[15]), and high secretory capacity (up to 10,000 Immunoglobulin (Ig) G molecules per second[16–18]*),* Furthermore, *ex-vivo* generated ePCs resemble endogenous human PCs, and can stably secrete therapeutically relevant levels of immunoglobulin for greater than one year in human IL6 transgenic mice[1]. Finally, B cells and PCs engineered to secrete mAbs have been shown to provide protection from RSV infection[12], produce mAbs against common leukemia targets[19] as well as produce mAb checkpoint inhibitors[8]. However, no work to date has demonstrated that mAb secreting human ePCs are able to provide functional therapeutic benefit over a long period of time (greater than 42 days) in a biologically relevant humanized small animal system.

Modeling anti-pathogen secreting ePCs in a humanized small animal model susceptible to human tropic disease would allow for the functional testing of disease protection. Models using mice bearing human hematopoietic cells are some of the only small animal models that allow for infection by many clinically important human tropic diseases such as HIV, EBV, dengue, and influenza.[20] A breakthrough in EBV modeling showed that immunodeficient, NOD.Cg-*Prkdc*^{scid} *Il2rg*^{tm1Wjl}/SzJ (NSG), mice that receive human CD34+ hematopoietic grafts (NSG-huCD34) become susceptible to human tropic EBV infection.[21,22] These NSG-huCD34 mice exhibit multilineage human hematopoietic engraftment which allows for EBV infection of the graft derived human B cells. Injections of a new potent anti-EBV neutralizing mAb, AMMO-1[23], into the NSG-huCD34 mice provided protection against EBV infection.[21] It may be possible that AMMO-1 secreting ePCs could also provide long-lasting protection in this model.

We anticipated that the NSG-huCD34 model would provide insight into both the protective capacity of anti-pathogen mAb secreting ePCs and human ePC biology such as

localization, longevity. Many cell lineages that play a role in PC homeostasis are present in NSG-huCD34 mice including CD4 T cells[24], and macrophages[25]. While NSG-huCD34 mice do develop human PCs, the PCs generated do not class switch and only express IgM without strong inflammatory stimuli.[26] Therefore, these mice do not develop human IgG PCs which allows for the tracking of ePCs by their secretion of IgG.[1,27] Thus, we predicted that adoptive transfer of AMMO-1 secreting ePCs into a syngeneic NSG-huCD34 model would allow for the study of mAb-secreting ePCs cellular kinetics, Ab kinetics and the potential to provide anti-pathogen neutralizing titers, and in parallel, permit detailed study of human PC biology in the context of a substantially reconstituted human hematopoietic system.

Herein we develop a biologically relevant *in vivo* NSG-huCD34 humanized mouse model for evaluating the engraftment and functionality of human ePCs. We observed the presence of various cytokine, cellular, and structural factors associated with PC homeostasis in mice bearing human $CD34^+$ hematopoietic grafts. We demonstrate that the engraftment of ePCs was more efficient in mice engrafted with syngeneic $CD34^+$ cells and resulted in significantly higher and more stable levels of ePC-derived endogenous polyclonal antibodies. Additionally, ePCs secreting anti-EBV antibodies demonstrated robust and sustained production for greater than 3 months. This syngeneic ePC NSG-huCD34 mouse model holds promise as a future therapeutic ePC testing platform as well as a model to help uncover additional fundamental features of long-lived PCs.

3.3. MATERIAL AND METHODS

3.3.1. *Generation and Analysis of NSG-huCD34 mice*

All animal studies were performed according to AAALAC standards and were approved by the Seattle Children's Research Institute (SCRI) Institutional Animal Care and Use Committee. NOD.Cg-Prkdcscid Il2rgtm1Wjl/SzJ-c (NSG) mice were purchased from Jackson Laboratory and all mice were kept in a designated pathogen-free facility at SCRI. Human peripheral blood stem cells (PBSCs) were obtained from healthy G-CSF mobilized donors in accordance with Seattle Children's Research Institute's institutional review board. Frozen human CD34-enriched PBSCs were thawed and then cultured in SCGM (CellGenix) with 100ng/mL each of human recombinant Thrombopoietin, stem cell factor, and Flt3-ligand at a cell density of 1×10^6 cells/mL in a humidified 37°C incubator with 5% CO2. After 24 hours in culture, cells were washed in phosphate buffered saline (PBS) and 1×10^6 $CD34^+$ cells delivered per busulfan-conditioned NSG mouse by retro-orbital injection. Busulfan conditioning was performed by intraperitoneal (i.p.) injection of 35 mg/kg clinical grade busulfan into 7-8 week-old NSG mice 24 hours prior to human PBSC transfer. 6-10 weeks post-cell transfer, successful human cell engraftment was confirmed by the presence of human CD45+ cells in peripheral blood using flow cytometry. 10 weeks post-cell transfer, NSG-huCD34 and matched NSG littermates were harvested for peripheral tissues. Half of the spleens were fixed in 10% neutral pH formalin and sent to the Fred Hutch Experimental Histopathology for H&E staining. Half of the spleens were processed and analyzed by flow cytometry (for flow antibodies see table S1). Peripheral blood was processed for sera and then cytokine concentrations were measured via multiplexed ELISA (U-Plex MSD).

3.3.2. *Homology directed repair of B cells using CRISPR Cas9 and AAV6 repair templates*

Mobilized peripheral mononuclear cells (PBMCS) were collected from the CD34- fraction from mobilized PBSC donors in accordance with Seattle Children's Research Institute's institutional review board. We isolated B cells from PBMCs using the EasySep Human B cell Enrichment Kit (Stem Cell Technologies). We obtained >95% purity for B cells defined by CD3 negativity and CD19 positivity. Isolated B cells were cultured in Iscove's modified Dulbecco's medium (Gibco), supplemented with 2-mercaptoethanol (55μM) and 10% FBS and various human cytokines. Cells were cultured in activating and differentiating conditions as described in Cheng et al (Figure 2A).28 Cells for in vivo experiments were purified via CD3 bead depletion column (Miltenyi) prior to tail vein injection. Cells were immunophenotyped by flow cytometry (for flow antibodies see table S1).

3.3.3. *Trackable ePCs generated through genome engineering via AAV6 Homology Directed*

B cells and subsequent PCs were engineered to express the trackable reporter firefly luciferase or blue fluorescent protein (BFP) as previously described in Cheng et al.[1] Digital droplet PCR was performed to calculate the HDR allele frequency as previously described in Hung et al27. BFP expression was confirmed by flow cytometry.

3.3.4. *Tracking and phenotyping of ePCs in NSG-huCD34 mice*

One to ten million Luciferase or BFP-expressing ePCs were injected intravenously into NSG and NSG that had been engrafted with CD34+ cells 10 weeks prior (ie NSG-huCD34). ePC engraftment was monitored by bioluminescence imaging using IVIS Lumina S5 (Perkin Elmer) following subcutaneous injection of luciferin (75-150 mg/kg). Peripheral blood was collected by

retro-orbital bleed or submandibular bleed and processed to collect sera and quantify peripheral IgG titers. A subset of mice was euthanized for ex vivo tissue imaging following subcutaneous injection of luciferin (75-150 mg/kg). A subset of the mice was euthanized for ex vivo spleen and bone marrow immunophenotyping by flow cytometry (for flow antibodies see table S1). A subset of the mice was euthanized for ex vivo spleen and bone marrow immunophenotyping by flow cytometry (for flow antibodies see table S1). Tissues were fixed in 10% neutral pH formalin and provided to Fred Hutch Experimental Histopathology for immunohistochemical analysis.

3.3.5. *Generation of AMMO1- secreting ePCs and detection of AMM0-1 and human total IgG*

B cells were engineered to express an engineered version of the anti-EBV antibody, AMMO-1, as previously described in Moffett et al (Figure 5A).12 Engineered B cells were differentiated to PCs as previously described in Cheng et al.28 Editing rates were calculated by intracellular Strep Tag II staining of AMMO-1 ePCS. AMMO-1 was detected via ELISA using a gHgL-based capture reagent (provided by Andy Mcguire) and human peroxidase conjugated anti-human IgG detection antibody (Jackson). Total human IgG was determined using a IgG (total) human ELISA kit (Invitrogen). The expected AMMO titers were determined by multiplying the STII+ cell frequency by the total IgG found in the sera or supernatant.

3.3.6. *Statistical analysis*

Statistical analyses using parametric tests were performed using Prism 7 (GraphPad, San Diego, CA) as described in figure legends.

3.4. RESULTS

3.4.1. *Immunodeficient mice engrafted with human peripheral hematopoietic stem cells reconstitute key cellular and soluble factors involved in plasma cell homeostasis*

We first wanted to establish whether or not immunodeficient mice engrafted with peripheral $CD34^+$ hematopoietic stem cells reconstituted several key factors known to influence human PC biology. NSG-huCD34 mice and control NSG were sacrificed, and their tissues harvested 10 weeks after initial adoptive transfer of $CD34^+$ hematopoietic stem cells. Spleens harvested from humanized mice were larger and contained ordered sections of white pulp (lymphoid compartment) while control mice had smaller spleens with little to no white pulp (Figure 1A). PC homeostasis is thought to be strongly influenced by the presence of myeloid cells, as well as both follicular and memory CD4 T cells[24]. Within the spleens of the NSG-huCD34 mice we found robust engraftment of CD34-derived human myeloid cells, B cells, and, to a lesser extent, CD4 T cells (Figure 1B). Additionally, PC homeostasis also relies on several cell extrinsic soluble factors such as human cytokine levels[1,27,29–34]. We were able to find measurable levels of human BAFF, IL-6 and IL-21 in the NSG-huCD34 mice but not in control mice. This data is consistent with the generation of an environment that recapitulates many features known to positively influence the generation and maintenance of long-lived PCs.

3.4.2. *Engrafted trackable ePCs show superior engraftment in humanized mice*

Next, we generated ePCs that expressed reporters that we could track in the syngeneic NSG-huCD34 mouse model. Mobilized PBMCs were collected at the same time as $CD34^+$ cells in order to have syngeneic ePC and NSG-huCD34 pairs. Subsequently, we engineered B cells from mobilized donors to express either blue fluorescent protein (BFP) or luciferase using

homology directed repair and then differentiated them into ePCs (previously published[1], schematized in Figure 2A). We confirmed robust integration of the transgene reporters via ddPCR (Figure 2B). Additionally, BFP expression was confirmed in greater than 20% of the BFP-ePCs via flow cytometry (Figure 2C). We immunophenotyped the ePCs to confirm that being sourced from mobilized PBMCS did not interfere with plasma cell differentiation. Similar to findings previously published with non-mobilized-PBMCs[1,27], greater than 20% of cells expressed the plasma cell markers ($CD38^+CD138^+$, Figure 2D) and greater than 75% of the $CD38^+CD138^+$ cells had class switched to IgG (Figure 2F). To our knowledge, this is the first demonstration that human ePCs can be generated from a G-CSF mobilized PBMC source.

We adoptively transferred luciferase expressing ePCs into syngeneic NSG-huCD34 and control NSG mice to assess whether humanization improved ePC engraftment (Figure 3A). Initial imaging of NSG-huCD34 with ePCs showed a bioluminescence pattern consistent with ePC engraftment in bone marrow of the limbs, spine, spleen and lungs (Figure 3B). Initial engraftment was relatively similar between control NSG and NSG-huCD34. However, the luminescence signal remained stable in the NSG-huCD34, whereas it deteriorated rapidly in the control NSG (Figure 3D). Consistent with the bioluminesce data, human IgG secreted from ePCs in the sera indicates a similar initial engraftment of ePCs followed by stable secretion in NSG-huCD34 and a steep decrease to below detectable levels in NSG (Figure 3E). Area under the curve analysis indicates that in all 4 independent experiments plasma cells showed superior long-term engraftment in NSG-huCD34 than in control mice as measured by luminescence (Figure 3F) and human total IgG serum titer (Figure 3G). Lastly, the sternum, lungs, spleen liver, jejunum and femurs were harvested and imaged *ex vivo* after perfusing the mice. Luminescence of all tissues was higher in all the tissues from NSG-huCD34, but most notably in the lungs and spleen (Figure 3H). We did not test whether perfusion potentially moves labile bone marrow ePCs and thus affects where signal is found in the tissues. NSG-huCD34 mice that received an

additional dose of Luciferase-ePCs exhibited higher levels of luminescence than mice that only received one dose suggesting that the PC niche is not saturated in this model (Figure S1). Collectively, these findings strongly suggest that humanization improves the engraftment and long-term survival of ePCs.

3.4.3. *Engineered plasma cells home to known plasma cell niches and retain their plasma cell phenotype in NSG-huCD34 mice*

While the above *in vivo* and *ex vivo* bioluminescence data strongly suggests that ePCs move to the bone marrow and spleen where they maintain their phenotype, it is not definitive. Thus, we collected tissues for immunohistology as well as for flow cytometry based immunophenotyping to confirm the presence and phenotype of ePCs in NSG-huCD34 that received adoptive transfer of either BFP expressing ePCs, luciferase expressing ePCs or PBS (Figure 4A). Human PCs ($huCD3^{-}CD38^{+}huCD45^{+}CD138^{+}$) could be found in the bone marrow and spleens of NSG-huCD34 five weeks after receiving ePCs (Figure 4B) and in NSG-huCD34 that received PBS (data not shown). However, only the NSG-huCD34 mice that received ePCs had class switched ($IgM^{-}IgG^{+}$) PCs in the bone marrow and spleen (Figure 4C). Importantly, we were only able to find BFP^{+} PCs in the spleens and bone marrow of ePC treated NSG-huCD34 and not PBS treated NSG-huCD34 (Figure 4D). We performed immunohistology to further demonstrate and understand localization of the engrafted ePCs. Luciferase expressing cells were found within the marrow space of the femur as well as the spleen in an evenly distributed manner (Figure 4E). Nearly all luciferase positive cells stained positive for human plasma cell marker CD138 (Figure 4E). Additional staining showed that $luciferase^{+}$ $CD138^{+}$ cells seem to preferentially colocalize with $huCD33^{+}$ myeloid cells in the spleen (Figure 4F). These data clearly demonstrate that ePCs are capable of migrating to the bone marrow and spleen niches of NSG-huCD34 mice where they can maintain a canonical PC phenotype, persist for months and potentially interact with myeloid cells derived from the $CD34^{+}$ graft.

3.4.4. *Monoclonal antibody secreting engineered plasma cells engrafted in humanized mice show robust long-term kinetics*

One potential use of the ePC adoptive transfer NSG-huCD34 model is to study the therapeutic potential of ePC that secrete mAbs that neutralize human pathogens. We used a previously published homology directed repair strategy to engineer B cells to express an anti-EBV engineered mAb (emAb) consisting of a light chain linked via the trackable StrepTag II (STII) linker to an anti-EBV heavy variable domain (AMMO-1,Figure 5A)[12]. After differentiation into ePCs, editing was detected via intracellular staining of the STII tag between the light and heavy chains of the AMMO-1 (Figure 5B). Secretion of AMMO-1-IgG was detected in the supernatants of AMMO-1 ePCs by antigen(gHgL)-specific ELISA (Figure 5C). Using total IgG levels in the supernatants (Figure 5D) and $STII^+$ editing rates, we calculated the expected concentration of AMMO-1-IgG in the supernatants. AMMO-1-IgG antibody levels in supernatants were roughly 20-fold lower than expected levels calculated from the editing levels and respective total IgG levels (Figure 5E). We confirmed that the difference was not due to an affinity difference caused by expressing AMMO-1 as an emAb with an STII linker (data not shown).

While the lower than expected supernatant levels of AMMO-1 was discouraging, we still wanted to test whether neutralizing titers could be achieved *in vivo* using these cells. ePCs secreting AMMO-1 or control GFP-ePCs were then injected into NSG-huCD34 mice according to the schema in Figure 5F. AMMO-1-IgG was detected in all mice that received AMMO-1-ePCs and could not be detected in mice that received GFP-ePCs (Figure 5G). Levels of AMMO-1-IgG decreased slowly over the course of 90 days. Similarly, total IgG in these mice also slowly decreased over the course of 90 days (Figure 5H). When adjusted for the decrease in total IgG we see that AMMO-1 remains stable indicating no selective disadvantage to cells expressing AMMO-1 vs PCs that do not (Figure 5I). Consistent with the *in vitro* data, AMMO-1-IgG levels

were ~20 fold lower than what we would have predicted assuming expression at levels equivalent to endogenous IgG(Figure 5J). Mouse sera were harvested between 30 and 60 days to perform pseudo neutralization assays. Not surprisingly, we were not able to neutralize EBV using sera from these mice likely due to the low titers of AMMO-1 (data not shown). Together, this data indicates that ePCs expressing anti-pathogen mAbs stably engraft in NSG-huCD34 mice for greater than 90 days and suggest that following improved secretion levels this approach may lead to generation of ePCs that generate neutralizing titers.

3.5. DISCUSSION

Engineered plasma cells comprise an emerging cell-based modality for high-level, sustained delivery of therapeutic proteins, but lack a biologically relevant small animal model for their study. Herein, we report the adoptive transfer of ePCs into immunodeficient mice bearing syngeneic human $CD34^+$ hematopoietic stem cells as a novel platform for assessing ePC biology, their potential for long-term persistence, and their ability to deliver therapeutic monoclonal antibodies (mAbs). We confirmed that immunodeficient mice engrafted with human hematopoietic stem cells exhibited key cellular (Mo, T cells) and soluble factors (BAFF, IL6, IL21) involved in plasma cell homeostasis (Figure 1). Importantly, adoptive transfer of these ePCs into NSG-huCD34 mice resulted in superior engraftment compared to control NSG mice (Figure 3). Furthermore, we confirmed the presence and phenotype of ePCs in the bone marrow and spleen of NSG-huCD34 mice (Figure 4). Lastly, we achieved stable levels of an anti-EBV mAb for over 90 days in NSG-huCD34 engrafted with anti-EBV secreting ePCs (Figure5).

Primary human PCs and *ex vivo* generated PCs are notoriously difficult to engraft in immunodeficient mice[1]. This is likely due in part to imperfect interactions between mouse cytokines and human receptors. For instance, the BAFF (72% conservation) and BAFFR (54% conservation) interaction is imperfect as evidenced in engraftment studies showing that human PBMCs into hBAFF knock-in mice led to increased immature B cell development[35]. Likewise, IL-6 (39% conservation) IL6R (52%) IL-21 (53% conservation) and IL-21R (63% conservation) are also poorly conserved between humans and mice. In this study we found that NSG-huCD34 mice had detectable levels of circulating human BAFF (mean 10,322pg/mL), IL-6 (17.53pg/mL) and IL-21(480pg/mL). Interestingly, all levels were elevated relative to normal human circulating levels (BAFF mean 906pg/mL[36], IL6 0.007-7pg/mL[37,38], IL21 28pg/mL[39]). These circulating

levels of human cytokines likely contributed in part to the increased engraftment and maintenance of ePCs seen in our adoptive transfer model. These findings open the possibility of future mechanistic studies exploring how blocking specific circulating cytokines may impact human PC engraftment or survival. This approach is likely to lead to advancement in the understanding of human PC biology as well as a potential mechanism(s) for targeting pathogenic PCs.

The increased engraftment of ePCs in humanized mice likely reflects a combination of paracrine signaling and human cell-cell interactions as well as potential differences in tissue architecture mediated by human hematopoietic engraftment. The limitations of NSG-huCD34 mice to recapitulate proper lymphoid structures such as lymph nodes, periarterial lymphoid structures and germinal centers is well documented[40,41]. Despite this, many ePCs were found within the white pulp compartment of NSG-huCD34 spleens suggesting that the reconstituted spleen maintains at least part of its capacity to form lymphoid structures that may support PCs. Additionally, we found that human PCs colocalized with myeloid ($CD33^+$) human cells in NSG-huCD34 spleens (Figure 4F). While it is known that myeloid cells play a critical role in maintaining long lived PCs, there is considerable debate as to which cell type within the myeloid compartment plays the most critical role [42–44]. Future studies using spatial transcriptomics in association with this adoptive transfer model could help elucidate the cellular components surrounding PCs and their potential role in the improved maintenance of ePCs in various tissues.

The enhanced long-term maintenance of ePCs in NSG-huCD34 mice led to relatively high and stable endogenous human Ab levels (Figure 3E) as well as stable anti-EBV mAb levels (Figure 5G) for greater than 90 days. Despite these improvements in engraftment, we did not move forward with EBV protection studies as we did not reach AMMO-1-IgG serum levels required for neutralization (B cell neutralization potency of AMMO-1-IgG1 is 160ng/mL[23]).

Importantly, the insufficient AMMO-1-IgG levels was primarily due to poorer expression of the emAb relative to endogenous IgG expression (Figure 5J) and not altered engraftment of AMMO-1-IgG expressing ePCs. Studies are underway to investigate ways to achieve higher emAb expression in ePCs. Regardless, the improvements seen in stable exogenous protein expression may allow for the study of other biologic-secreting ePCs that would otherwise not reach sufficient biologic levels for long-term function or for biologics that require human hematopoietic cells to be present for functional testing.

In summary, we have developed a robust ePC adoptive transfer humanized mouse model that recapitulates many biological features of human PC homeostasis. Future studies using this ePC adoptive transfer platform will help to uncover additional fundamental features of long-lived PCs, and in parallel, support the capacity to build and test ePC-based cell therapies.

3.6. FIGURES

3.6.1. *Humanization of NSG mice with human CD34+ hematopoietic stem cells partially reconstitute human plasma cell niches*

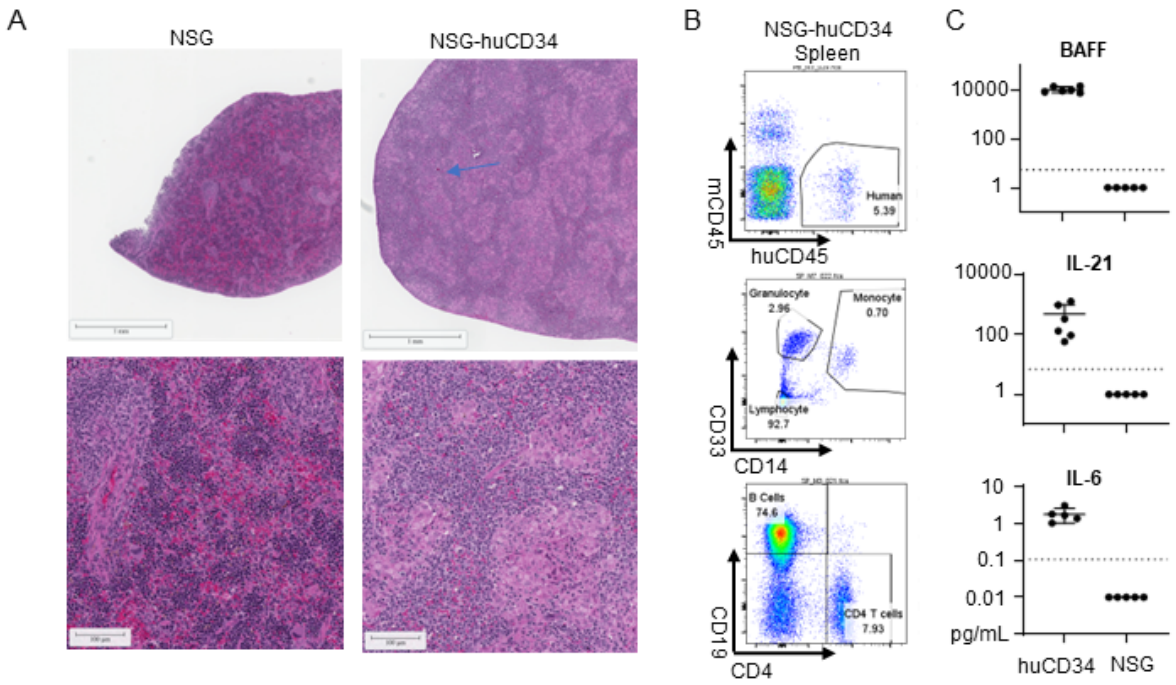

Immunodeficient NSG mice were injected with huCD34^{+} hematopoietic stem cells via tail vein injection. Mouse tissues and peripheral sera were harvested 10 weeks after engraftment. **A)** Representative H&E images of spleens from NSG and NSG-huCD34^{+}. **B)** Representative flow plots of cells harvested from a NSG-huCD34 spleen that was processed, stained for human surface markers and then analyzed by flow cytometry. **C)** Cytokine concentrations in the sera of NSG-huCD34 and NSG mice were measured by MSD ELISA and graphed as shown. Dotted line indicates lower limit of detection.

3.6.2. *Genome-engineering of mobilized primary human B cells followed by differentiation generates trackable ePCs*

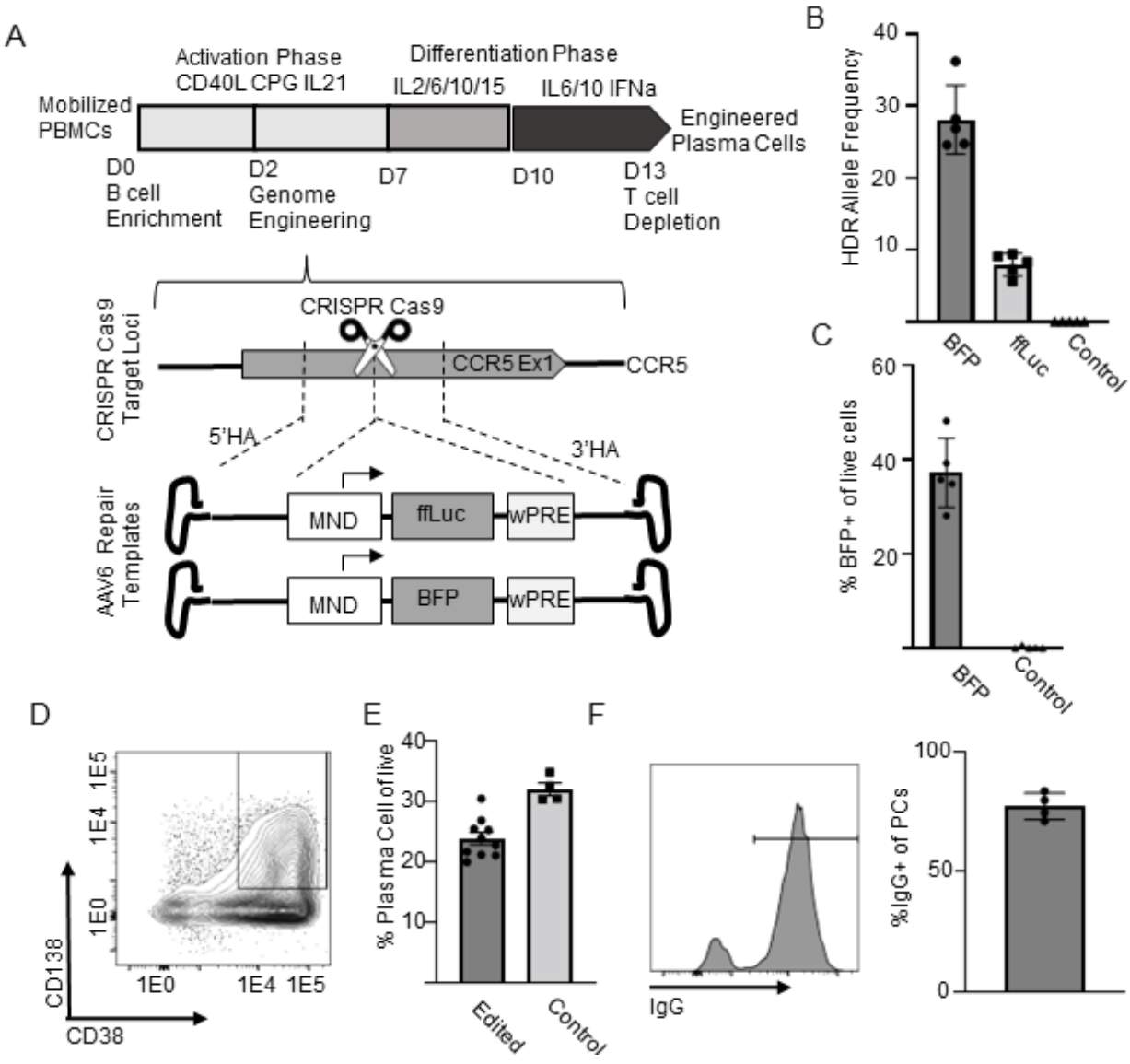

A) Schematic indicating the *in vitro* culturing and genome engineering strategies to generate ePCs from mobilized PBMCs. **B)** HDR allele frequency as calculated by ddPCR of genomic DNA from ePCs. **C)** The percent BFP^{+} of day 13 ePCs as measured by flow cytometry. **D)** Representative flow cytometry plot of ePCs at the end of the differentiation phase. Gate shown for the **E)** quantification of cells expressing both plasma cell markers CD38 and CD138. Intracellular staining IgG was performed on D13 ePCs. **F)** Representative flow plot and

quantified percent IgG^+ staining of $CD38^+$ $CD138^+$ plasma cells.

3.6.3. Hematopoietic stem cell humanization of immunodeficient mice leads to robust engraftment of human engineered plasma cells for over 100 days

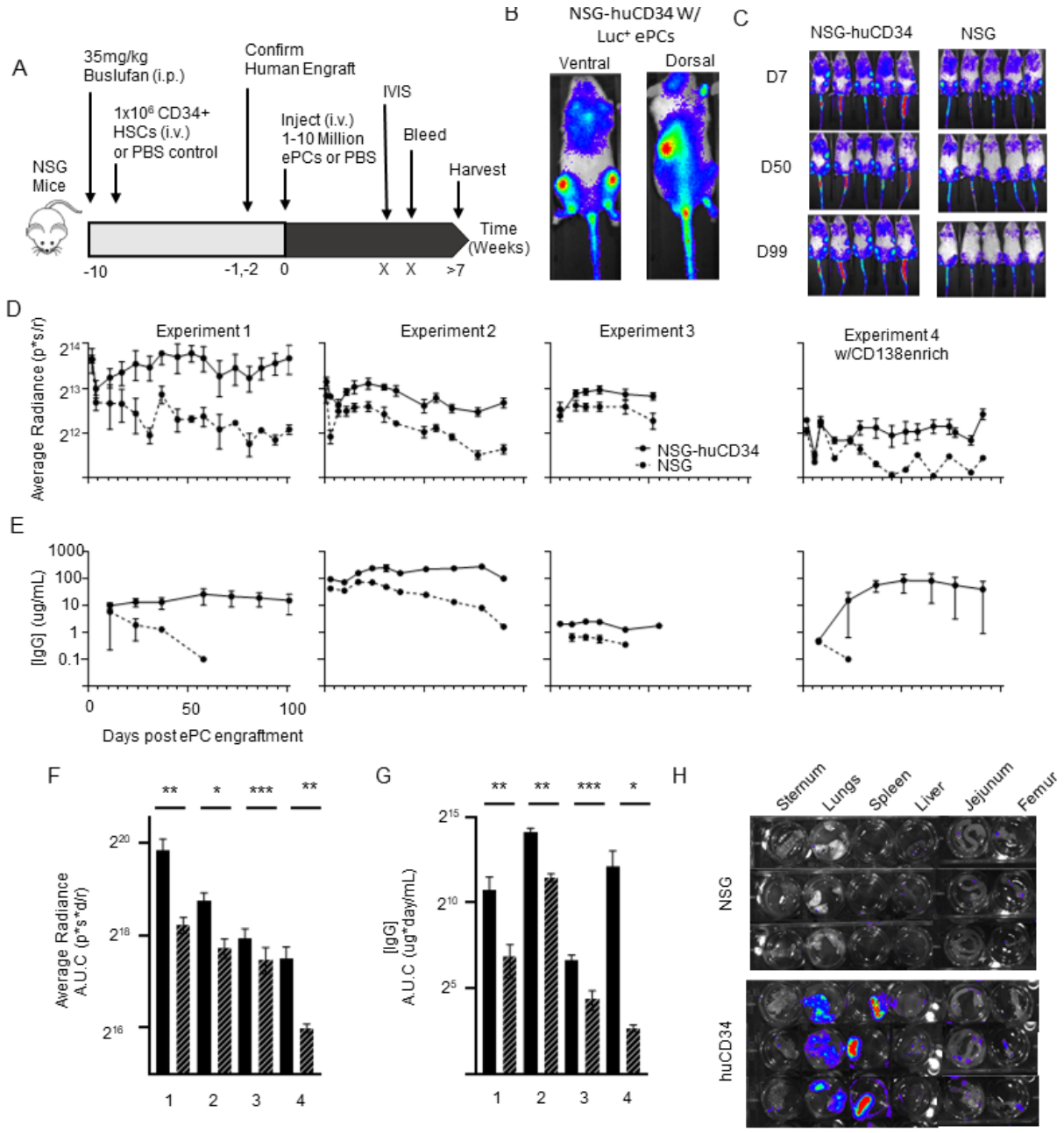

A) Experimental timeline for the assessment of luciferase expressing ePCs in NSG and NSG-huCD34 mice. Mice were injected (s.c.) with luciferin and bioluminescence was measured at

various time points. **B)** Representative bioluminescence dorsal and ventral images of NSG-huCD34 mice 21 days after engraftment with ePC were obtained via *in vivo* imaging **C)** Representative bioluminescence ventral images of NSG and NSG-huCD34 mice at various times after ePC are shown. **D)** Bioluminescence was quantified from each mouse as average radiance and graphed over time for each experiment and graphed over time. **F)** Area under the curve analysis of average radiance was conducted with baseline correction of $2x10^3$ average radiance. **E)** The concentration of human IgG was measured via ELISA of peripheral sera and graphed over time for each experiment. **F)** Area under the curve analysis of the [IgG] was conducted and graphed as shown. **E)** Mice 21 days after engraftment with ePCswere perfused with PBS containing luciferin and tissues were harvested for ex vivo bioluminescence imaging. E-G) Data across 4 donors in 4 independent experiments with p-value calculated by unpaired student's t test for each experiment (* $p < 0.05$, ** $p < 0.01$, *** $p < 0.001$).

3.6.4. *Engineered plasma cells maintain plasma cell phenotype and persist in the bone marrow and spleen of humanized mice*

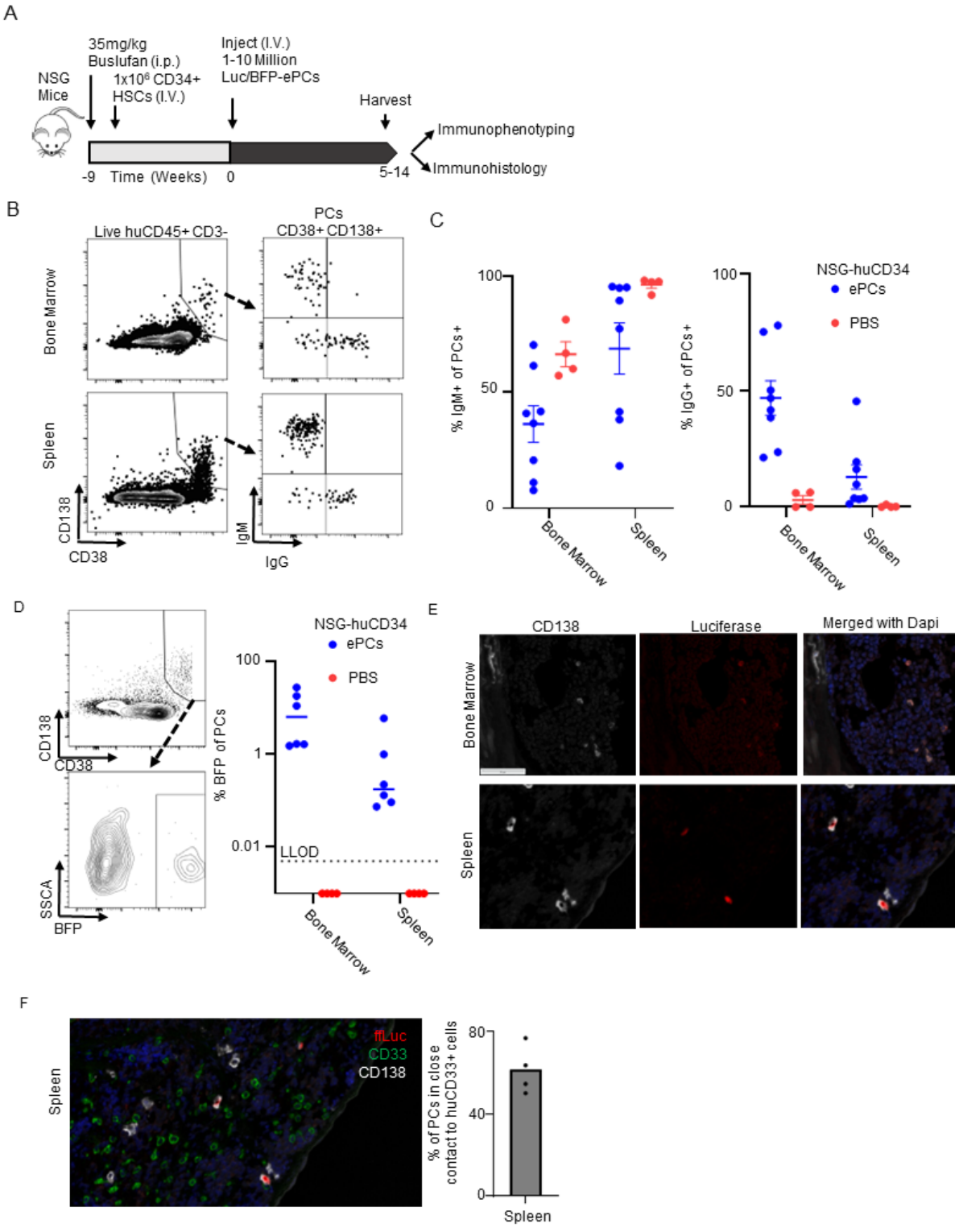

A) Experimental timeline for the assessment of plasma cell phenotype and localization in NSG-huCD34 mice. Mouse bone marrow and spleen were harvested between 5 and 10 weeks post ePC engraftment. **B)** Representative flow plots showing the staining and gating strategy to determine the isotype of plasma cells found in the bone marrow and spleens of ePC engrafted NSG-huCD34 mice. **C)** The percentage of PCs (huCD45$^+$,CD38$^+$,CD138$^+$) that express IgM and IgG were quantified and graphed to show that only mice receiving ePC have IgG$^+$ PCs. **D)** Representative flow plots and quantification of the percent of PCs that express BFP. **E)** Immunohistology of bone marrow and spleens from ePC engrafted NSG-huCD34 mice showing colocalization of Luciferase with CD138 positive cells. **F)** Spleens were also stained for human CD33. The percentage of PCs in close contact was calculated and graphed as shown. B-D) Data across two donors in two independent experiments. F) Data across four mice from one experiment.

3.6.5. *ePCs produce stable titers of anti-pathogen mAb for over 100 days*

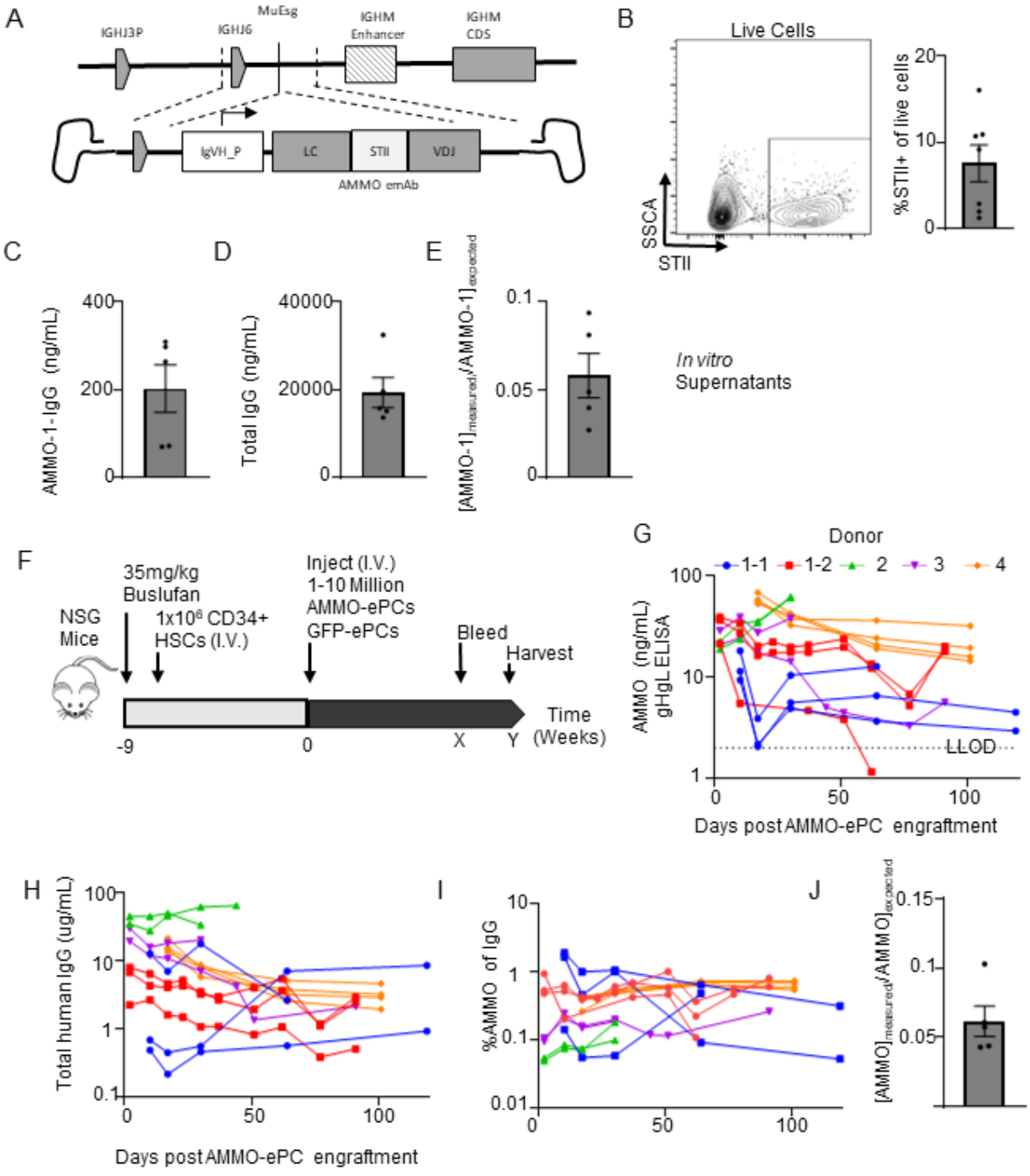

A) Schematic showing the genome editing approach used to generate ePCs that produce AMMO-1 emAb. **B)** Day 13 ePCs were intracellularly stained for the STII epitope tag within the

linker of the AMMO-1 emAb. **C)** Secreted AMMO-1 IgG in the supernatants of D13 AMMO-1 ePCS was measured by antigen specific (gHgL) ELISA and graphed. **D)** Total secreted IgG in the supernatants of D13 AMMO-1 ePCS was measured and graphed. **E)** Using total IgG levels in the supernatants and $STII^{+}$ editing rates, we calculated the expected concentration of AMMO-1 in the supernatants. We then compared the measured AMMO-1 to the expected AMMO-1. **F)** Experimental timeline for the assessment of AMMO-1 emAb engraftment and secretion kinetics in NSG-huCD34 mice. and localization in NSG-huCD34 mice. **G)** Secreted AMMO-1 IgG in the sera of AMMO-1 ePCS engrafted mice was measured by antigen specific (gHgL) ELISA and graphed. **H)** Total secreted IgG in the sera of AMMO-1 ePCS engrafted mice was measured. **I)** AMMO-1 IgG levels was compared to total IgG levels and graphed to show a steady ratio between AMMO-1 IgG levels and total IgG levels. **J)** We compared the measured AMMO-1 to the expected AMMO-1 based on AMMO-1 editing rates and graphed the ratio. B-E) data across 3 biologic donors in 2 independent experiments. G-H) data across 4 biologic donors in 5 independent experiments.

3.6.6. *NSG-huCD34 can be engrafted with multiple doses of ePCs*

NSG-HuCD34 mice were engrafted with luciferase expressing ePCs. A second dose of luciferase expressing ePCs was administered to two mice on day 24 (arrow). Engraftment was monitored via in vivo imaging studies (IVIS).

3.6.7. *STII-emAb-AMMO-IgG has similar binding affinity to AMMO-IgG.*

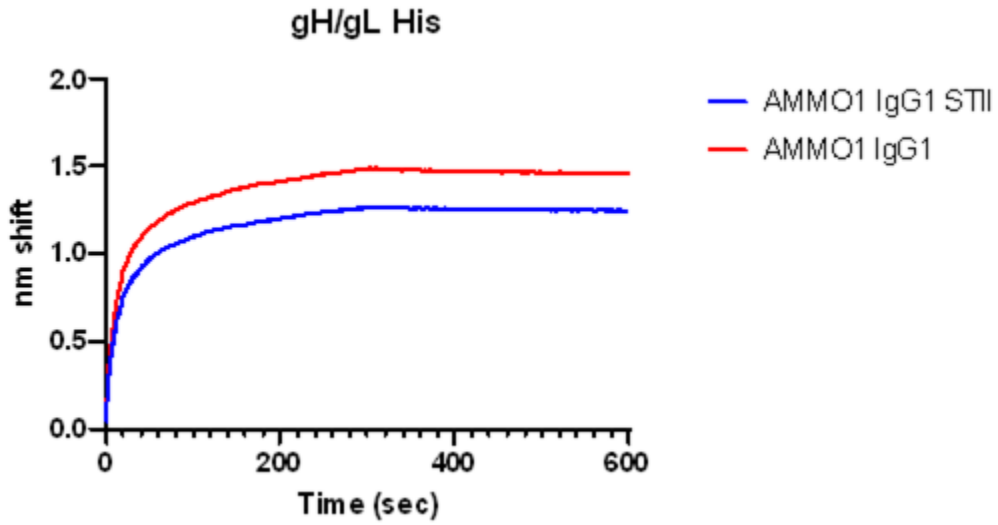

Surface plasmon resonance was used to measure antibody binding kinetics to EBV antigen gHgL.

3.7. BIBLIOGRAPHY

1. Cheng RYH, Hung KL, Zhang T, et al. Ex vivo engineered human plasma cells exhibit robust protein secretion and long-term engraftment in vivo. *Nat Commun*. 2022;13(1):6110.

2. Lyu X, Zhao Q, Hui J, et al. The global landscape of approved antibody therapies. *Antib Ther*. 2022;5(4):233-257.

3. Mullard A. FDA approves 100th monoclonal antibody product. *Nat Rev Drug Discov*. 2021;20(7):491-495.

4. Marengo MF, Suarez-Almazor ME. Improving treatment adherence in patients with rheumatoid arthritis: what are the options? *Int J Clin Rheumtol*. 2015;10(5):345-356.

5. Baryakova TH, Pogostin BH, Langer R, McHugh KJ. Overcoming barriers to patient adherence: the case for developing innovative drug delivery systems. *Nat Rev Drug Discov*. 2023;22(5):387-409.

6. Gatault P, Brachet G, Ternant D, et al. Therapeutic drug monitoring of eculizumab: Rationale for an individualized dosing schedule. *MAbs*. 2015;7(6):1205-1211.

7. Jain T, Litzow MR. Management of toxicities associated with novel immunotherapy agents in acute lymphoblastic leukemia. *Ther Adv Hematol*. 2020;11:2040620719899897.

8. Luo B, Zhan Y, Luo M, et al. Engineering of α-PD-1 antibody-expressing long-lived plasma cells by CRISPR/Cas9-mediated targeted gene integration. *Cell Death Dis*. 2020;11(11):973.

9. Nahmad AD, Lazzarotto CR, Zelikson N, et al. In vivo engineered B cells secrete high titers of broadly neutralizing anti-HIV antibodies in mice. *Nat Biotechnol*. 2022;40(8):1241-1249.

10. Andrews CD, Luo Y, Sun M, et al. In Vivo Production of Monoclonal Antibodies by Gene Transfer via Electroporation Protects against Lethal Influenza and Ebola Infections. *Mol Ther Methods Clin Dev*. 2017;7:74-82.

11. Hartweger H, McGuire AT, Horning M, et al. HIV-specific humoral immune responses by CRISPR/Cas9-edited B cells. *J Exp Med*. 2019;216(6):1301-1310.

12. Moffett HF, Harms CK, Fitzpatrick KS, Tooley MR, Boonyaratanakornkit J, Taylor JJ. B cells engineered to express pathogen-specific antibodies protect against infection. *Sci Immunol*. 2019;4(35).

13. Voss JE, Gonzalez-Martin A, Andrabi R, et al. Reprogramming the antigen specificity of B cells using genome-editing technologies. *Elife*. 2019;8. doi:10.7554/eLife.42995

14. Manz RA, Thiel A, Radbruch A. Lifetime of plasma cells in the bone marrow. *Nature*. 1997;388(6638):133-134.

15. Amanna IJ, Carlson NE, Slifka MK. Duration of humoral immunity to common viral and vaccine antigens. *N Engl J Med*. 2007;357(19):1903-1915.

16. Eyer K, Doineau RCL, Castrillon CE, et al. Single-cell deep phenotyping of IgG-secreting cells for high-resolution immune monitoring. *Nat Biotechnol*. 2017;35(10):977-982.

17. Radbruch A, Muehlinghaus G, Luger EO, et al. Competence and competition: the challenge of becoming a long-lived plasma cell. *Nat Rev Immunol*. 2006;6(10):741-750.

18. Hibi T, Dosch HM. Limiting dilution analysis of the B cell compartment in human bone marrow. *Eur J Immunol*. 1986;16(2):139-145.

19. Tyler F. Hill, Parnal Narvekar, Gregory Asher, Nathan Camp, Kerri R. Thomas, Sarah K. Tasian, David J. Rawlings, Richard G. James. Human plasma cells engineered to secrete bispecifics drive effective in vivo leukemia killing. *Blood*.

20. Douam F, Ploss A. The use of humanized mice for studies of viral pathogenesis and immunity. *Curr Opin Virol*. 2018;29:62-71.

21. Singh S, Homad LJ, Akins NR, et al. Neutralizing Antibodies Protect against Oral Transmission of Lymphocryptovirus. *Cell Rep Med*. 2020;1(3). doi:10.1016/j.xcrm.2020.100033

22. Islas-Ohlmayer M, Padgett-Thomas A, Domiati-Saad R, et al. Experimental infection of NOD/SCID mice reconstituted with human CD34+ cells with Epstein-Barr virus. *J Virol*. 2004;78(24):13891-13900.

23. Snijder J, Ortego MS, Weidle C, et al. An Antibody Targeting the Fusion Machinery Neutralizes Dual-Tropic Infection and Defines a Site of Vulnerability on Epstein-Barr Virus. *Immunity*. 2018;48(4):799-811.e9.

24. Slamanig SA, Nolte MA. The Bone Marrow as Sanctuary for Plasma Cells and Memory T-Cells: Implications for Adaptive Immunity and Vaccinology. *Cells*. 2021;10(6). doi:10.3390/cells10061508

25. Xu W, Joo H, Clayton S, et al. Macrophages induce differentiation of plasma cells through CXCL10/IP-10. *J Exp Med*. 2012;209(10):1813-1823, S1-S2.

26. Seung E, Tager AM. Humoral immunity in humanized mice: a work in progress. *J Infect Dis*. 2013;208 Suppl 2(Suppl 2):S155-S159.

27. Hung KL, Meitlis I, Hale M, et al. Engineering Protein-Secreting Plasma Cells by Homology-Directed Repair in Primary Human B Cells. *Mol Ther*. 2018;26(2):456-467.

28. Cheng RYH, de Rutte J, Ott AR, et al. SEC-seq: Association of molecular signatures with antibody secretion in thousands of single human plasma cells. *bioRxiv*. Published online August 26, 2022:2022.08.25.505190. doi:10.1101/2022.08.25.505190

29. Avery DT, Kalled SL, Ellyard JI, et al. BAFF selectively enhances the survival of plasmablasts generated from human memory B cells. *J Clin Invest*. 2003;112(2):286-297.

30. Tellier J. BAFF bestows longevity on splenic plasma cells. *Blood*. 2018;131(14):1500-1501.

31. O'Connor BP, Raman VS, Erickson LD, et al. BCMA is essential for the survival of long-lived bone marrow plasma cells. *J Exp Med*. 2004;199(1):91-98.

32. Jourdan M, Cren M, Robert N, et al. IL-6 supports the generation of human long-lived plasma cells in combination with either APRIL or stromal cell-soluble factors. *Leukemia*. 2014;28(8):1647-1656.

33. Ettinger R, Sims GP, Fairhurst AM, et al. IL-21 induces differentiation of human naive and memory B cells into antibody-secreting plasma cells. *J Immunol*. 2005;175(12):7867-7879.

34. Moens L, Tangye SG. Cytokine-Mediated Regulation of Plasma Cell Generation: IL-21 Takes Center Stage. *Front Immunol*. 2014;5:65.

35. Lang J, Zhang B, Kelly M, et al. Replacing mouse BAFF with human BAFF does not improve B-cell maturation in hematopoietic humanized mice. *Blood Adv*. 2017;1(27):2729-2741.

36. Kiyama K, Kawabata D, Hosono Y, et al. Serum BAFF and APRIL levels in patients with IgG4-related disease and their clinical significance. *Arthritis Res Ther*. 2012;14(2):R86.

37. Kado S, Nagase T, Nagata N. Circulating levels of interleukin-6, its soluble receptor and interleukin-6/interleukin-6 receptor complexes in patients with type 2 diabetes mellitus. *Acta Diabetol*. 1999;36(1-2):67-72.

38. Said EA, Al-Reesi I, Al-Shizawi N, et al. Defining IL-6 levels in healthy individuals: A meta-analysis. *J Med Virol*. 2021;93(6):3915-3924.

39. Chao PZ, Hsieh MS, Lee FP, et al. Serum level of interleukin-21 is elevated in chronic rhinosinusitis. *Am J Rhinol Allergy*. 2015;29(1):e1-e6.

40. Rongvaux A, Takizawa H, Strowig T, et al. Human hemato-lymphoid system mice: current use and future potential for medicine. *Annu Rev Immunol*. 2013;31:635-674.

41. Kenney LL, Shultz LD, Greiner DL, Brehm MA. Humanized Mouse Models for Transplant Immunology. *Am J Transplant*. 2016;16(2):389-397.

42. Matthes T, Dunand-Sauthier I, Santiago-Raber ML, et al. Production of the plasma-cell survival factor a proliferation-inducing ligand (APRIL) peaks in myeloid precursor cells from human bone marrow. *Blood*. 2011;118(7):1838-1844.

43. Winter O, Moser K, Mohr E, et al. Megakaryocytes constitute a functional component of a plasma cell niche in the bone marrow. *Blood*. 2010;116(11):1867-1875.

44. Chu VT, Fröhlich A, Steinhauser G, et al. Eosinophils are required for the maintenance of plasma cells in the bone marrow. *Nat Immunol*. 2011;12(2):151-159.

Chapter 4.

ENGINEERING TOOLS FOR THE SCREENING OF ANTIBODIES BASED ON B CELL SIGNALING AND ANTIBODY EXPRESSION IN HUMAN B CELLS

4.1. INTRODUCTION

In Chapter 3, we established a powerful engineered plasma cell (ePC) adoptive transfer humanized mouse model as a tool for the functional testing of biotherapeutic-secreting ePC. Unfortunately, we were not able to test whether anti-EBV monoclonal antibody (mAb)-secreting ePCs could protect humanized mice from EBV infection. This was due in part to lower than expected secretion of the anti-EBV mAb from the ePCs. In this chapter, we seek to develop a tool that will help screen libraries of antigen-specific B cell receptors (BCRs) for both functional BCR signaling and for robust expression levels in human B cells. An antigen-specific BCR and its corresponding secreted antibody share a nearly identical structure except for a cTerminal transmembrane domain. Thus, screening BCRs using a BCR signaling reporter may prove to be a biologically relevant tool to help identify high affinity mAbs that will express and secrete well when used in ePCs.

Monoclonal antibody therapies are a form of immunotherapy that uses mAbs to bind monospecifically to certain cells or proteins to treat a wide range of diseases. The first monoclonal antibody was generated in 1975 by Köhler and Milstein[1]. The first mAb therapy, muromonab-CD3, was approved for clinical use in 1986[2]. Now there are over 162 mAb therapies approved by at least one regulatory agency (more than half in the last decade) and the global mAb market is estimated to grow from $205 billion dollars in 2022 to $534 billion by 2025[3]. This rapid growth in mAb therapeutics has been due in part to the expansion in powerful technologies used for antibody discovery and development. Nevertheless, when it comes to tackling challenging antigen targets, predicting the expressibility of a mAb in mammalian cells, elucidating strong BCR (and mAb) functionality, and producing optimized therapeutic antibodies, conventional *in vitro* methods fall short.

The majority of antibody discovery and development methodologies rely on mouse hybridoma, phage display, and single-B cell screening techniques[4]. Hybridoma technology leverages the natural ability of the host to generate B cells capable of producing antibodies that exhibit specific isotype functionality and high affinity towards foreign antigens. The considerable time frame, typically lasting 3-4 months, and the animal-derived nature of the antibodies produced through hybridoma technology present substantial constraints on the widespread application of this approach for human therapeutics[5]. In the 1990s, the introduction of phage display technology brought about a revolutionary change in the field, enabling the creation of fully human monoclonal antibodies against virtually any desired target utilizing combinatorially rearranged human Ab libraries[6]. To generate phage-displayed antibody repertoires, human variable regions of heavy (VH) and light (VL) chains are interconnected by a flexible linker and then fused to the coat proteins (pIII or pVIII) of the filamentous bacteriophage M13 effectively displaying them as surface molecules. Phages expressing antigen-specific Abs are then enriched for target antigen binding. However, the selection and screening process of phage antibody libraries for human mAb is inherently limited by expression bias, folding errors, off-target binding and the number of clones that can be evaluated through downstream validation assays[7]. Alternatively for the development of pathogen-specific mAbs, antigen-specific memory B cell repertoires derived from naturally infected individuals can provide many high affinity BCRs (and subsequent mAbs). Our group has established robust protocols for BCR sequencing of rare, antigen-specific memory B cells[8–11]. The full utilization of single-cell memory B cell repertoires are still often limited by labor intensive *in vitro* antibody expression and validation ELISAs. Therefore, new methods are needed that allow for the rapid screening of BCRs from single-cell memory B cell libraries for Abs that are functional, antigen-specific, high-affinity and can be expressed from ePCs.

In this study, we develop and validate a novel human B cell-based BCR screening platform to address the validation bottleneck in mAb development, to better understand BCR biology, and to develop highly expressed mAbs for ePC therapies.

4.2. MATERIAL AND METHODS

4.2.1. *Generation of Nur77 (NR4A1) reporter Cell Line*

OCI-Ly7 cells were obtained from the Leibniz Institute DSMZ and cultured in IMDM (Gibco) media supplemented with 10% FBS. Clustered regularly interspaced short palindromic repeats (CRISPR) RNAs (crRNAs) targeting the c-terminus of *NR4A1* were identified using the Broad Institute GPP sgRNA Designer (http://portals.broadinstitute.org/gpp/public/analysis-tools/sgrna-design) and synthesized (IDT) containing phosphorothioate linkages and 2′O-methyl modifications (sequences in Table S1). crRNA and trans-activating crRNA (tracrRNA; IDT) single guide hybrids were mixed with 3uM Cas9 nuclease (Berkeley Labs) at a 1.2:1 ratio and delivered to cells by Lonza 3D electroporation (Pulse code: CM-137). After electroporation, cells were incubated in the presence of adeno-associated virus 6 (AAV6) vectors carrying homologous DNA repair templates consisting of 400bp homology flanking the remaining cTerminal *NR4A1* sequence (codon optimized) followed by a T2A ribosomal skip element and enhanced green fluorescent protein (20% AAV by volume, Figure 1A schema). Engineered Ly-7 cells were then serially diluted into monoclonal lines. Monoclonal lines were screened for reporter activity (see methods Stimulation and Sorting of eBCRs) and one was carried forward herein referred to as *NR4A1-GFP* reporter cell line.

4.2.2. *Engineering the BCRs of Ly7*

NR4A1-GFP reporter cell line was cultured in IMDM (Gibco) media supplemented with 10% FBS. Clustered regularly interspaced short palindromic repeats (CRISPR) RNAs (crRNAs) targeting the second exon of IGHM (sequences in Table S1) were identified using the Broad Institute GPP sgRNA Designer and synthesized (IDT) containing phosphorothioate linkages and 2′O-methyl modifications. crRNA and tracrRNA; single guide hybrids were mixed with 3uM Cas9 nuclease (Berkeley Labs) at a 1.2:1 ratio and delivered to cells by Lonza 3D (CM-137) electroporation. After electroporation, cells were incubated in the presence of adeno-associated virus 6 (AAV6) vectors carrying homologous DNA repair templates consisting of a T2A ribosomal skip element in cis with a light chain linked via a 3x strep tag II (STII) sequence to the variable domain of a heavy chain linked to a codon optimized version of the first exon of IGHM flanked by 400bp homology (20% AAV, Figure 2A schema). NR4A1-GFP cells expressing eBCRs were sorted via FACS ARIA II based on staining of the STII linker.

4.2.3. *Stimulation and sorting of eBCRs*

To assess the reporter activity, WT BCR expressing *NR4A1-GFP* reporter cell line was cultured for various amounts of time with various concentration of anti-AffiniPure $F(ab')_2$ Fragment Goat Anti-Human IgG + IgM (H+L) (Jackson ImmmunoResearch). Reporter expression was assessed by flow cytometry. Recombinant Spike RBD-His was purified from supernatants of HEK 293T cells transfected with a SARS-CoV2 Spike RBD-His expression plasmid. Recombinant hen egg lysozyme (HEL) was purchased from Sigma (L4919). Both RBD and HEL were biotinylated using EZ-Link Pentylamine-Biotin (Thermo 21345) and desalted using Zeba Spin columns (Thermo). M-280 beads (Invitrogen) were labeled with biotinylated HEL and RBD and subsequently washed 3 times with PBS. One million *NR4A1-GFP* cells

expressing a mixture of eBCRs were incubated with $3x10^7$ antigen coated beads for 6 hours. Cells were then washed with PBS, stained for IgM, and sorted on FACS ARIA II. The sorted cells were cultured for 2 days at which point gDNA was collected and eBCRs were using a miseq nano kit v3.

4.2.4. *Generation of eBCR library and library analysis*

We developed a gibson assembly-based drop in cloning method to rapidly generate a library of gene pAAV transfer plasmids containing 95 eBCR sequences. The majority of the pool of sequences consisted of antibodies targeting the RBD of SARS-CoV2 spike protein (14 clinical mAbs, 29 published[10–12], 14 unpublished). An additional 10 known control eBCRs that do not bind RBD (ie Palivizumab, VRC01, MSP1 etc), 6 nonsense controls and 10 eBCR sequences that were codon optimized (codon optimization tool, IDT) away from germline sequence were included in the library. Another 5 of the eBCR sequences had their signal peptide swapped to each of three VH signal peptides for an additional 15 sequences. Each eBCR sequence had its IgHM exon 1 silently mutated to a unique barcode sequence to allow for easy sequencing and tracking of each sequence. These barcodes were amplified by nested PCR and sequenced using a miseq nano kit v3. Barcodes were counted using 2Fast2Q.[13] Each eBCR count was normalized to total counts from each sample to get sequence prevalence. By comparing sequence prevalence in the high STII group to the low STII group we were able to calculate an enrichment score.

4.2.5. *Statistical analysis*

Statistical analyses using parametric tests were performed using Prism 7 (GraphPad, San Diego, CA) as described in figure legends.

4.3. RESULTS

4.3.1. *Fluorescent reporter expressed under NR4A1 control generates a BCR signal reporter cell line*

We first wanted to establish a human B cell line that could report surface BCR stimulation via expression of a fluorescent reporter. Previous labs have shown that *NR4A1* (also known as Nur77) is a specific indicator of antigen receptor signaling in human T and B cells[14]. Leveraging this knowledge, we used homology directed repair (HDR) to link the expression of a fluorescent reporter expression to the expression of *NR4A1*. Briefly, OCI-Ly7 (diffuse large B cell lymphoma) cells were electroporated in the presence of Cas9 ribonucleoprotein complexes containing guide RNAs targeting the C-terminal sequence within *NR4A1,* and were subsequently transduced with rAAV6 HDR donor vector containing a transgene cassette consisting of *NR4A1* homology followed by a P2A ribosomal skip element and green fluorescent reporter (GFP) (Figure 1A). The cell line was serially diluted to create a monoclonal reporter line with high GFP expression upon BCR stimulation (referred herein as *NR4A1-GFP*, data not shown). *NR4A1-GFP* cells were stimulated with αIgM $F(ab')_2$. Upon stimulation we found a decrease in surface IgM consistent with BCR internalization (Figure 1B). Importantly, we saw an increase in GFP reporter expression in stimulated cells (Figure 1C). The level of GFP expression reflected both the amount of stimulation as well as the duration of the stimulation (Figure 1D). This data supports that the *NR4A1-GFP* reporter cell line is capable of reporting BCR signaling.

4.3.2. *NR4A1-GFP reporter cells engineered to express a variety of engineered BCRs demonstrate antigen-specific reporter activity*

To begin to test whether *NR4A1-GFP* reporter cells were capable of reporting antigen-specific signaling in response to cognate antigens, we next replaced the endogenous BCR with various BCRs of interest. Moffett et al. previously showed that inserting a full light chain linked to the heavy chain variable domain between the *IGHJ6* and *IGHM* loci in B cells results in the expression of engineered BCRs and engineered antibodies (emAbs)[15]. We modified the

Moffett engineering strategy to edit directly into exon 2 of the *IGHM* locus. This design was utilized to directly link eBCR expression with the abrogation of endogenous BCR expression. The resulting BCR engineered *NR4A1-GFP* cells express an exogenous immunoglobulin light chain linked by a strep tag II linker (STII) to an exogenous IgM heavy chain (herein referred to as an eBCR, Figure 2A). We used this strategy to individually express a series of eBCRs specific to hen egg lysozyme (αHEL) or the receptor binding domain of the SARS-CoV2 spike protein (αRBD), respectively. *NR4A1-GFP* cells treated with a CRISPR guide targeting exon 2 of IGHM in the absence of repair templates resulted in loss of IgM surface expression, whereas cells edited using eBCR repair templates showed restoration of IgM surface expression (Figure 2B). Consistent with surface expression of the eBCR, FACS staining for the STII linker demonstrated eBCR expression in engineered but not in control cell lines (Figure 2B). Importantliy, expression of the eBCRs did not impact the baseline GFP reporter expression consistent with the concept that eBCRs do not mediate tonic BCR signaling (Figure 2C). These data indicate that the endogenous BCR of *NR4A1-GFP* cells can be replaced with various eBCRs of interest.

Next, we determined if antigen-specific stimulation of cells expressing eBCRs would result in detectable *GFP* reporter expression and eBCR internalization. We treated *NR4A1-GFP* cells expressing either an αHEL-eBCR or an αRBD-eBCR with beads that were coated with

either HEL or RBD (Figure 3A). Consistent with antigen triggered cellular activation and subsequent integrin signaling, in response to addition of beads, αRBD-eBCR cells formed clusters in culture following the addition of RBD-coated- but not with HEL-coated beads. Conversely, αHEL-eBCR cells clustered with HEL coated beads but not with RBD coated beads (Figure 3B). Consistent with antigen driven eBCR internalization, IgM surface staining decreased on eBCR-cells stimulated with cognate antigen but not with control antigen (Figure 3C). Finally, GFP expression increased in eBCR-cells stimulated with cognate but not with control antigen (Figure 3D). These data indicate antigen-specific stimulation of eBCR expressing *NR4A1-GFP* cells leads to detectable eBCR internalization and BCR signaling reporter expression.

4.3.3. *Sorting on reporter expression and eBCR internalization correctly enriches for cells expressing eBCRs specific to target antigens*

Having established that antigen stimulation of eBCR expressing *NR4A1-GFP* cell lines results in antigen-specific reporter activity, we next wanted to determine whether this reporter system could be used to screen for antigen-specific eBCRs within a mixed population of cells expressing different eBCRs. To test this, we mixed an αRBD-eBCR cell line with an αHEL-eBCR cell line to create a mixed population of eBCR expressing cells. We then stimulated this mixed population with either HEL or RBD coated beads, sorted on reporter positive cells and sequenced their eBCRs (Figure 4A). Both HEL and RBD bead stimulations resulted in a sortable population of $GFP^{+}IgM^{low}$ from the mixed population (Figure 4B). eBCRs were sequenced from the genomic DNA of the sorted cells and bulk control cells. The control bulk cells resulted in roughly equal counts of αRBD and αHEL-eBCRs, whereas HEL stimulated cells enriched for the αHEL-eBCR and RBD stimulated cells enriched for the αRBD-eBCR (Figure 4C). We repeated the experiment with a more complex mixture of cells expressing 2 different αHEL-eBCR (D1.3 and HyHel10)[16] and 3 different αRBD-eBCRs (284, 300[11], 2B04[12]). We were

able to enrich for cells expressing eBCRs that had corresponding specificity to the antigen used to stimulate (Figure 4DE). This data suggests that one could use the eBCR *NR4A1-GFP* to screen for antigen-specific eBCRs from a population of unknown eBCRs.

4.3.4. *NR4A1-GFP reporter cells can be edited to express libraries containing many eBCRs*

Next, we wanted to express a large library of eBCR sequences in the *NR4A1-GFP* cell line to test whether the system was compatible with screening BCRs for features including: the level of protein expression (surface STII staining), binding specificity (enrichment with differing antigen stimulations), and binding affinity (enrichment upon repeat low dose antigen stimulations). To accomplish this we gathered 95 eBCR sequences from both published and unpublished antibodies targeting a variety of antigens with a variety of affinities and specificities. The majority of the library focused on antibodies targeting the RBD of SARS-CoV2 spike protein (14 clinical mAbs, 29 published[11,12], 14 unpublished). Additionally, to test how nucleotide sequence alterations and signal peptides might affect surface eBCR expression, we included 10 codon optimized sequences along with their analogous germline sequences and 15 sequences using 3 different signal peptide sequences. In parallel, we added 6 sequences containing stop codons at various locations within the eBCR sequence that should act as negative controls for eBCR expression.

The eBCR library sequences were cloned into eBCR transfer vectors to generate a plasmid library containing 95 unique sequences (Figure 5A). The plasmid library was sequenced to reveal that all sequences were present within a normal distribution (Figure 5B). We then engineered the *NR4A1-GFP* cell line with a low MOI of AAV6 containing the eBCR library to reduce the chance of double edits and passenger effects. We confirmed successful engineering by surface staining of STII which stained 9.36% of the library engineered cells (Figure 5C). Additionally, library engineered cells showed a wide continuous STII staining

pattern instead of a discrete positive population (Figure 5C). Finally, we sequenced the genomic DNA from the library engineered *NR4A1-GFP* cells and found all unique eBCR sequences represented in a normal distribution (Figure 5D). This data is consistent with the successful generation of *NR4A1-GFP* cells that express a large library of eBCRs with sufficient sequence coverage for further hypothesis testing.

We hypothesized that the variability of STII staining (Figure 5C) may be due to differences in the expression levels of each eBCRs. To test this hypothesis, we sorted eBCR library engineered *NR4A1-GFP* cells based on high, medium and low/negative STII staining (Sort gating shown in Figure 6A). Two days after the sort, we confirmed that we had three distinct populations by surface staining of STII (Figure 6B). Genomic DNA was harvested from each of the three populations and their eBCRs were sequenced. All controls with nonsense mutations were present in the low/negative but were absent from the high STII population (Figure 6C) indicating that the STII sort likely correctly screen out eBCR sequences that fail to express properly. We assigned an STII enrichment score to each eBCR sequence by comparing the prevalence of each eBCR in the high STII sort group to the prevalence in the low/negative STII sort group. We then plotted each eBCR sequence based on enrichment score from low to high (Figure 6D). As expected, nonsense control eBCR sequences were disproportionately found in the low expressors (Figure 6E). The top 10 eBCR sequences by STII enrichment score are shown (Figure 6F). OCI-Ly7 cells express endogenous kappa light chain which could interfere with expression of kappa light chain eBCRs. We compared the enrichment scores between kappa and lambda chain containing eBCRs and saw no difference indicating that our eBCR expression system is compatible with eBCRs containing either light chain (Figure 6G). Lasty, we were curious whether codon optimization of the human germline nucleotide sequences would improve expression. We did not see any difference in enrichment score between germline (median: 0.9715) and codon optimized sequences (median 0.9042, Figure

6H), suggesting that both germline and codon optimized sequences are compatible in our system. This data suggests that enrichment for STII staining may predict the level of mammalian expression level of a given BCR or antibody sequence.

4.4. DISCUSSION

Here we describe the use of a human B cell line to screen single-cell memory B cell derived Ab/BCR libraries based on their capacity to signal when in the presence of antigen as a platform to rapidly evaluate high-affinity mAbs with optimal expression in mammalian cells.

Antigen specific single-cell antibody discovery often leads to discovery of hundreds to thousands of potential antigen-specific BCRs[10,17,18]. Many of the potential hits are not truly antigen-specific because the low frequency of antigen-specific cells, even after a robust immune reaction, is only between 0.01–0.1% of total circulating B cells[19,20]. Additionally, not every sequence will lead to expressed BCR (sequences from recombined but silenced alleles). Similar to other antibody discovery platforms, it is often costly and labor intensive to screen all clones to evaluate and identify the best mAb candidates to develop using traditional methods (e.g., plasmid-based cloning, transfection, cell-based protein expression, protein purification, binding assessment through enzyme-linked immunosorbent assays (ELISAs), etc.)[21,22]. Our NR4A1-GFP system could be applied to create a short optimal list of mAbs to characterize by in vitro expression and therefore reduce the time needed to discover mAbs. While we show *NR4A1-GFP* screening data for a library of 95 unique sequences, the true limit is likely to be limited by FACs sorting capacity at ~10^4. However, this limitation is likely to be circumvented by performing a magnetic enrichment with antigen coated nanoparticles prior to antigen stimulation prior to sorting. Combining magnetic enrichment data with BCR signaling information would also provide insight regarding BCRs that bind to antigen but are incapable of signaling, potentially providing information on the biochemical constraints required for BCR signaling.

In addition to magnetic selection, computation pipelines could further enhance the screening efficiency of the *NR4A1-GFP* platform by shortlisting BCR repertoires prior to eBCR library generation. Cao *et al* use a computation pipeline to consider the frequency of somatic-hypermutations (SHMs) and potentially, other antigen-specific features; for example, focusing on already known antigen-specific VH–VL combinations, or specific IgG isotypes to shortlist potential Ab candidates[23,24]. However, this potentially risks the biasing towards immunodominant epitopes which may or may not provide protection[25]. Skewing towards immunodominant clones could potentially be counteracted by modifications to the epitope used in the *NR4A1-GFP* screen. For example by using subsequent positive screens with antigens that lack problematic immunodominant epitopes or with the use of immunodominant epitope blocking antibodies (as F'ab$_2$ to prevent BCR signaling negative feedback)[26–28]. This is critical for the development of neutralizing mAbs against pathogens known for their highly polymorphic immunodominant epitopes such as HIV and Influenza A[29,30].

Another strength of the *NR4A1-GFP* platform is that it is derived from a human B cell line. Many methods for screening large memory B cell repertoires use non-human display systems such as yeast and phage display to further screen antigen-specific memory B cell Ab libraries. However, Abs expressed in phage and yeast display have folding errors and glycosylation differences[31]. Human B cells offer a highly advantageous environment for a screening platform, as they facilitate proper folding, human B cell glycosylation patterns, and other essential B cell post-translational modifications[32,33]. Additionally, the majority of commercially available antibody therapeutics are manufactured using mammalian cell systems such as human PER.C6 cells[34]. Therefore, Abs screened via the *NR4A1-GFP* platform are more likely to succeed as manufacturable human therapeutics than Ab screened from other non-mammalian discovery technologies.

The *NR4A1-GFP* platform may prove useful for discovery of emAbs for engineered B cell and engineered plasma cell therapeutics, which are emerging cell-based modalities for high-level sustained delivery of therapeutic biologics. In the previous chapter we engineered PCs (ePC) to express an engineered anti-EBV antibody, AMMO-1[15,35]. We found that AMMO-1 expressed ~20 fold lower than expected. Consistent with the poor expressibility of this sequence, we found that the AMMO-1 eBCR sequence had the sixth lowest STII enrichment score (Figure 6E). This finding suggests that STII enrichment score may predict the expressibility of an emAb in human ePCs. Further experiments are underway to establish whether The *NR4A1-GFP* platform will accurately predict secretion levels of a variety of emAbs.

In summary, we developed an Ab screening platform that uses a *NR4A1* reporter in human B cell line to screen antigen-specific memory B cells libraries for BCR signaling in order to discover high-affinity mAbs. This platform shows promise for the discovery of antibodies for use as manufacturable mAb therapies and as emAb secreting ePC therapeutics.

4.5. FIGURES

4.5.1. *Fluorescent reporter of NR4A1 expression allows for readout of BCR signaling in a human B cell line*

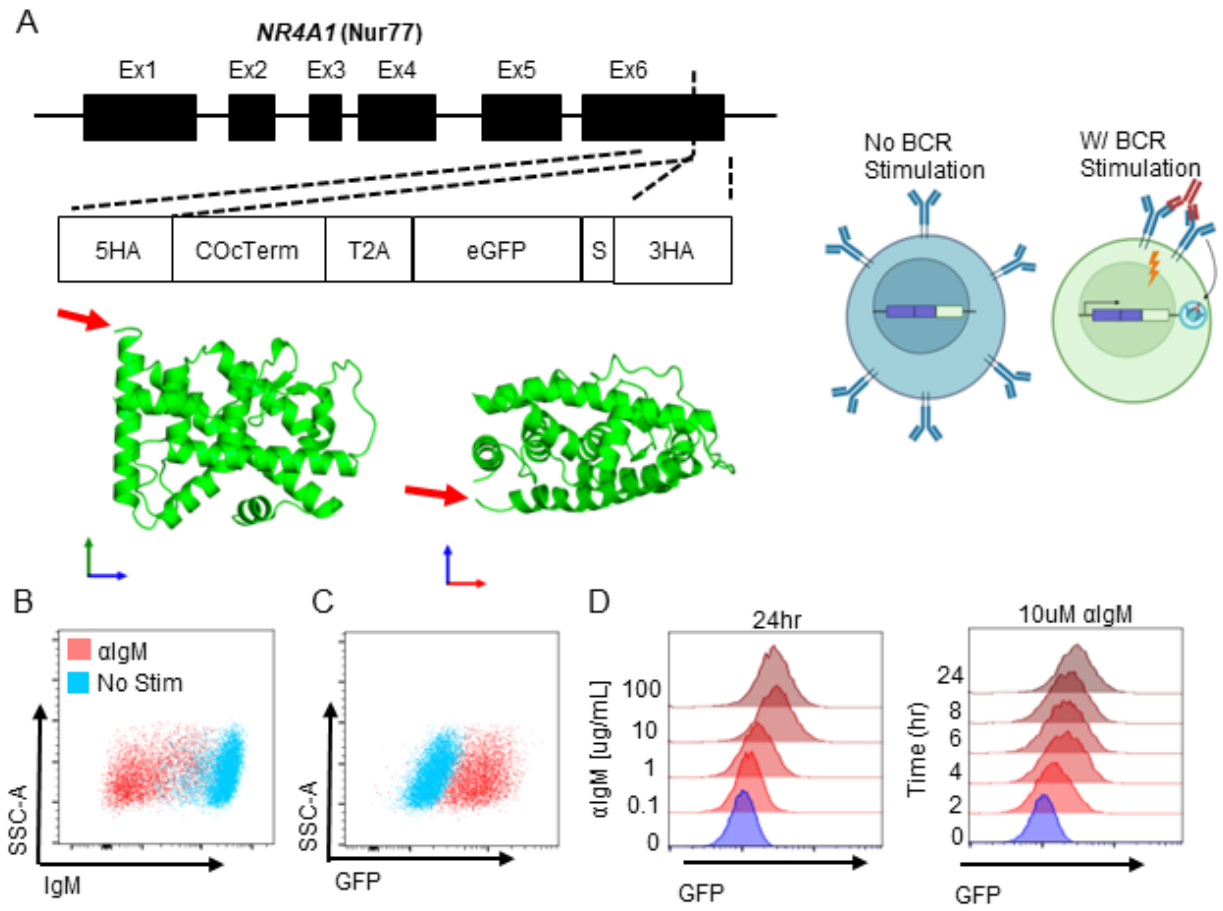

A) Schematic showing the genome engineering strategy used to produce a BCR signaling reporter. Red arrows indicate C terminus of NR4A1. **B)** Flow cytometry surface IgM staining of *NR4A1-GFP* cells after 24 hour hours of stimulation with 10uM αIgM (Blue) or with media only (Red). **C)** GFP expression as measured by flow cytometry. **D)** *NR4A1-GFP* cells were simulated using various concentrations of αIgM for various amounts of time and GFP expression was measured.

4.5.2. *NR4A1-GFP cells engineered to replace endogenous BCR with surface trackable exogenous eBCRs*

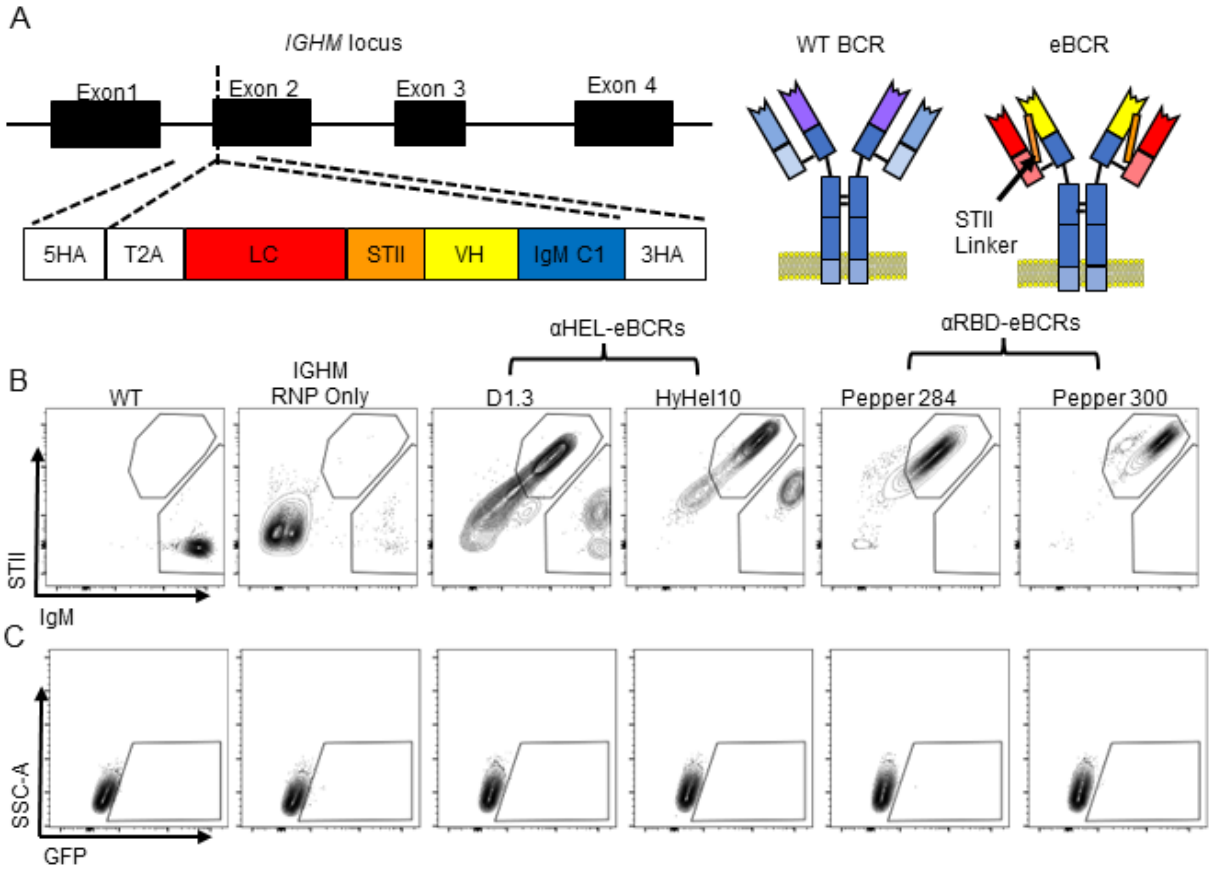

A) Schematic showing the genome engineering strategy used to replace the endogenous BCR with exogenous eBCRs. eBCRs contain a stainable strep tag II linker (STII) between the heavy and light chain. *NR4A1-GFP* cells were engineered to express 4 different eBCRs targeting HEL or Spike RBD. **B)** Flow cytometry surface IgM staining and strep tag II. **C)** GFP expression as measured by flow cytometry.

4.5.3. *Antigen-specific stimulation of eBCR induces BCR signaling reporter expression*

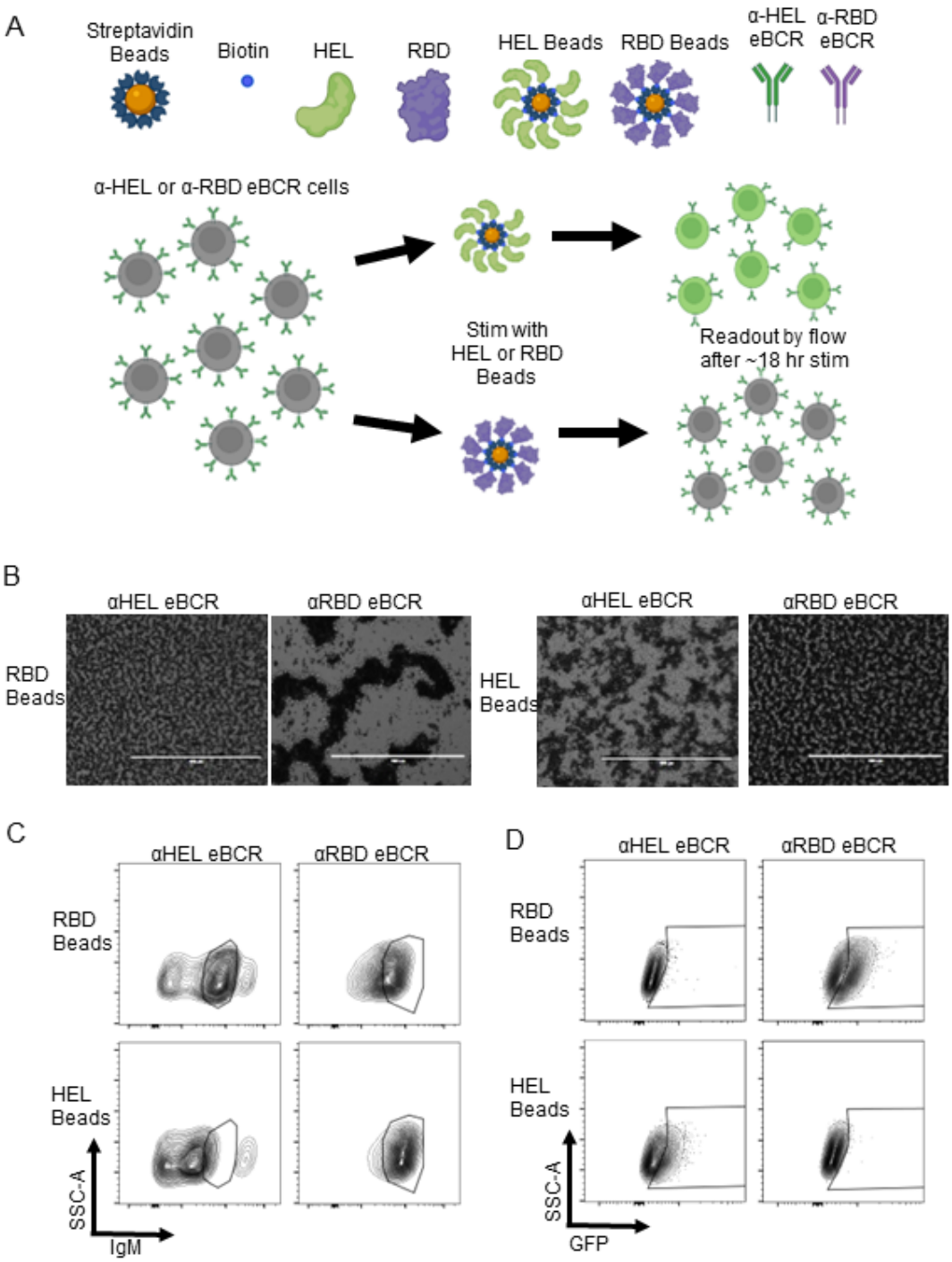

A) Schematic showing *NR4A1-GFP* cells expressing either an αHEL-eBCR or an αRBD-eBCR stimulated with either RBD or HEL coated beads. **B)** Light microscopy of eBCR *NR4A1-GFP* in

the presence of antigen-coated beads. **C)** Cells were stained for surface IgM and analyzed by flow cytometry to assess eBCR internalization. Gates indicate BCR internalization **D)** Cells were analyzed by flow cytometry to measure GFP positivity as a read out for BCR signaling. Gates indicate GFP positive cells.

4.5.4. Antigen-specific cells can be enriched from a mixed population of eBCR-cells

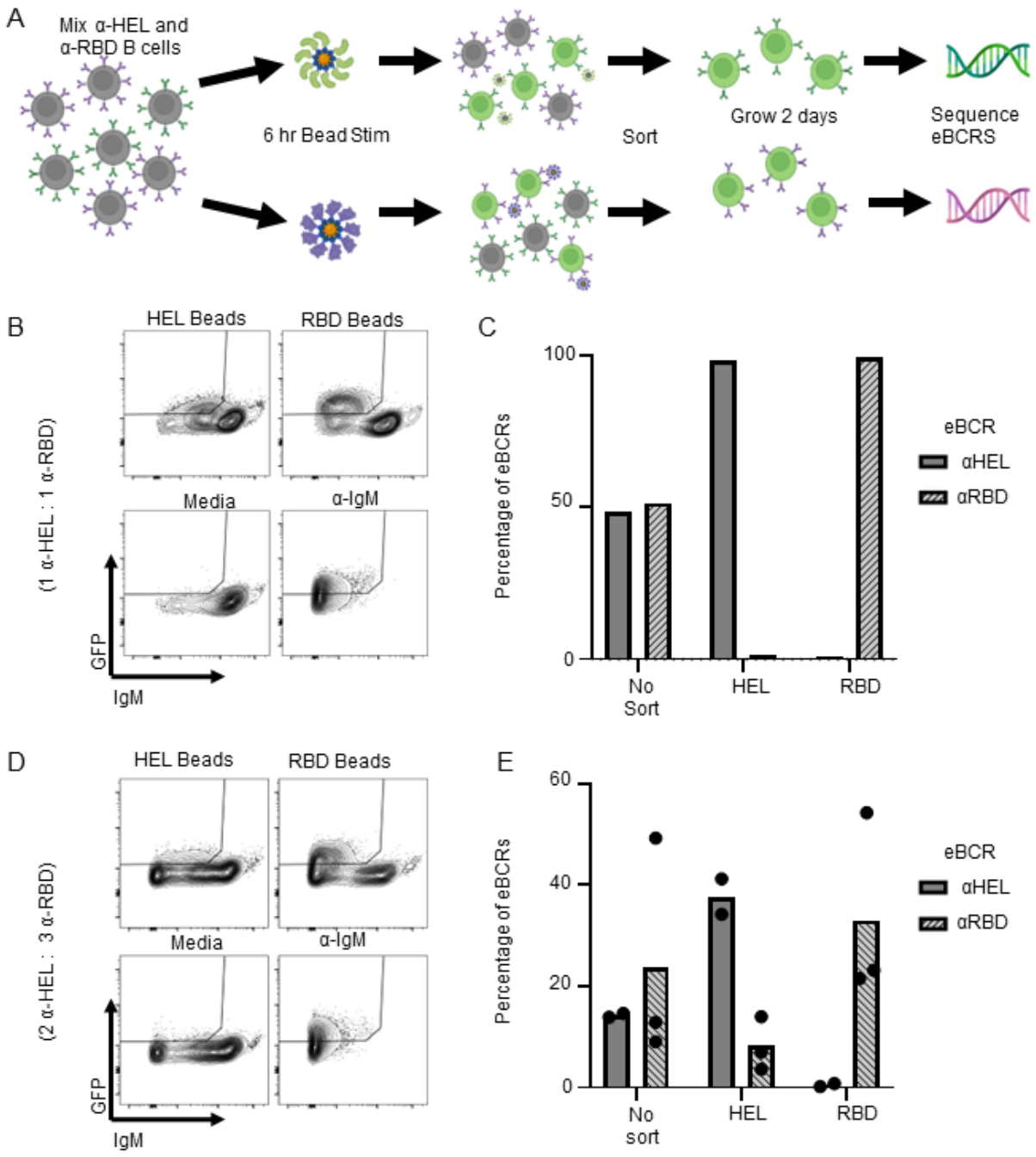

A) Schematic depicting the workflow for screening eBCRs based on GFP expression. A mixture of *NR4A1-GFP* cells expressing various αHEL and αRBD-eBCRs is stimulated with either RBD

or HEL coated beads. GFP cells are then sorted and grown for 2 days. Cells are then lysed and the eBCRs are sequenced. **B)** Cells were sorted according to flow cytometry gates shown. **C)** Sequence reads for each eBCR were counted and then graphed as a percentage of total eBCR sequence counts for each sorted population. **D)** Cells were sorted according to flow cytometry gates shown. **E)** Sequence reads for each eBCR were counted and then graphed as a percentage of total eBCR sequence counts for each sorted population.

4.5.5. *NR4A1-GFP cells engineered to express an eBCR library containing 95 unique sequences*

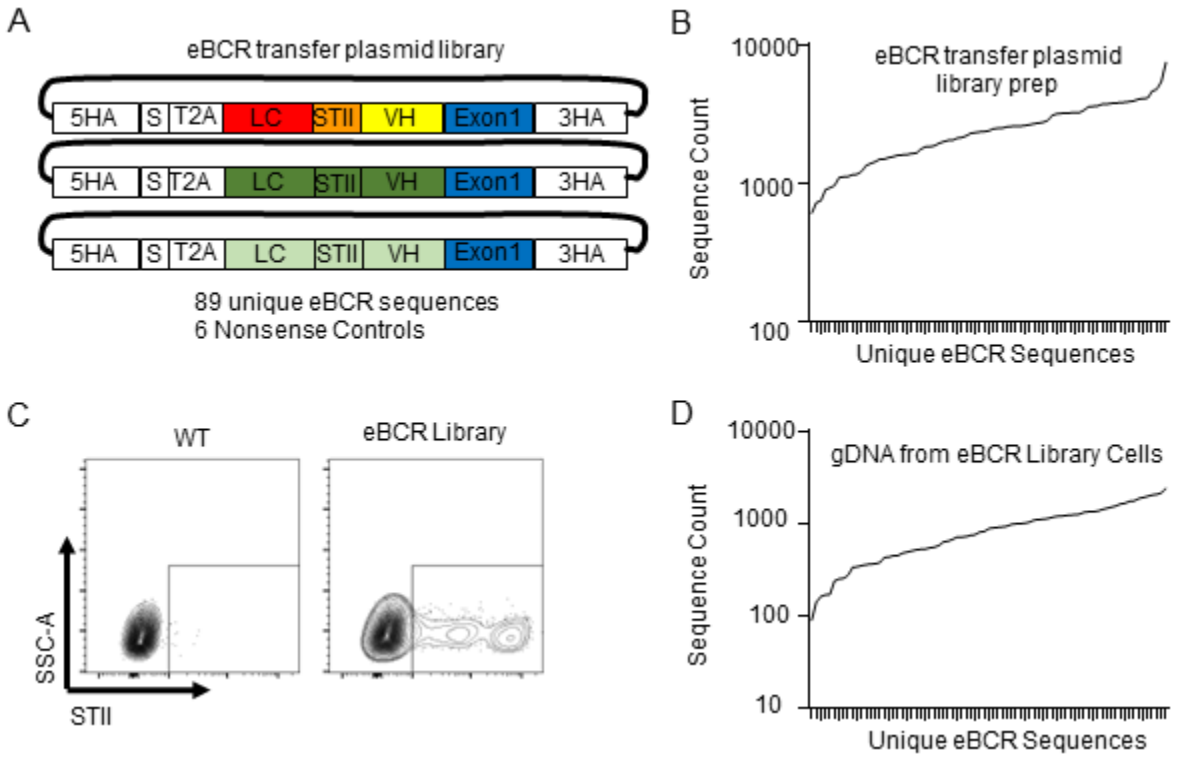

A) Representation of eBCR transfer plasmid library. **B)** eBCRs were sequenced from the library plasmid prep and graphed according to sequence count. **C)** *NR4A1-GFP* cells were engineered with the eBCR library. Two days later engineering success was determined by staining for STII surface expression. **D)** eBCRs were sequenced from genomic DNA that was harvested from library engineered cells. Sequence counts were graphed for each unique eBCR sequence.

4.5.6. Expressibility of eBCRs determined by surface STII staining and sorting

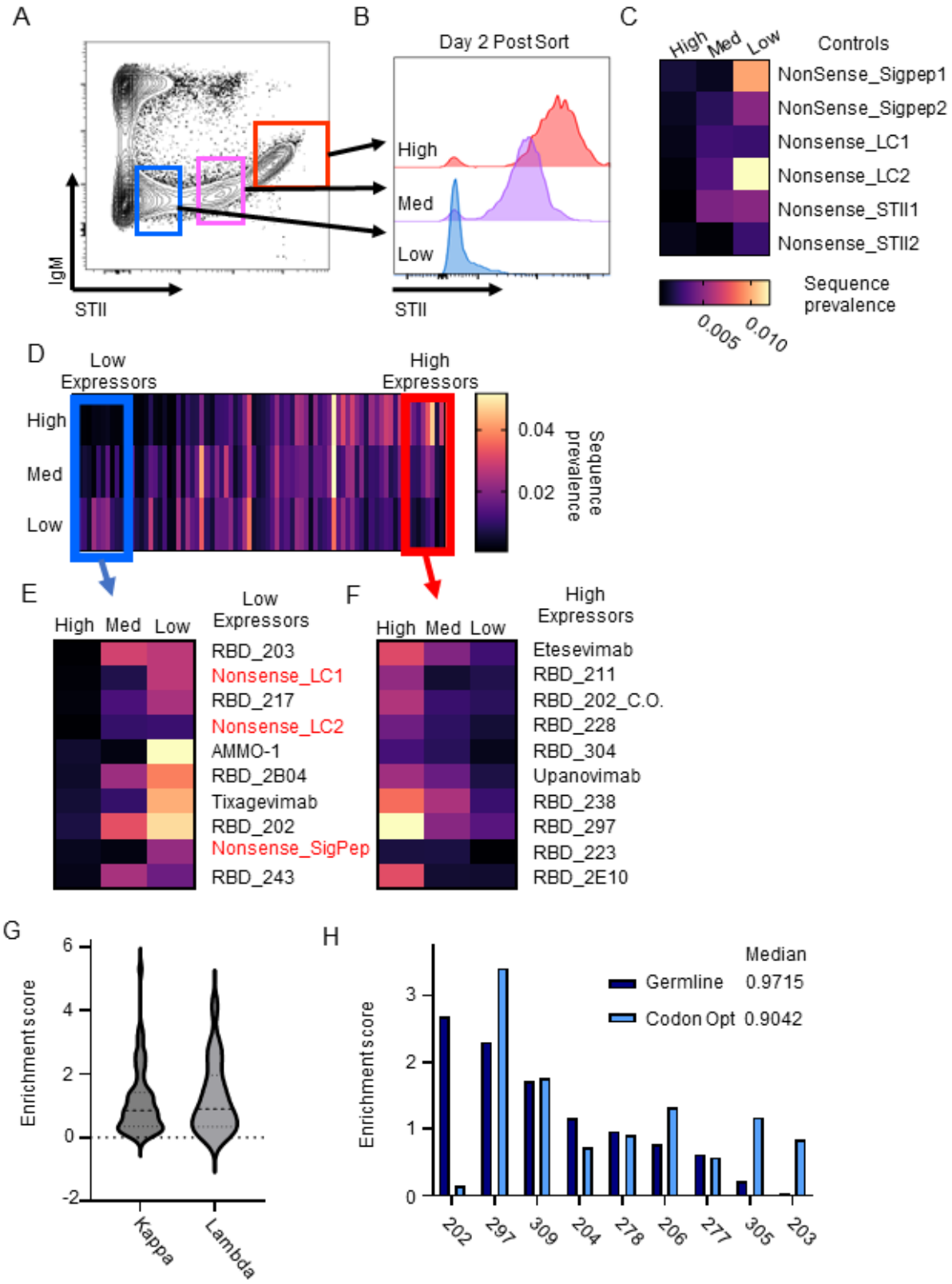

A) eBCR library engineered NR4A1-GFP cells were stained for surface IgM and for STII. The stained cells were then sorted according to the gates shown. **B)** Two days after sorting, each sorted population was stained for STII. Genomic DNA was then harvested from each sorted population and their eBCRs were sequenced. Each eBCR sequence count was normalized to total sequence counts of each population to calculate the sequence prevalence. **C)** Sequence prevalence for each nonsense control was mapped by a heat map for each sorted population. **D)** Enrichment scores were calculated by comparing the sequence prevalence of each eBCR in the high STII sorted group to the low STII sorted group. Sequence prevalence for each eBCR was plotted from low to high STII enrichment score. The blue box indicates eBCR sequences that have low STII enrichment scores while the red box indicates sequences with high STII enrichment scores. **E)** Heat map showing the 10 worst expressing eBCRs by STII enrichment score. **F)** Heat map showing the 10 highest expressing eBCRs by STII enrichment score. **G)** Violin plot showing the enrichment score of eBCRs with kappa light chains or lambda light chains. **H)** Enrichment score of eBCRs expressed as germline sequence or as codon optimized sequence.

4.6. BIBLIOGRAPHY

1. Köhler G, Milstein C. Continuous cultures of fused cells secreting antibody of predefined specificity. *Nature*. 1975;256(5517):495-497.

2. Van Wauwe JP, De Mey JR, Goossens JG. OKT3: a monoclonal anti-human T lymphocyte antibody with potent mitogenic properties. *J Immunol*. 1980;124(6):2708-2713.

3. Research, Markets. Global Monoclonal Antibody Therapeutics Market Report 2023: Sector is Expected to Reach $534.2 Billion by 2030 at a CAGR of 12.7%. Published June 8, 2023. Accessed July 11, 2023. https://www.globenewswire.com/en/news-release/2023/06/08/2684545/28124/en/Global-Monoclonal-Antibody-Therapeutics-Market-Report-2023-Sector-is-Expected-to-Reach-534-2-Billion-by-2030-at-a-CAGR-of-12-7.html

4. Wang Z, Wang G, Lu H, Li H, Tang M, Tong A. Development of therapeutic antibodies for the treatment of diseases. *Mol Biomed*. 2022;3(1):35.

5. Moraes JZ, Hamaguchi B, Braggion C, et al. Hybridoma technology: is it still useful? *Curr Res Immunol*. 2021;2:32-40.

6. Parray HA, Shukla S, Samal S, et al. Hybridoma technology a versatile method for isolation of monoclonal antibodies, its applicability across species, limitations, advancement and future perspectives. *Int Immunopharmacol*. 2020;85:106639.

7. Pedrioli A, Oxenius A. Single B cell technologies for monoclonal antibody discovery. *Trends Immunol*. 2021;42(12):1143-1158.

8. Krishnamurty AT, Thouvenel CD, Portugal S, et al. Somatically Hypermutated Plasmodium-Specific IgM(+) Memory B Cells Are Rapid, Plastic, Early Responders upon Malaria Rechallenge. *Immunity*. 2016;45(2):402-414.

9. Thouvenel CD, Fontana MF, Netland J, et al. Multimeric antibodies from antigen-specific human IgM+ memory B cells restrict Plasmodium parasites. *J Exp Med*. 2021;218(4). doi:10.1084/jem.20200942

10. Rodda LB, Netland J, Shehata L, et al. Functional SARS-CoV-2-Specific Immune Memory Persists after Mild COVID-19. *Cell*. 2021;184(1):169-183.e17.

11. Hale M, Netland J, Chen Y, et al. IgM antibodies derived from memory B cells are potent cross-variant neutralizers of SARS-CoV-2. *J Exp Med*. 2022;219(9). doi:10.1084/jem.20220849

12. Alsoussi WB, Turner JS, Case JB, et al. A Potently Neutralizing Antibody Protects Mice against SARS-CoV-2 Infection. *J Immunol*. 2020;205(4):915-922.

13. Bravo AM, Typas A, Veening JW. 2FAST2Q: a general-purpose sequence search and counting program for FASTQ files. *PeerJ*. 2022;10:e14041.

14. Ashouri JF, Weiss A. Endogenous Nur77 Is a Specific Indicator of Antigen Receptor Signaling in Human T and B Cells. *J Immunol*. 2017;198(2):657-668.

15. Moffett HF, Harms CK, Fitzpatrick KS, Tooley MR, Boonyaratanakornkit J, Taylor JJ. B cells engineered to express pathogen-specific antibodies protect against infection. *Sci Immunol*. 2019;4(35).

16. Batista FD, Neuberger MS. Affinity dependence of the B cell response to antigen: a threshold, a ceiling, and the importance of off-rate. *Immunity*. 1998;8(6):751-759.

17. Hurtado J, Rogers TF, Jaffe DB, et al. Deep repertoire mining uncovers ultra-broad coronavirus neutralizing antibodies targeting multiple spike epitopes. *bioRxiv*. Published online March 31, 2023:2023.03.28.534602. doi:10.1101/2023.03.28.534602

18. Zost SJ, Gilchuk P, Chen RE, et al. Rapid isolation and profiling of a diverse panel of human monoclonal antibodies targeting the SARS-CoV-2 spike protein. *Nat Med*. 2020;26(9):1422-1427.

19. Franz B, May KF Jr, Dranoff G, Wucherpfennig K. Ex vivo characterization and isolation of rare memory B cells with antigen tetramers. *Blood*. 2011;118(2):348-357.

20. Hoven MY, De Leij L, Keij JF, The TH. Detection and isolation of antigen-specific B cells by the fluorescence activated cell sorter (FACS). *J Immunol Methods*. 1989;117(2):275-284.

21. Vazquez-Lombardi R, Nevoltris D, Luthra A, Schofield P, Zimmermann C, Christ D. Transient expression of human antibodies in mammalian cells. *Nat Protoc*. 2018;13(1):99-117.

22. Gieselmann L, Kreer C, Ercanoglu MS, et al. Effective high-throughput isolation of fully human antibodies targeting infectious pathogens. *Nat Protoc*. 2021;16(7):3639-3671.

23. Cao Y, Su B, Guo X, et al. Potent Neutralizing Antibodies against SARS-CoV-2 Identified by High-Throughput Single-Cell Sequencing of Convalescent Patients' B Cells. *Cell*. 2020;182(1):73-84.e16.

24. Goldstein LD, Chen YJJ, Wu J, et al. Massively parallel single-cell B-cell receptor sequencing enables rapid discovery of diverse antigen-reactive antibodies. *Commun Biol*. 2019;2:304.

25. Angeletti D, Kosik I, Santos JJS, et al. Outflanking immunodominance to target subdominant broadly neutralizing epitopes. *Proc Natl Acad Sci U S A*. 2019;116(27):13474-13479.

26. Schaefer-Babajew D, Wang Z, Muecksch F, et al. Antibody feedback regulates immune memory after SARS-CoV-2 mRNA vaccination. *Nature*. 2023;613(7945):735-742.

27. Bournazos S, Ravetch JV. Fcγ Receptor Function and the Design of Vaccination Strategies. *Immunity*. 2017;47(2):224-233.

28. Heyman B. Regulation of antibody responses via antibodies, complement, and Fc receptors. *Annu Rev Immunol*. 2000;18:709-737.

29. Altman MO, Angeletti D, Yewdell JW. Antibody Immunodominance: The Key to

Understanding Influenza Virus Antigenic Drift. *Viral Immunol*. 2018;31(2):142-149.

30. Mayr LM, Su B, Moog C. Non-Neutralizing Antibodies Directed against HIV and Their Functions. *Front Immunol*. 2017;8:1590.

31. Wildt S, Gerngross TU. The humanization of N-glycosylation pathways in yeast. *Nat Rev Microbiol*. 2005;3(2):119-128.

32. Majewska NI, Tejada ML, Betenbaugh MJ, Agarwal N. N-Glycosylation of IgG and IgG-Like Recombinant Therapeutic Proteins: Why Is It Important and How Can We Control It? *Annu Rev Chem Biomol Eng*. 2020;11:311-338.

33. Wang TT, Ravetch JV. Functional diversification of IgGs through Fc glycosylation. *J Clin Invest*. 2019;129(9):3492-3498.

34. Li F, Vijayasankaran N, Shen AY, Kiss R, Amanullah A. Cell culture processes for monoclonal antibody production. *MAbs*. 2010;2(5):466-479.

35. Snijder J, Ortego MS, Weidle C, et al. An Antibody Targeting the Fusion Machinery Neutralizes Dual-Tropic Infection and Defines a Site of Vulnerability on Epstein-Barr Virus. *Immunity*. 2018;48(4):799-811.e9.

CONCLUDING THOUGHTS

In conclusion, the remarkable strides achieved in genome-engineering and human B cell biology have paved the way for the creation of human engineered plasma cells with transformative potential for long term therapeutic protein delivery with applications across a wide variety of human diseases. This dissertation encompasses a trio of pivotal investigations that collectively provide evidence and tools for the clinical translation of ePCs from basic research to bedside cure. The first study demonstrates that ePCs that secrete functional bispecific antibodies can suppress growth of leukemia xenografts, thus providing evidence that ePCs can mediate a clinically beneficial response in a clinically relevant model of human disease. The second study establishes a humanized mouse model that serves as an essential platform for demonstrating that autologously transplanted ePCs are capable of long term therapeutic secretion *in vivo*.The third study introduces an innovative B cell signaling-based screening method, facilitating the identification of high-expression monoclonal antibodies for secretion by ePCs. Collectively, these discoveries lend strong support to the advancement of ePC therapies. Nonetheless, uncertainties persist regarding ePCs.

An unresolved concern for the application of ePCs to humans pertains to the effective elimination or control of therapeutic protein secreted by ePCs subsequent to their administration. For example, ePC therapies targeting lymphoid malignancies have the potential to cause on-target off-tumor toxicity such as B cell aplasia, hypogammaglobulinemia and long-term dysfunction of the immune system. While such toxicities can be effectively managed via antibiotics, intravenous immunoglobulin replacement therapy as well as vaccinations, it may be preferably or necessary to remove ePCs therapeutics after a desired treatment period. For ePCs targeting lymphoid malignancies as a bridge to hematopoietic stem cell transplant, ePCs may be naturally removed via allo-rejection upon allogeneic immune reconstitution. The allo

rejection of host PCs is well documented[1] and may occur for ePCs as well. This could be a preferred method for ePC removal as it eliminates the ePCs right at the moment in which their therapeutic benefit is no longer necessary. In addition, ePCs may be removed using plasma cell targeting therapeutics such as daratumumab[2] or carfilzomib[3]. Lastly, a kill switch such as an inducible caspase suicide gene system may be required to eliminate ePCs[4]. The James lab is investigating engineering methods to generate ePCs that can be eliminated via inducible degradation of essential proteins. As an alternative to elimination, researchers are developing systems in which ePCs only secrete therapeutic protein when induced[5]. Various strategies, ranging from natural allo-rejection mechanisms to targeted therapies and engineered systems, are being developed to ensure the timely removal or controlled functioning of ePCs, allowing for the safe and optimized application of ePC therapies.

Another outstanding concern for ePC therapies is whether or not ePCs will contribute to the immunogenicity of a given therapeutic protein or promote immune tolerance towards the therapeutic protein. A major challenge for therapeutic proteins is their propensity to cause anti-drug antibodies (ADA). ADAs develop in around 25–30% of patients with severe hemophilia A within the initial 50 exposure days[6,7]. Both dose, route of administration, frequency, and the interval of dosing play a role in anti-drug antibody responses[8,9]. ePCs represent a novel route of drug administration that circumvents many of the treatment regimen factors most highly associated with ADA formation such as high injection frequency, and or subcutaneous administration. Moreover, these ePCs may present the exogenous protein peptides as a self-antigen, potentially reducing the immunogenicity associated with exogenous replacement protein therapies[10,11]. One study found the use of retrovirally transduced primary B cells expressing FIX antigen could prevent antibody formation and desensitize animals against FIX[12]. While lacking for ePCs, current evidence suggests that ePCs may induce therapeutic protein tolerance when compared to the immunogenicity of conventional recombinant protein

replacement therapy. We suggest that studies in immunocompetent animals and future clinical trials design their studies so that a direct comparison between the immunogenicity of ePCs and standard of care can be assessed.

Another unknown is how ePCs will traffic and localize in fully immunocompetent humans and whether this localization can be manipulated to direct ePCs to target tissues. We report in chapter 2 evidence that αCD19 expressing plasma cells mediate a potent anti-tumor response which may in turn be due to engineered plasma cells homing to the same bone marrow niche as the patient derived ALL cells. However, these studies were done in immunodeficient mice that lack the “normal” human plasma cell microenvironments[13]. We go on to show in Chapter 3 and in previous studies that ePCs are capable of long-term engraftment in the bone marrow of humanized mice[14]. This feature of plasma cells could be particularly useful for the local delivery therapeutics that have on-target but off-tissue side effects such as CD33 and CD123 targeting agents[15–17]. IgA PCs are also known for their localization in mucosal tissues, suggesting a link between PC and plasma cell localization[18]. Further studies in rhesus macaques examining tissue localization are warranted to further understand the tissue homing of ePCs and whether it can be manipulated to boost therapeutic protein levels in target tissues.

At this juncture, the data collected from in vitro and in vivo studies strongly emphasize the considerable potential of ePCs as a platform for delivering therapeutic proteins and peptides. Nonetheless, much remains to be uncovered about ePCs, and future studies will not only unveil their therapeutic prospects but also contribute to the broader understanding of plasma cell biology. This growing knowledge holds the promise of revealing mechanisms and targets for diseases influenced by plasma cell dysfunction. Further studies in humanized mice, non-human primates and humans are warranted to fully understand the therapeutic potential of ePCs

CONCLUDING THOUGHTS BIBLIOGRAPHY

1. Kamboj M, Shah MK. Vaccination of the Stem Cell Transplant Recipient and the Hematologic Malignancy Patient. *Infect Dis Clin North Am*. 2019;33(2):593-609.

2. Mateos MV, Sonneveld P, Hungria V, et al. Daratumumab, Bortezomib, and Dexamethasone Versus Bortezomib and Dexamethasone in Patients With Previously Treated Multiple Myeloma: Three-year Follow-up of CASTOR. *Clin Lymphoma Myeloma Leuk*. 2020;20(8):509-518.

3. Dimopoulos MA, Moreau P, Palumbo A, et al. Carfilzomib and dexamethasone versus bortezomib and dexamethasone for patients with relapsed or refractory multiple myeloma (ENDEAVOR): a randomised, phase 3, open-label, multicentre study. *Lancet Oncol*. 2016;17(1):27-38.

4. Di Stasi A, Tey SK, Dotti G, et al. Inducible apoptosis as a safety switch for adoptive cell therapy. *N Engl J Med*. 2011;365(18):1673-1683.

5. Page A, Delles M, Nègre D, Costa C, Fusil F, Cosset FL. Engineering B cells with customized therapeutic responses using a synthetic circuit. *Mol Ther Nucleic Acids*. 2023;33:1-14.

6. van den Berg HM, Fischer K, Carcao M, et al. Timing of inhibitor development in more than 1000 previously untreated patients with severe hemophilia A. *Blood*. 2019;134(3):317-320.

7. Peyvandi F, Mannucci PM, Garagiola I, et al. A Randomized Trial of Factor VIII and Neutralizing Antibodies in Hemophilia A. *N Engl J Med*. 2016;374(21):2054-2064.

8. Schellekens H. Factors influencing the immunogenicity of therapeutic proteins. *Nephrol Dial Transplant*. 2005;20 Suppl 6:vi3-vi9.

9. De Groot AS, Scott DW. Immunogenicity of protein therapeutics. *Trends Immunol*. 2007;28(11):482-490.

10. Van Meerhaeghe T, Néel A, Brouard S, Degauque N. Regulation of CD8 T cell by B-cells: A narrative review. *Front Immunol*. 2023;14:1125605.

11. Bennett SR, Carbone FR, Toy T, Miller JF, Heath WR. B cells directly tolerize CD8(+) T cells. *J Exp Med*. 1998;188(11):1977-1983.

12. Wang X, Moghimi B, Zolotukhin I, Morel LM, Cao O, Herzog RW. Immune tolerance induction to factor IX through B cell gene transfer: TLR9 signaling delineates between tolerogenic and immunogenic B cells. *Mol Ther*. 2014;22(6):1139-1150.

13. Hung KL, Meitlis I, Hale M, et al. Engineering Protein-Secreting Plasma Cells by Homology-Directed Repair in Primary Human B Cells. *Mol Ther*. 2018;26(2):456-467.

14. Cheng RYH, Hung KL, Zhang T, et al. Ex vivo engineered human plasma cells exhibit robust protein secretion and long-term engraftment in vivo. *Nat Commun*. 2022;13(1):6110.

15. Kenderian SS, Ruella M, Shestova O, et al. CD33-specific chimeric antigen receptor T cells exhibit potent preclinical activity against human acute myeloid leukemia. *Leukemia*. 2015;29(8):1637-1647.

16. Guy DG, Uy GL. Bispecific Antibodies for the Treatment of Acute Myeloid Leukemia. *Curr Hematol Malig Rep*. 2018;13(6):417-425.

17. Lamble AJ, Eidenschink Brodersen L, Alonzo TA, et al. CD123 Expression Is Associated With High-Risk Disease Characteristics in Childhood Acute Myeloid Leukemia: A Report From the Children's Oncology Group. *J Clin Oncol*. 2022;40(3):252-261.

18. Wang X, Hao GL, Wang BY, et al. Function and dysfunction of plasma cells in intestine. *Cell Biosci*. 2019;9:26.

VITA